REPORT DOCUMENTATION PAGE

Form Approved
OMB No. 0705-0188

1. AGENCY USE ONLY (Leave Blank)	2. REPORT DATE	3. REPORT TYPE AND DATES COVERED
	940131	ANNUAL REPORT 2/1/93-1/31/94

4. TITLE AND SUBTITLE

"EFFECT OF SURFACE FORCES ON THE RHEOLOGY OF PARTICLE-LIQUID SYSTEMS AND THE CONSOLIDATION OF CERAMIC POWDERS"

5. FUNDING NUMBERS

N00014-90-J-1441

AD-A277 092

6. AUTHOR(S)

FRED F. LANGE

DTIC
ELECTE
MAR 16 1994
C

7. PERFORMING ORGANIZATION NAME(S) AND ADDRESS(ES)

MATERIALS DEPARTMENT
COLLEGE OF ENGINEERING
UNIVERSITY OF CALIFORNIA
SANTA BARBARA, CA 93106

8. PERFORMING ORGANIZATION REPORT NUMBER

9. SPONSORING/MONITORING AGENCY NAME(S) AND ADDRESS(ES)

OFFICE OF NAVAL RESEARCH
MATERIALS DIVISION
800 NORTH QUINCY STREET
ARLINGTON, VA 22217-5000

10. SPONSORING/MONITORING AGENCY REPORT NUMBER

11. SUPPLEMENTARY NOTES

12A. DISTRIBUTION/AVAILABILITY STATEMENT

Approved for public release

12B. DISTRIBUTION CODE

13. ABSTRACT (Maximum 200 words)

More reliable ceramics require improved processing reliability. Heterogeneities bought with powders and those inadvertently introduced during processing as well as non-uniform and undefined phase distributions contribute to unreliable processing. Colloidal powder treatments can eliminate many heterogeneities and ensure more uniform phase distributions. To ensure that new heterogeneities are not introduced, colloidally treated powders must be piped, as slurries, directly to a die cavity. Slurry consolidation methods based on particle partitioning, e.g., pressure filtration and centrifugation are emphasized in this review. Interparticle potentials play a dominant role in governing the slurry viscosity, maximum particle packing density and the rheology of the consolidated body. These roles will be reviewed with the objective to understand how damage free bodies can be consolidated from slurries to increase the structural reliability of ceramics and their composites.

14. SUBJECT TERMS	15. NUMBER OF PAGES
Ceramics, Heterogeneities, Slurry, Colloidal Powder	80
	16. PRICE CODE

17. SECURITY CLASSIFICATION OF REPORT	18. SECURITY CLASSIFICATION OF THIS PAGE	19. SECURITY CLASSIFICATION OF ABSTRACT	20. LIMITATION OF ABSTRACT
UNCLASSIFIED	UNCLASSIFIED	UNCLASSIFIED	

94-08523

94 3 16 081

DISCLAIMER NOTICE

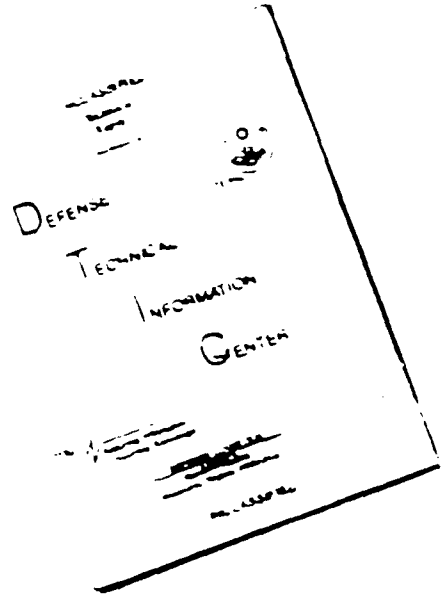

THIS DOCUMENT IS BEST QUALITY AVAILABLE. THE COPY FURNISHED TO DTIC CONTAINED A SIGNIFICANT NUMBER OF PAGES WHICH DO NOT REPRODUCE LEGIBLY.

MATERIALS

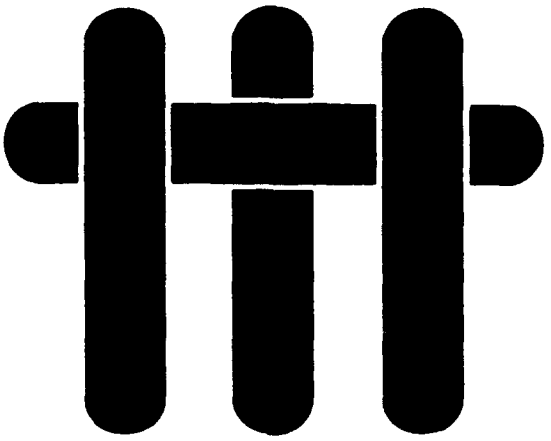

Effect of Surface Forces on the Rheology of Particle-Liquid Systems and the Consolidation of Ceramic Powders

Annual Technical Report
and
Technical Reports 8, 9, 10, 11 and 12

February 1, 1993-January 31, 1994

Office of Naval Research

Grant No. N00014-90-J-1441

Fred F. Lange

Principal Investigator

Materials Department
University of California
Santa Barbara, CA 93106

MATERIALS

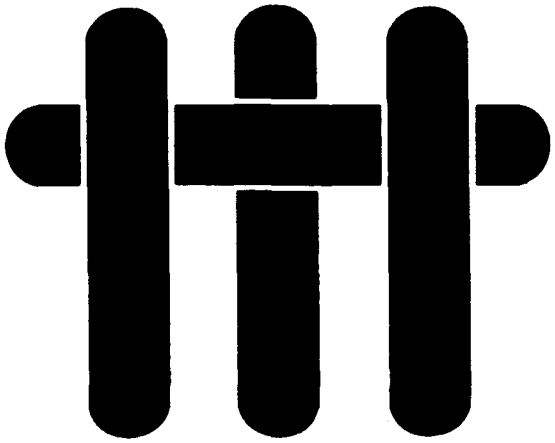

Technical Report Number 8

Effect of Interparticle Potentials on Particle Packing for Ceramic Processing

F. F. Lange

Office of Naval Research

Grant No. N00014-90-J-1441

Fred F. Lange

Principal Investigator

Materials Department
University of California
Santa Barbara, CA 93106

Powders & Grains 93, Thornton (ed.) © 1993 Balkema, Rotterdam, ISBN 90 5410 323 X

Effect of interparticle potentials on particle packing for ceramic processing

F. F. Lange
Materials Department, University of California, Santa Barbara, Calif., USA

ABSTRACT: Engineering shapes made of ceramics are first formed as powder compacts which are made dense by a heat treatment. High packing densities are desired, but more critically, powders must pack with a uniform density despite pressure gradients within the die cavity. As reviewed below, short- or long-range repulsive interparticle potentials that persist during packing enable ceramic powders to pack to high, pressure insensitive, relative densities. To appreciate how interparticle potentials effect particle packing, this review will first discuss how one develops different interparticle potentials, the relation between particle size distribution and the maximum packing density, and the mechanics of particle packing, viz., particle rearrangement during pressure consolidation.

1 INTRODUCTION

Interparticle potentials can be neglected when particles are large, i.e., when their separation force (particle mass x differential acceleration) in gravitational flow is much larger than either their attractive or repulsive force caused by different surface phenomena described below. This is not the case for powders used in ceramic processing where smaller particles (< 1 μm) are highly desireable to minimize the densification temperature and period and to develop microstructures that optimize properties. High relative densities also minimize the shrinkage strain during densification. For small particles, interparticle potentials strongly affect particle packing.

Although a high relative density is desired, modest densities ($\phi < \phi_{max}$) are certainly acceptable provided density gradients are not present. Density gradients cause shrinkage gradients that cause warping and cracking. Because pressure gradients always exist within die cavities, powders that pack to the same density over a wide range of pressures are desired. In addition, some forming methods can not be used if the relative density is pressure sensitive, e.g., centrifugation, which naturally produces large pressure gradients, can be used to form shapes when particle packing is pressure sensitive only at very low pressures. Thus, in ceramic processing, the pressure sensitivity of particle packing is a greater issue, relative to the maximum relative density.

Particles are either attractive or repulsive. The van der Waals potential, always cause particles with similar dielectric properties to be attractive when they are surrounded by a fluid with different dielectric properties. By itself, the van der Waals potential can produce a network of particles in elastic contact which are difficult to rearrange due to friction. A long-range repulsive potential can be produced by several practical methods provided the chemistry of the surface and/or the chemistry of the fluid near the surface can be sufficiently altered. To used these methods, the powder must be placed within an appropriate liquid. The net interparticle potential can be repulsive when the magnitude of the long-range repulsive potential is larger than the van der Waals potential. Repulsive potentials cause the particles to be dispersed. Even when the volume fraction of particles is small, dispersed particles form an interactive network because their movement is hindered by neighbors. Surface chemistries can also be modified to produce a repulsive potential that is only 'felt' once the particles are close enough to be attracted by the van der Waals potential. These short-range repulsive potentials keep the attractive particles from touching. As reviewed below, short-range repulsive potentials can produce a weaker attractive network relative to the touching network produce by the van der Waals potential alone. Provided that they persist as particles are pushed together, both long- and short-range repulsive potentials can ease particle rearrangement and produce pressure insensitive packing at practical pressures which allows particles to pack to their maximum relative density.

2 INTERPARTICLE POTENTIALS

The reader is referred to Horn's (1990) review of most phenomena, and their functional forms, that contribute to the interactive potential between

particles in liquid media appropriate to ceramics. Here, only the van der Waals attractive potential and several methods of achieving repulsive potentials will be briefly outlined so that their effect on particle packing can be coherently discussed.

The van der Waals interparticle potential always describes an attractive force between like particles in a fluid with different dielectric properties. It arise from the correlated, attractive interaction of oscillating, electric dipoles associated with atoms and molecules. In the absence of any repulsive potential, the van der Waals potential produces very strong, attractive forces at small (< 5 nm) interparticle separations. The magnitude of the van der Waals potential depends on the Hamaker constant, which depends on the high frequency dielectric properties of the particles and their surrounding fluid, the particle diameter and the distance between particles.

When the volume fraction of particles is very small, initially separated particles moving about via Brownian motion, will form small, low density clusters with fractal dimensions when they bump into one another. As the cluster become larger, they sediment and pile on one another to form a continuous, touching network. For particle-liquid systems (slurries) containing volume fractions of practical interest for ceramic processors (>0.1), a connective network of touching particles quickly forms as the vigorously stirred slurry becomes quiescent. Since the particles are in elastic contact, the network is 'strong' i.e., it requires the greatest effort to break apart. It is called a flocced network, schematically illustrated in Fig. 1a. To avoid this strong network, one must develop a repulsive interparticle potential sufficient to counter the attractive van der Waals potential. Although the van der Waals potential is effective in all fluids, common methods of producing repulsive potentials require a liquid medium.

Two methods of producing long-range repulsive potentials and two methods of producing short-range repulsive potentials will be outlined. A net repulsive potential is produced when a long-range repulsive potential is added to the van der Waals potential. As shown in Fig. 1b & c, the dispersed particles form a non-touching, but interactive network. An attractive particle network, which is repulsive at short separation distances (< 5 nm), is produce when a short-range repulsive potential is added to the van der Waals potential; as shown in Fig. 1d, the combined function has a potential well. The particles in this network are attractive, but non-touching. Particles that form this weak, attractive network are call coagulated (or weakly flocced).

One method to produce a long-range, repulsive potential is to produce surfaces with a net charge density which is neutralized by ions of opposite charge that surround the particle. This potential is called an electrical double-layer. Charged oxide surfaces can be produced in water when the -M-OH surface sites react with either H_3O^+ or OH^- ions. By controlling the pH, the net surface charge can be either positive (acidic conditions), neutral, or negative (basic conditions). The pH that produces a neutral surface is called the iso-electric point (iep). The pH required to maximize the surface charge density (either positive or negative) depends on the surface chemistry and its equilibrium with H_3O^+ and OH^-. The surface is neutral at an intermediate pH (iep), where the surface contains a large fraction of neutral -M-OH sites and equal proportions of hydrated, positive sites ($-M-H_2O^+$) and negative ($-M-O^-$) sites. Counterions, ions in the solution with an opposite charge relative to the surface are introduced by ions used to change the pH, ions produced by the slight solubility of the particles, and ions purposely added as a salt.. Counterions attempt to neutralize the surface by forming a diffuse 'cloud' layer around each particle. The 'cloud' layer contains both positive and negative ions, but with a concentration gradient of counterions that decreases from the surface into the liquid. The thickness of this layer, generally called the Debye length, decreases with increasing concentration of counterions. The charged surface and its diffuse cloud of opposite charged counterions is the electrical double layer. Although an easy way to understand this repulsive potential is to simply state that like charged particles repel one another because of electrostatics, the repulsive potential is really due to an osmotic pressure caused by the increased concentration of ions within the diffuse layer when the particles are brought closer together. The Debye length is large when few counterions are present and decreases with increasing counterion concentration. The largest electric double-layer repulsion is achieved for a high surface charge density (or surface potential) and a large Debye length (fewer counterions). The magnitude of the electric double-layer potential can be reduced to zero by either adding salt and/or by changing the pH to the iep to produce a neutral surface.

The DLVO (Derjaguin, Landau, Verwey and Overbeek) theory adds the van der Waals, attractive potential and the repulsive electrical double-layer potential together to produce a combined interparticle potential that can be either repulsive or attractive, depending on the magnitude of the repulsive potential. One form of a combined interactive potential (high surface charge and low salt content) is shown in Fig. 1b. For this condition, as particles approach one another, they encounter a repulsive energy barrier. The particles remain separate and repel one another if the energy barrier is many times their kinetic energy. When particles crowd together at moderate volume fractions, they attempt to 'sit' at positions that minimize their interaction potential, viz., at a separation distance (usually > 10 nm) to form a non-touching, but interactive network schematically shown in Fig. 1b. Since the particles in the network are not touching one another, the system is called a 'dispersed' slurry. Because the electrical double-layer potential is

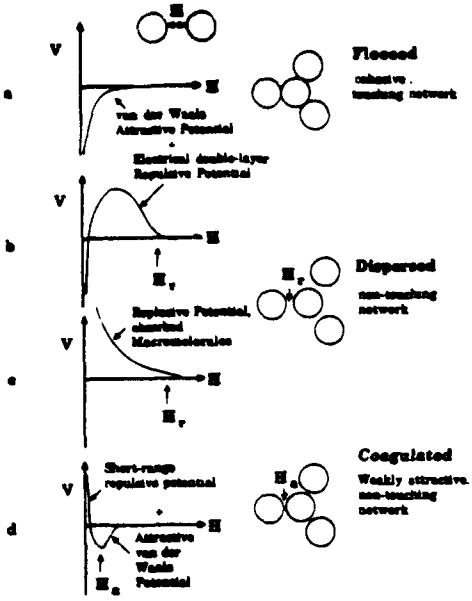

Figure 1 Schematic of different interparticle potentials and their particle networks.

estimated by an exponential function and the van der Waals potentials is a power law function, the latter 'wins' at very small separations (< 0.5 nm). Thus, if the particles are pushed together by a larger force, they will 'fall' into the deep potential well to form a touching network.

If the repulsive contribution to the DLVO potential is reduced (e.g., decreasing the surface charge by changing pH), a condition can be achieved where the repulsive barrier is no longer sufficient to prevent particles from slipping into the deep potential well and produce a strongly cohesive, touching network as described above. Thus, the DLVO theory teaches that although the combined repulsive interaction (magnitude of the repulsive barrier and equilibrium separation distance) can be controlled and optimized (by controlling pH and salt content), particles should always fall into a deep potential well to form a cohesive, flocced network when conditions are much less than optimum. That is, DLVO theory offers no help in understanding how one might control the depth of the attractive well.

A second method to produce a long-range repulsive potential is to either chem- or phys-adsorb macromolecules on the surface of the particles as shown in Fig. 2a. These macromolecules would prefer to be in solution if the surface was not present. The molecules can either be attached to the surface at one end (bi-functional molecules) or attached at different places along its length with loops extending into the liquid. If the molecule is attached with extended loops, the surface of each particle must be fully saturated so that macromolecules from one particle can not link

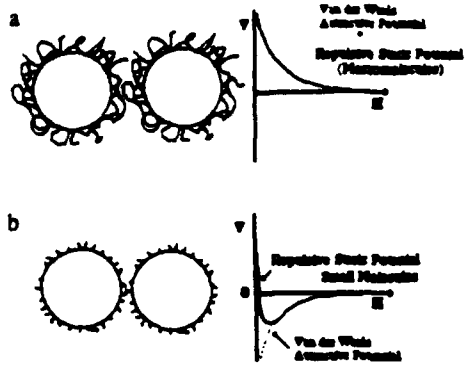

Figure 2 Adsorbed molecules can produce a) long-range repulsive potentials and b) short-range repulsive potentials.

to another to cause flocculation. The repulsive potential due to the molecules becomes finite at approximately twice the molecule (or loop) length, and increases as the molecules (or loops) are pushed together as shown in Fig. 2a. This phenomena is called steric stabilization; it is commonly used to disperse particles in non-polar liquids where the electrical double-layer approach can not be used. If the molecules are weakly attached to the surface (phys-adsorbed), experience suggests that they can pushed away during particle packing. Thus, strongly attached (chem-adsorbed) molecules are desired.

One of the easiest methods of producing a short-range repulsive potential is simply to attach short molecules to the surface as shown in Fig. 2b. When the molecule is < 5nm, the repulsive steric potential only begins when the particles are already attractive due to the van der Waals potential. Although the long- and short-range repulsive steric potential can be estimated with a complex function (Napper, 1983), it is nearly as accurate to estimate the interaction length of this potential by truncating the van der Waals potential at twice the length of the adsorbed molecule (each of the two surfaces have adsorbed molecules) when it is know that the molecule is attached at one end. This is the case when low molecular weight alcohol molecules, dissolved in toluene, are reacted with the -M-OH surface sites of different powders to attach their carbon chain (-M-OH + ROH → -M-OR + H_2O) at ≈ 150 °C (Iler, 1979). Figure 3 illustrates the van der Waals potential for 0.4 μm diameter Si_3N_4 particles in dodecane (Hamaker Constant = 20 x 10^{-20} J), and illustrates how 3 different chem-adsorbed, carbon chains would truncate this potential to produce 3 different potential wells (Kramer and Lange, 1993)

The strength of the 3 attractive Si_3N_4 powders networks produced with each of the 3 chem-adsorbed molecules is inversely proportional to the depth of the potential well, viz., the deeper the well, the stronger the network. The network

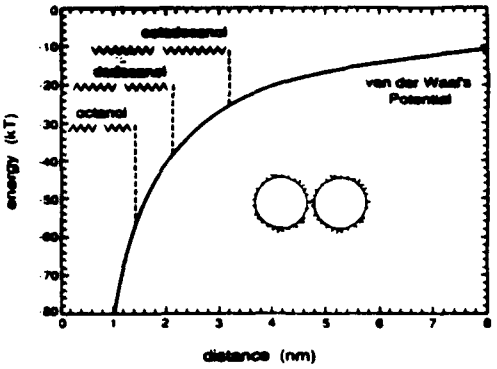

Figure 3 Van der Waals potential for silicon nitride particles (0.4 μm dia., Hamaker Const. = 20 x 10^{-20} J) truncated with three different chem-adsorbed alcohol molecules. (Kramer and Lange, 1993)

strength can be determined in one of three ways: i) The viscosity of attractive particle networks decreases with increasing shear rate, i.e., the network breaks into smaller and smaller units with increasing shear rate. Stronger networks have a higher viscosity at a given shear rate (Velamakanni, et al. 1990) ii) Attractive networks have a yield stress, i.e., they are elastic before they flow. Stronger networks have a higher yield stress. (Chang et al., 1993) iii) Prior to flow, the attractive network has an elastic shear modulus. Stronger networks have a greater shear modulus (Yanez, et al. 1993).

In general, the short-range repulsive potential is commonly called a solvation potential (see Horn, 1990). The term solvation arises from the recognition that molecules within the liquid can lower their free energy by, for one reason or another, either weakly bonding or ordering themselves at the surface. Attempting to remove them by forcing two solvated surfaces together requires work, and thus can give rise to a very short-range, highly repulsive potential. Since the molecules are very small and/or form a very thin layer of ordered molecules, the particles are attractive due to the reasons discussed above, but sit apart within a potential well. The second method of producing a short-range repulsive potential is more difficult to understand because, although it is obvious that short-range repulsive potentials are due to strongly-adsorbed small molecules (or layers of small molecules) that require work to remove, the type of molecule(s) is really unknown for this second case.

Under certain conditions, the basal surface of mica is believed to develop a special solvation potential called the hydration potential. Using the surface force apparatus, Israelachvili and Adams (1978) and Pashley (1981) showed that when mica is placed in water, the potassium ion in its structural surface site can be strongly hydrated by water molecules to produce a layer of 'structured' water molecules. A sufficient concentration of K^+ ions must exist in solution to keep the hydrated K^+ ions in the surface from dissolving into the water. In effect, when a sufficient amount of a K-salt is dissolved in the water, water molecules become bound to the surface through the hydrated potassium ions which, in turn, are bound within their structural surface sites. They also showed that by adding other salts to the water, the hydrated potassium ion can be exchanged with another hydrated cation to change the 'strength' of the hydration potential. When no long-range repulsive potential is present, their surface force measurements show that the net surface potential has a functional form similar to that shown in Fig. 1d, i.e., attractive at separation distances > ≈ 2 nm, and highly repulsive at smaller separations. Because of the structural similarities with mica and a host of other evidence, it is believed that clay surfaces (Olphen, 1977) also develop a hydrated surface layer and, thus, a repulsive hydration potential.

Velamakanni et al. (1990) have shown that a short-range repulsive potential can also be developed on the surfaces of Al_2O_3 particles. This short range, repulsive potential was developed when salt was added to an aqueous Al_2O_3 slurry prepared at a pH known to produce a positive surface charge and, thus, a highly dispersed particle network. When sufficient salt was added to the slurry it was noted that the dispersed network was altered to what superficially appeared as a flocced network predicted by *DLVO theory*. After further experiments, primarily concerned with packing (Velamakanni et al., 1990) and network strength determinations (Chang, et al. in press), it was concluded that the salt did change the dispersed network to an attractive network, but this new, attractive network was much weaker than in the flocced system. That is, unlike a flocced network produced by changing the pH to the iso-electric point, the particles in this new network could easily be rearranged. Different rheological measurements of network strength also showed that the strength of the attractive network could be increased to a maximum value, still below the strength of the flocced network, with a certain salt concentration.

All evidence now shows that when the salt is added, the counterions diminish the magnitude of the repulsive, long-range electrostatic potential as predicted by DLVO theory, but they also produce a short-range, repulsive potential not suggested by classical DLVO theory. The short-range repulsive potential due to added salt has been recently confirmed with sapphire plates in the surface force apparatus by Ducker et al. (1993). The short-range interparticle potential is currently believed to be due to a hydrated layer of counterions similar to that found for mica surfaces (Israelachvili and Adams, 1978, and Pashley, 1981), and for clay surfaces (van Olphen, 1977). Chang et al. (1993) have recently modeled this behavior summing the functions for the electrical double-layer potential (V_{LR}), the van der Waals potential (V_A) and an exponential function used to describe the short-range potential

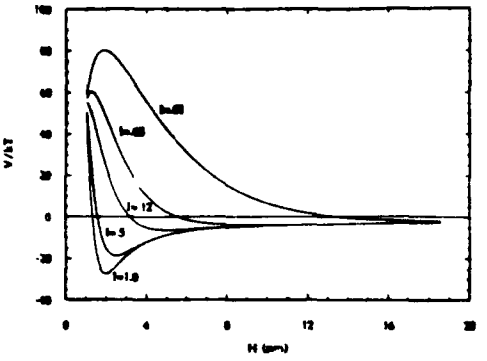

Figure 4 Sum of van der Waals (HC = 4.9 x 10^{-20} J, 0.25 μm dia.), electrical double-layer (V_z = 40 mV), and exponential, short-range repulsive potentials (see text) for different ionic (I, molar, NH_4Cl) strengths. (Chang et al. to be pub)

(V_{SR}) for Al_2O_3 particles with a radius of 0.125 μm, a surface potential of 40 mV, and a Hamaker constant of 4.9 x 10^{-20} J:

$$V = V_{LR} + V_A + V_{SR}. \quad (1)$$

The short-range potential was described by

$$V_{SR} = C \exp\left(-\frac{H}{B}\right), \quad (2)$$

where H is the separation distance between surfaces of the particles, the pre-exponential factor C represents how strongly the molecules (hydrated counterions) are bonded to the surface, and B described the range of the interaction. Based on experimental determinations of the lowest concentration of salt needed to first form an attractive network (known as the critical coagulation concentration (CCC), e.g., for NH_4Cl, CCC = 0.12 molar, Chang, et al., 1993) and the assumption that the network would be attractive when the potential well is < - 5 kT, values of C = 30 kT and B = 5 nm were calculated. Figure 4 illustrates the total potential, V, for different ionic strengths (I), which only affect the magnitude of the electrical double-layer potential (V_{LR}). As shown in Fig. 4, when I > 0.12 molar, the particles are repulsive, and when I ≤ 0.12 molar, the particles are attractive and 'reside' in a potential well that increases in depth from ≈ - 5 kT (I = 0.12 molar) to ≈ - 30 kT (I = 1.0 molar); larger salt concentrations do not significantly deepen the potentials well. The change in the depth of the well is consistent with the strength of the attractive network for increasing salt concentrations. (Chang et al., 1993) This modeling, combined with rheological properties shows that the salt additions have two effects. First, the added salt produces a short-range repulsive potential for reasons not clearly understood (current thinking suggests that hydrated counterions produce the short-range potential). Second, as predicted by DLVO, the salt decreases the long range repulsive potential, which in turn, causes the potential well to deepen with increasing salt content to a maximum depth of ≈ - 30 kT.

In comparing the two methods of producing a short-range repulsive potential, the salt-added method can be used to change a dispersed slurry (particles repulsive) to a coagulated slurry (non-touching, but attractive particles), and it can be used to control the depth of the potential well, and thus, the strength of the attractive particle network. On the other hand, the first method described above, viz., the chem-adsorption of small molecules, does not start with a dispersed slurry, nor can the potential well be continuously changed (without changing temperature or solvent conditions). That is, in the short-range steric method, only two potentials are added together: the van der Waals and short-range steric potentials, and the depth of the potential well is governed by the length of the chem-adsorbed molecule.

3 PARTICLE PACKING

3. 1 Maximum packing density, ϕ_{max}

Ignoring particle fracture during packing, the maximum packing density is governed by the particle shape (neglected here) and size distribution. The random packing of identical spheres always produces a relative packing density of 0.638 when they are unaffected by interparticle potentials. This particle network does not contain space for another identical sphere. (Scott and Kilgour, 1969; Finney, 1970) Smaller, spherical particles can increase the maximum density by either fitting into interstices formed by the larger spheres (R < 0.15) or replacing the larger spheres (R > 0.15) to form denser (Dodds, 1980) tetrahedral units. Tetrahedral units are the dominate building blocks of the dense, random network (Frost, 1982).

Furnas (1928) described the relative density of binary mixtures, ϕ_{max}^F, by two different regimes for the case where the radius ratio, R, of the small to large spheres → 0. In the first regime, where the volume fraction (relative to total solid volume) f_l of the larger spheres is < f_l^o, the larger spheres replace the matrix formed by the smaller spheres and its void space to produce a relative composite density of:

$$\phi_{max}^F = \frac{\phi_s^o}{1-\left(1-\phi_s^o\right) f_l}, \quad \left[f_l \le f_l^o\right], \quad (3)$$

where ϕ_s^o is the relative density of powder formed with the smaller spheres. f_l^o is the volume fraction where the larger spheres form a dense, randomly packed network within the binary mixture; the maximum relative density for the binary mixture occurs when $f_l = f_l^o$. In the second regime, defined

by $f_l > f_l^o$ the smaller spheres pack within the interstices of the network formed by the random dense packed larger spheres, producing a relative density for the binary mixture of

$$\phi_{max}^o = \frac{\phi_l^o}{f_u}, \quad [f_l > f_l^o], \tag{4}$$

where ϕ_l^o is the maximum relative density of the larger spheres by themselves. It can be shown that

$$f_l^o = \frac{\phi_l^o}{\phi_l^o + \phi_s^o(1-\phi_l^o)}. \tag{5}$$

When the relative density of powders formed with either the matrix spheres or larger spheres is equal to that of random dense packing ($\phi_s^o = \phi^o = 0.64$), the maximum idealized density of the mixture is = 0.87 and occurs at $f_l = f_l^o = 0.735$. The relative packing density of powders formed with three, four or more different spherical powders can be treated in the same manner.

Neglecting for the moment the effect of interparticle potentials, the idealized maximum packing density described by eq (3) and (4) is rarely achieved because, in practice, the size ratio (R) of binary mixtures is > 0. One reason for the discrepancy between ideal and observed maximum packing density is known to be caused by the 'wall effect'. It is well know that the walls of a container reduce the packing density of large, identical spheres from 0.636. The reduction increases with the surface to volume ratio of the container and, for a given container, with the ratio of the particle radius to container radius. Because fractions of particles can not exist between the container wall and the first layer of particles as would be the case if an imaginary plane replaced the wall in a dense packed network, this space contains a greater void volume, per unit volume, relative to all other portions of the powder (Ridgeway and Tarbuck, 1966). Zok et al. (1991) recognized that the 'wall effect' always exists when small particles pack around larger particles. They showed that each larger sphere within a binary mixture increases the relative void volume in proportion to its surface area per unit volume (related to f_l) and the radius ratio, R. In addition to the 'wall effect', Zok et al. (1991) pointed out that contacts between larger spheres will also disrupt the packing of the smaller spheres, and thus increase the relative void volume of the binary mixture. The 'contact effect' was related to the average number of large spheres that contact one another, which is also related to f_l. Although the wall and contact effects are significant, they can only contribute to the less than ideal packing described by Furnas when the particles are sufficiently small to pack around the larger particles, viz., when R < 0.1.

When the R > 0.155, the Furnas concept is invalid because the smaller particles can not pack around networks formed by the larger particles. Instead, the smaller and larger particles form tetrahedra. Dobbs (1980) reasoned that because the relative density of tetrahedra formed with a mixture of large and small particles is larger relative to the tetrahedron formed by 4 identical, large particles, the mixed system will have a higher density relative to the random dense packing of either end-member. Unfortunately, this conceptual idea has not been fully formalized to produce an exact solution.

3.2 Mechanics of particle packing

When the fluid surrounding the particles is a gas (or vacuum), powders contained within a container can be consolidated (made denser) by either uniaxial pressing (die cavity and plunger) or iso-pressing (e.g., rubber bag in pressurized water). In this case the container walls or plunger apply pressure directly to the powder. When the fluid is a liquid, the particles within the slurry can be consolidated via gravity or centrifugal sedimentation, filtration or several other consolidation methods not discussed here (electrophoresis, evaporative drying, etc). Because particles must displace their respective fluids during consolidation, and because the viscosity of liquids is much greater than gases, much longer periods are required to consolidate powders from the slurry state. After consolidation, the powder compact is saturated. The relative density of the particle network in the saturated compact can be determined by simply weighing the compact before and after the liquid is removed (usually by evaporative drying). Knowledge of the solid and liquid density is needed for the relative density calculation. Namely, the volume of the powder is determined by dividing its dry weight by its density, and the volume of the liquid is determined by dividing the differential weight by the density of the liquid.

An applied pressure is not required to consolidate powders made of large particles. When large, identical spheres (e.g., ball bearings, coriander seeds, etc.) are poured into a container with a small surface to volume ratio, they immediately produce a relative density of ≈ 0.60 (termed, loose random packing); the relative density quickly increases to 0.636 after some tapping. On the other hand, when a dry powder, composed of very small, strongly attractive particles is poured into a container, the relative tap densities can be < 0.4. When such a powder is either uniaxial pressed or iso-pressed, its relative density increases with the applied pressure. The shrinkage of the powder compact due to consolidation stops when the pressure is held constant; each incremental increase in pressure produces an incremental shrinkage in the powder compact, and thus an incremental increase in the relative density. As discussed below, the relative density vs applied pressure is a continuous function in which the normal and tangential forces at every particle contact are in static equilibrium with the applied pressure.

Insight into how particles can be arranged to produce a very low tap density is obtained by watching a small volume fraction of dispersed particles, too small to be resolved by the eye, as

they are attracted to one another when the interparticle potential is suddenly made attractive, e.g., by changing the pH to the isoelectric point by stirring in acid or base. As the stirred system becomes quiescent, one observes small, wispy 'clouds' of particles that grow larger and begin to settle. Scattering experiments show (Schaefer et al, 1984) that the agglomerates have a fractal geometry, i.e., their density decreases with increasing distance from their center of gyration. Larger agglomerates are observed to fall onto and collect the smaller, slower moving agglomerates during sedimentation. At the top of the test tube, the initially opaque slurry becomes clear, whereas the opacity at the bottom increases as the agglomerates pile up to form a continuous network. Because of their fractal nature in suspension, it might be suspected that the continuous particle network, formed by the packed agglomerates is also fractal at some dimension between the particle size and the agglomerate size. Since the volume fraction of particles that form the initial, continuous network is initially much lower than .t the percolation threshold, $\phi_p \approx 0.16$, (Zallen, 1983), it must be concluded that the network is not a random distribution, but it must have some fractal character due to its fractal building blocks, i.e., the agglomerates. That is, a random distribution of particles at or below its percolation level could not be self supporting. Thus, low tap densities in dry powders and low network densities formed by the sedimentation of agglomerates must be due to the fewer connective particles between agglomerates, relative to higher connectivity within the agglomerates.

As the test tube is allowed to sit for hours, days, weeks, etc., it is observed that the height of the sediment decreases, but given time, its height becomes constant. When the tube is centrifuged, the height of the sediment continuously decreases, but after a given period, becomes constant. Collimated, gamma ray absorption measurements show that the packing density continuously increases from the top of the sediment to the bottom of the tube (Schilling, 1988). The mass of particles above a given height exerts a known pressure on the particle network below. Density determinations vs the applied network pressure results in a continuous function that will be discussed below.

Pressure filtration is another method of consolidating particles in a slurry. In this method the slurry is poured into a cylindrical die cavity containing a filter on one end that can pass the liquid, but not the particles. When pressure is exerted on the slurry via either a pressurized gas or a plunger, a consolidated layer of particles builds on the filter as liquid passes through the particle layer and the filter. After some period (Tiller and Tsai, 1986; Lange and Miller, 1987) the slurry forms a fully consolidated layer (as much liquid as possible has passed through the filter) and the consolidated layer, which now completely supports the applied pressure, has a uniform packing density. As in the other consolidation methods, the relative density of the saturated powder compact is a continuous function of the applied pressure.

All of the experimental methods described above show that a) the particle network can be in static equilibrium with an applied pressure, and b) the relative density (ϕ) of the particle network increases with the applied pressure until $\phi = \phi_{max}$.

Figure 5 illustrates photoelastic discs placed in biaxial compression a) before and b) after an incremental increase in stress that caused particle

Figure 5 Photoelastic discs under bi-axial compression showing isochromatic fringes due to contact stresses a) before and b) after incremental increase in stress. (Kuhn et al. 1991)

rearrangement and thus, an increase in the 2-D packing density (Kuhn et al., 1991). The isochromatic fringes illustrate the Hertzian contact stresses at positions where touching particles are compressed by the remote, applied stress. The greater the density of fringes within a particle, the greater the stress within the particle. It should be noted that: i) not all particles support the same stress. In fact, some particles, although touching others, do not support any of the applied stress, while others are highly stressed. ii) For any particle, the force (or stress) at every contact is not identical. iii) the contact positions are not symmetrical around any particle, and the stress at each contact is not identical, yet the network of particles is in static equilibrium with the applied pressure. Namely, the vector sum of all forces at each particle is zero. iv) At most contacts the fringe pattern is not perfectly symmetrical across the contact; i.e., both normal and shear stresses exist at most contacts. v) After rearrangement (Fig. 5 b) the density of isochromatic fringes is reduced in each particle despite the incrementally greater applied stress.

The photoelastic observations support computer simulations (Cundall and Strack, 1979) which show that: i) that many interpenetrating, percolative particle networks exist within a powder compact that collectively support the applied stress. ii) A distribution of normal forces exist between particle pairs which spans between zero (a significant fraction of particles do not support any applied stress) and a value much larger than an average value.

Based on the fact that the contact positions and their stresses are not symmetrical and on direct observations that 'keystone' particles are 'pushed' into a vacant region as the applied pressure is incrementally increased, Kuhn et al. (1991) proposed that the powder increases its relative density via a particle rearrangement phenomenon that involved an instability phenomenon designated 'snap-through-buckle' illustrated in Fig 6a. It was reasoned that although the percolative network of contact forces can be in static equilibrium during an applied compressive stress, some particles, located adjacent to vacancies, would undergo incremental displacement upon incremental stressing until their geometrical arrangement suddenly became unstable. This phenomena would be analogous to the instability of the keystone in the Roman arch due to an overload which not only leads to the catastrophic collapse of the arch, but also the catastrophic collapse (densification) of the cathedral. Each catastrophic event results in a new network of connective particles and a new network of percolating forces in static equilibrium with a slightly larger pressure.

Figure 6 describes the sequential analytical steps used to determine critical force for the 'snap-through-buckle' event for the 2 dimensional example where the vacant position, which can just accommodate one unit sphere, is surrounded by 6 identical spheres. The pressurized, cylindrical shell (Fig. 6b) of powder confining the 6 touching particles has the elastic properties associated with Hertzian elasticity ($\sigma \propto \varepsilon^{3/2}$) described by Walton (1987). An extra force, F, directed towards the vacancy, is applied to one of the 6 particles. This 'extra' force represents the differential force above an average value for which all other particles within the ring are subjected. The problem consists of determining the relation between the 'extra' force and the change in the particle configuration described, e.g., through the angle (Φ) between adjacent particles. Figure 6c describes the incremental displacement of the particle with increasing Φ. Figure 6d shows the calculated F vs Φ plot, illustrating that the system is stable for $60° \leq \Phi \leq 70.5°$, but unstable when $\Phi > 70.5°$, where F exceeds its maximum (and critical) value. It can be shown that the critical value of F decreases with

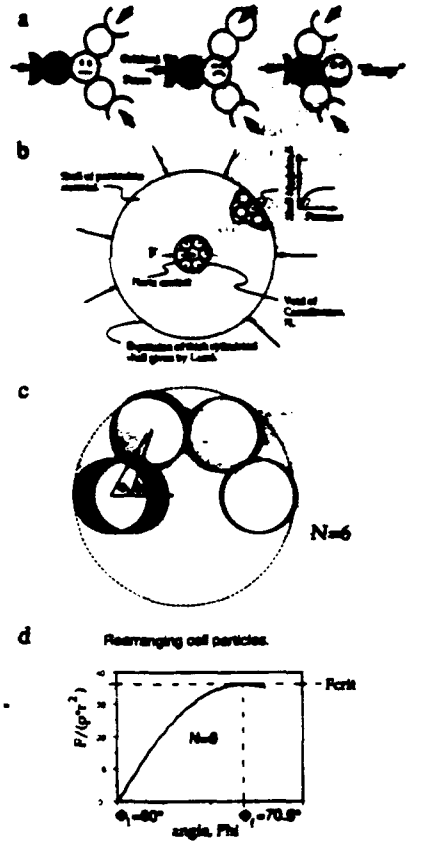

Figure 6 Rearrangement of particles via the 'snap-through-buckle' mechanism. a) pictorial, b) the Lamé shell of powder, c) progressive displacement of particles with increasing force, d) force vs angle showing critical phenomenon. (Kuhn et al, 1991)

increasing pressure applied to the powder 'shell'. The analysis reported by Kuhn et al. (1991) assumed frictionless particles. It can be imagined that higher critical values of F are required when the coefficient of friction is finite.

With an incremental increase in the applied pressure, the original equilibrium network can be suddenly disrupted by catastrophic events described as 'snap-through-buckle'. These events lead to particle rearrangement, the formation of a new particle network in equilibrium with the incrementally increased pressure and an incremental increase in relative density. Although the rearrangement event leading to the increase in density can be described, the relation describing the equilibrium relative density vs the applied pressure has yet to be derived from first principals. The two common empirical relations describing the experimental relative density vs pressure data are power law and logarithmic functions, viz.,

$$\phi = C P^{m} \quad (m < 1, \text{and } \phi \le \phi_{max}) \quad (6)$$

and

$$\phi = A \ln(P) + B \quad (\phi \le \phi_{max}). \quad (7)$$

In a slightly different form, the power law relation was used by Buscal and White (1987) to 'back calculate' the density gradient within a centrifuged compact with knowledge of the pressure gradient. The logarithmic function is the dominant function used by processing engineers; many other empirical relations exist (Benbow, 1983). Figure 5 schematically illustrates the logarithmic function with 3 different powders, each related to different friction coefficients between particles via interparticle potentials discussed below. Each describe the range of pressure where the relative density is pressure sensitive.

Particle rearrangement leading to densification via the 'snap-through-buckle' mechanism dramatically changes the distribution contact stresses because it dramatically changes the particle distribution, and thus the percolative networks that transmit the applied pressure. Another way to dramatically change the percolative network is to simply unload the stressed network. During unloading, relatively large strains, stored primarily at the contact positions and described by Hertz (Timoshenko and Goodier, 1951) are relieved, causing particle rearrangement without significant densification. Upon reloading, a new connective, pressure transmitting network forms. This new network has, statistically, a greater probability of undergoing rearrangement during reloading via the 'snap-through-buckle' mechanism relative to the network that existed prior to unloading. For this reason, the Hertzian elastic behavior expected for a powder compact ($\sigma \propto \epsilon^{3/2}$) can not be observed during loading a previously consolidated powder compact until its relative density has reached its maximum value ($\phi = \phi_{max}$). Instead, during reloading, one observes an inflection in the load vs deflection curve at relatively low stresses (Lange and Miller, 1987). Each cycle increases the inflection point to higher loads. Prior to the inflection, the data suggests Hertzian behavior. After each cycle, one observed an incremental, non-recoverable strain, viz., each loading and unloading cycle increases the relative density. Hertzian behavior can only be observed during unloading (Lange and Miller, 1987). The effect of cyclic loading on the relative density of an alumina powder, agglomerated by spray drying has recently been reported by Kim and Son (1992). Their data, plotted in a linear-log format in Fig. 8, illustrates that cyclic compaction can significantly increase the relative density.

Figure 5 also shows that the average contact stress decreases after rearrangement although the applied stress is incrementally larger. This is to be expected because an increase in relative density means that a more percolative network now supports the slightly higher pressure, and thus, the average force between contacts is expected to be

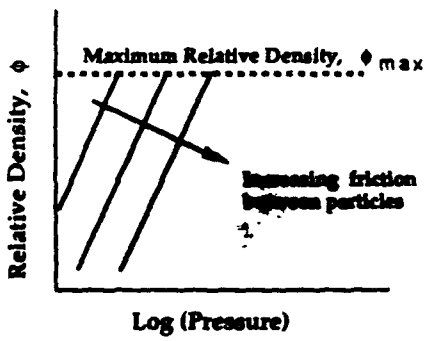

Figure 7 Schematic of linear-log function describing pressure sensitivity of particle packing.

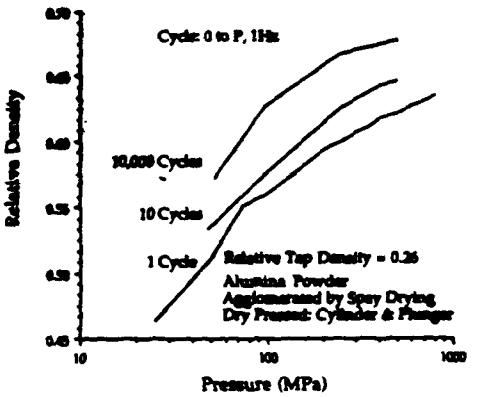

Figure 8 Effect of cyclic stressing on packing density of dry alumina powder. (Kim and Son, 1992).

smaller. Assuming that each contact force is identical to all others, Helle et al (1985) used the principle of virtual work to determine the average contact force between identical spheres (radius R), subjected to a remote pressure (P) as a function of their average coordination number (Z, average number of neighboring spheres touching any other sphere), and volume fraction (ϕ, relative density). By equating the incremental work done on the particle by the contact forces to the incremental work done by the applied pressure on a unit network of radius R_o ($= R\,\phi^{-1/3}$) surrounding the particle

$$Z\,F\,dR = P\left[4\pi R_o^2\right] dR_o , \qquad (8)$$

the average force per contact can be determined as

$$F = \frac{4\pi P R^2}{Z\phi} . \qquad (9)$$

Knowing that the average coordination number of any identical particle is given by (Zok et al., 1991)

$$Z = \frac{\phi}{\phi_{max}} Z_{max} , \qquad (10)$$

then the average contact force can be related to P, R and ϕ as

$$F = \frac{4\pi P R^2 \phi_{max}}{\phi^2 Z_{max}} , \qquad (11)$$

where ϕ_{max} is the maximum packing density (ϕ_{max} = 0.636 for identical spheres) and Z_{max} is the average coordination number when the particles are packed to their maximum density (for identical spheres Z_{max} is between 7 and 8, when ϕ_{max} = 0.636). Eq (11) shows that the average contact force will dramatically decrease with an increase in relative density as shown in Fig. 5; also, the average contact force will be much larger, at the same pressure and relative density, when the particle size is smaller.

It might be noted that the average coordination number of identical spheres touching the container wall is $Z_{wall} = 0.75\,Z_{max}$, (Bouvard and Lange, 1992) and thus, the average force between these particles is 4/3 greater than between interior particles. A density gradient should exist from the wall to the interior because of the greater contact forces between particles near the wall.

4 EFFECT OF INTERPARTICLE POTENTIALS

As schematically illustrated in Fig. 9, long-range repulsive potentials generally produce high, and relatively pressure insensitive packing densities when the applied pressure is > 0.5 MPa. (Lange and Miller, 1987, Fennelly and Reed, 1972) The pressure sensitivity of dispersed systems is generally only observed at very low network pressures observed, e.g. during sedimentation or low 'g' centrifugation experiments (Chang et al, 1993). On the other hand, attractive interparticle potentials due to the van der Waals potential alone, whether the powder is dry or in the slurry state, alway produce a much lower, very pressure sensitive relative density. Although the data is very recent, Fig. 9 also suggests that short-range repulsive potentials can impart pressure insensitivity and high packing densities to powders.

Figure 10 summarizes recent data of Chang et al. (1993) where dispersed (pH 4), flocced (iep = pH 9) and coagulated (pH 4 + NH_4Cl) slurries were consolidated by centrifugation. At very low centrifuge speeds, the packing density was determined by a calibrated, x-ray absorption method; at high speeds, any density gradients were ignored, and the reported density is an average value. Figure 4 shows the estimated interparticle potentials for these slurries. At network pressures < 0.5 MPa, the packing density of both dispersed and

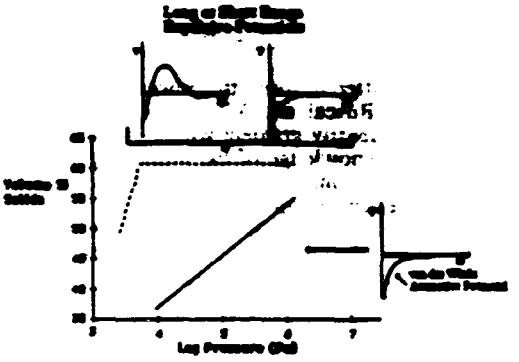

Figure 9 Relative density vs pressure observed for different interparticle potentials.

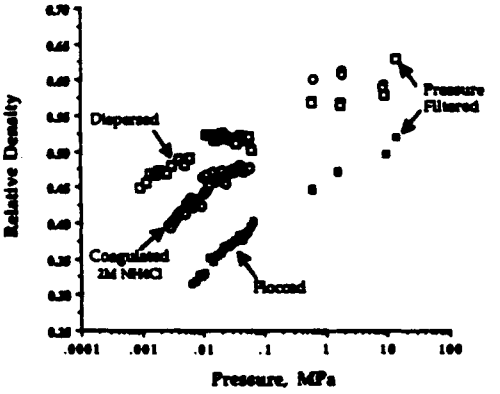

Figure 10 Centrifugation packing of Al_2O_3 powder vs interparticle potential. (Chang, et al, 1993)

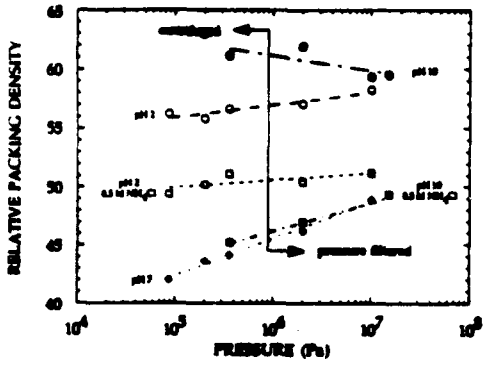

Figure 11 Packing of Si_3N_4 powder vs interparticle potential. (Luther et al, 1993)

coagulated particles are pressure sensitive, with the density of the bodies produced with the coagulated slurries lower than those produced with the dispersed slurry. As observed by others for this powder (Lange and Miller, 1987; Fennelly and Reed, 1972), the flocced slurry is very pressure sensitive and their relative densities are significantly lower. Similar, but much less extensive data was reported by Velamakanni et al. (1990), with the discovery of the short-range repulsive potential for salt added slurries. Chang et al. (1991) also showed that the coagulated slurries are sufficiently strong to prevent mass segregation during centrifugation of two-phase ($Al_2O_3 + ZrO_2$) slurries, but sufficiently weak to produce a relative density that is either near or identical to the maximum relative density. This observation is significant for the ceramic processor who can now form engineering components via centrifugation without mass segregation and achieve a uniform packing density.

As shown in Fig. 11, attempts by Luther et al. (1993) to produce a short-range repulsive potential by the method of adding salt to aqueous, dispersed Si_3N_4 slurries, have not been as successful. Although rheological data show that the added salt (>CCC) does produce a weaker particle network relative to the van der Waals potential alone, the packing densities are intermediate to those achieved with dispersed and flocced slurries, and they never achieve the maximum packing density, ϕ_{max}, over the pressure range investigated. In addition, although the Al_2O_3 bodies formed with the coagulated (salt added) slurries are plastic after consolidation (desired for many reasons, e.g., new shape forming technologies), bodies formed from dispersed and coagulated Si_3N_4 slurries are brittle, viz., they fracture before they undergo plastic deformation. The Hamaker constant, and thus magnitude of the van der Waals potential, of Si_3N_4 is 4 to 5 times greater than that fof Al_2O_3 for a comparable particle size. This and other differences can only be correlated to particle packing and rheology once the phenomena responsible for the

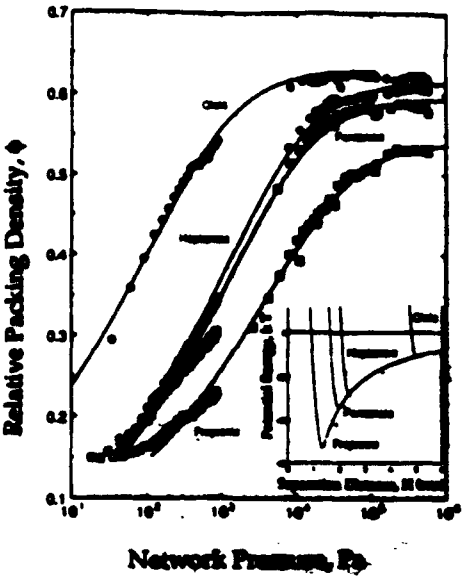

Figure 12 Packing of Al_2O_3 powder with phys-adsorbed fatty acids. Insert shows truncated van der Waals potential due to adsorbed surfactants of different length. (Bergström et al., 1992)

short-range repulsive potential in salt added systems is better known.

Although short-range repulsive potentials induced in dispersed slurries with added salt may not be currently effective in Si_3N_4 slurries, Kramer and Lange (1993) have recently shown that chem-absorbed hydro-carbon chains bound by the surface hydroxide/alcohol reaction discussed above is very effective for organic liquid slurries, when the chain length is > 1 nm, but < 2 nm. Rheology measurements show that the alkylated powders are weakly attractive. Although extensive consolidation experiments have not been performed for these different alkylated powders, the maximum packing for this powder (ϕ_{max} = 0.60) is achieved at modest pressures during pressure filtration, whereas powders which are not alkylated, only pack to a relative density of 0.52. In addition, although phys-adsorbed alcohols also produce weakly attractive networks in the slurry state (= 10 times the amount of alcohol is required relative to the chem-adsorbed slurries), the weakly bonded, phys-adsorbed molecules are pushed away during particle packing as demonstrated by the packing densities intermediate to ϕ_{max} and that of the flocced. These consolidated bodies are also brittle instead of plastic.

Data reported by Bergström et al. (1992) and shown in Fig. 12 is the only other systematic study of the effect of short-range repulsive potentials on particle packing known to the author. In this case, the Al_2O_3 slurries were formulated with phys-

adsorbed fatty acids of different molecular weight. Less pressure sensitivity and higher packing densities were achieved for the organic slurry with the largest phys-adsorbed molecule, but in all other cases, the maximum packing density was never achieved. Instead, at higher pressures, the relative density plateaus at a relative density that decreased with the molecular weight (or molecule length) of the fatty acid. This observation suggests that the phys-adsorbed molecules were pushed away from the surface when the force between particles exceeded the strength of the phys-adsorbed, molecular bond.

Yen and Chaki (1992) have recently reported packing simulations with an algorithm that includes the van der Waals potential and/or the coefficient of friction. Their simulation starts with a low density ($\phi = 0.36$) distribution of identical, iron spheres that pack under the force of gravity alone; they include Hertzian contact forces, frictional forces and the van der Waals potential. Table I illustrates that without friction, they simulate random dense packing ($\phi_{max} = 0.633$) and the attractive van der Waals potential has a major effect on particle packing.

Table 1 Simulation Results, Yen and Chaki (1992)

Diameter (Iron Spheres)	50 μm	100 μm
No Friction	---	0.633
With Friction*, $\mu = 0.3$	---	0.578
With van der Waals and friction, $\mu = 0.3$	0.420	0.528
$\mu = 0.7$	---	0.505

* Hamaker Constant = 21.1×10^{-20} J

Finally, it should be noted that when the particles are very small, e.g., diameters < 100 nm, long-range repulsive potentials can limit their maximum relative density because the particles appear larger than their true volume. That is, when their equilibrium separation distance (H_e in Fig. 1c) is a significant fraction of their radius, their effective volume will control their maximum packing density. For this reason, short-range repulsive potentials, where equilibrium separation distances are < 5 nm, are important in achieving high packing densities.

5 SUMMARY

It is obvious that touching particles, in elastic contact, i.e., particles affected by the van der Waals potential alone, will resist rearrangement due to sliding friction. Using the surface force apparatus in a sliding mode, Homola et al. (1989) have shown that the short-range, repulsive hydration potential on mica surfaces produces a low coefficient of friction. They also showed that when the mica surfaces are in contact due to the van der Waals potential alone, the surface fractures during sliding. It is also obvious that, in some way, both short- and long-range repulsive potentials make the particles slippery. In both cases, the particles are not touching, but held apart by some separation distance, even though the contact positions can undergo some elastic deformation. Holding surfaces apart during sliding, so that fewer surface asperities rub one another, is a design feature of air bearings. Although the effect of the repulsive potentials is a theoretical problem for the tribologist, it is well known to all of us that the apparent 'lubrication' felt between two south pole magnets as they are pushed together is not due to the air, but caused by the repulsive potential itself. Like-wise, the ease in which instabilities can occur between particles that repel one another at either short- or long-ranges, must be due to the repulsive force field. Experimental data also suggests that the phenomena that gives rise to the repulsive force can also be pushed away as the particles are pushed into contact. Namely, even if a potential barrier exists between particles as is the case when the repulsive potential is due to an elastic double-layer (Fig. 1 b), if the compressive force is large enough, the particles can be pushed 'over the barrier' and into elastic contact. Like-wise, molecules used to develop either short- or long-range potentials can be pushed away by the compressive force. Boldizzar suggests that this can occur for weakly bonded (phys-adsorbed) molecules, relative to strongly (chem-adsorbed) molecules. Needless to say, this subject is rich and ripe for research, and easily simulated with known interparticle potentials.

Interparticle potentials also govern the rheological properties of the slurry and saturated, consolidated body. The yield stress is one of these important properties. If the yield stress is not large enough, then after forming, the body deforms due to its weight. If the yield stress is too large, the body is brittle, i.e., it fractures before it flows. Short-range potentials impart desirable plastic behavior--a subject of another review.

ACKNOWLEDGMENTS

The Office of Naval Research supported this work under contract #N00014-90-J-1441.

REFERENCES

Benbow, J. J. 1983. "Mechanisms of Compaction," p 167 in Enlargement and Compaction of Particulate Solids. Ed. by Stanley-Wood, Butter worth, Boston, MA.

Bergström, L.,Schilling, C. H., and Aksay, I. A., 1992. J. Am. Ceram. Soc. 75:3305-14.

Bouvard, D. and Lange, F. F., 1992. Phys. Rev. A 45: 5690-3.

Buscall, R. and White, L.R., 1987. J. Chem. Soc. , Faraday Trans. 1, 83: 873-91.

Chang, J.C., Velamakanni ,B.V., Lange, F.F. and Pearson, D.S. 1991. J. Am. Ceram. Soc., 74:2201-204.
Chang, J. C., Lange, F.F., Pearson, D.S., 1993. in press. J. Am. Ceram. Soc.
Chang, J.C. Lange, F.F. Pearson, D.S. and Pollinger J. P. 1993. in press. J. Am. Ceram. Soc.
Cundall, P. A. and Strack, O.D.L. 1977, NSF Rept for Grant ENG76-20711, Dept. Civil and Mineral Eng., University of Minnesota, 1979.
Dodds, J. A., 1980. J. Coll. Interface Sci., 77:317-27.
Fennelly, T. J. and Reed, J. S., 1972. J. Am. Ceram. Soc. 55[5] 264-8.
Finney, J. L., 1970 Proc. Royal Soc. (London) A 319:479.
Frost, H. J. 1982. Acta. Met. 30: 899-904.
Furnas, C. C., Oct. 1928. U.S. Dept. of Commerce, Bureau of Mines, R. I. 2894.
Helle, A.S., Easterling K.E. and Ashby, M.F., 1985. Acta Metall. 33:2163.
Homola, A. M.,Israelachvili, J. N., Gee, M. L. and McGuiggan, P. M. J. 1989. Tribology, 111:675.
Horn, R. G., 1990. J. Am. Ceram. Soc. 73:1117-1135
Iler, R.K., 1979. The Chemistry of Silica, Wiley-Interscience, New York.
Israelachvili, J. N. and Adams, G. E., 1978. J. Chem. Soc. Faraday Trans. 1 74:975-1001.
Kim, K. T. and Son, G., 1992. J. Am. Ceram. Soc. 75:3157-59.
Kramer, T. and Lange, F. F., 1993, to be published
Kuhn, Liisa T., McMeeking, R. M. and Lange, F. F., 1991. J. Am. Ceram. Soc. 74: 682-5.
Lange, F. F. and. Miller, K. T., 1987. Am. Cer. Soc. Bull. 66:1498.
Luther, E. P. Kramer, T, M.. Lange , F. F and Pearson, D. S., 1993. sent to J. Am. Ceram. Soc.
Napper, D. H., 1983. Polymeric Stabilization of Colloidal Dispersions, Academic Press, London.
Olphen, H. van, 1977. An Introduction to Clay Colloid Chemistry, p 99 John Wiley, NY.
Pashley, R. M. 1981. J. Colloid Interface Sci, 83:531-46.
Ridgeway, K. and Tarbuck, K. J. 1966. J. Pharm. Pharmac., 18, Suppl., 168S-175S.
Davis, K. E., Russel, W. B., and Glantschnig, W. J., 1991. Chem. Soc. Faraday Trans., 87:411.
Schaefer, D. W., Martin, J. E.. Witzuis, P. and Cannell, D. J., 1984. Phys. Rev. Lett., 52:2371.
Schilling, C. H. and Aksay, I. A., 1988, Ceram. Trans. vol 1, Ceramic Powder Sci. II, B, pp 800-8, Ed. by G. L. Messing, E. R. Fuller, and H. Hausner, Am. Ceram. Soc.,Westerville, Ohio.
Scott, G. D. and Kilgour, D. M., 1969. J. Phys. D, Appl. Phys 2: 863.
Tiller, F. M., and Tsai, C. D., 1986. J. Am. Ceram. Soc., 69:882-7.
Timoshenko, S. and Goodier, J. N., 1951. Theory of Elasticity, pp 409-14, McGraw-Hill, NY.
Velamakanni, B.V., Chang, J. C., Lange, F.F., Pearson, D.S., 1990. Langmuir 6:1323-5.
Walton, K., 1987. J. Mech. Phys. Solids. 35: 213.
Yanez, J., Pearson, D. S., and Lange, F. F., 1993. to be published.
Yen, K. Z. Y. and Chaki, T. K., 1992. J. Appl. Phys., 71:3164-73.
Zallen, R. 1983. Physics of Amorphous Solids, Chapt. 4, "The Percolation Model" John Wiley and Sons.
Zok, F., Lange, F. F., and Porter, J. R., 1991. J. Am. Ceram. Soc. 74: 1880-5.

MATERIALS

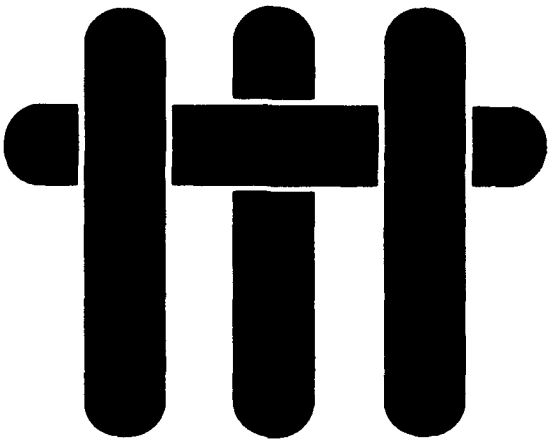

Technical Report Number 9

Compaction of Al_2O_3 Slurries by Centrifugation: The Effect of Interparticle Potentials

Jeanne C. Chang, F. F. Lange, Dale S. Pearson and John P. Pollinger*

* Garrett Ceramic Components, Allied-Signal Aerospace Company
Torrance, CA 90509

Office of Naval Research

Grant No. N00014-90-J-1441

Fred F. Lange
Principal Investigator

Materials Department
University of California
Santa Barbara, CA 93106

Compaction of Al_2O_3 Slurries by Centrifugation: The Effect of Interparticle Potentials

Jeanne C. Chang, Fred F. Lange*, Dale S. Pearson, and John P. Pollinger†*

Materials Department, College of Engineering, University of California
Santa Barbara, California 93106
†Garrett Ceramic Components, Allied-Signal Aerospace Company,
19800 Van Ness Avenue, Torrance, CA 90509

The relation between relative packing density and applied network pressure has been studied by centrifugation for aqueous slurries of Al_2O_3 powder prepared with different interparticle potentials. Attractive interparticle potentials were obtained by either changing the pH to the isoelectric point or adding an electrolyte in excess of that required to produce coagulation. A range centrifugal speeds produced consolidation pressures between 10^{-3} MPa and 10 MPa. At lower centrifugal speeds, the packing density gradient was determined with an X-ray absorption technique. It was determined that a maximum packing density (0.62 ± 0.02) was achieved for both dispersed and coagulated slurries at network pressures in excess of 0.5 MPa. At lower network pressures, the packing density of these slurries was pressure dependent. Significantly, slurries flocculated by adjusting the pH to the isoelectric point never reached high packing densities at the largest pressure. Our findings are discussed in terms of the relationship between the consolidation stress required to achieve a given particle packing density and the expected interparticle potentials in the slurries that were studied.

*Member of the American Ceramic Society

Introduction

The properties of ceramic bodies prepared from colloidal slurries can be improved by controlling the interparticle potential. Lange and Miller[1] and Velamakanni and Lange[2] have found that the highest packing fractions are obtained when the starting slurry is fully dispersed, i.e. when the pH is adjusted so that the

interparticle force is dominated by long-range repulsive potentials. Also, bodies consolidated from these dispersed slurries are less prone to cracking because they can more easily relieve internal stresses during the strain recovery that occurs when the pressure is released.[3] Long-range repulsive potentials in the dispersed slurry are responsible for both the ease of particle rearrangement during packing and the body's 'plastic' behavior that helps relieve residual strain after consolidation. In contrast, the highly attractive interparticle potentials in slurries flocculated at the isoelectric point produce a very cohesive particle network which hinders particle rearrangement during packing. They also produce a relatively 'elastic' body after consolidation that dissipates stored strain energy by cracking. However, there are disadvantages associated with compacts made from dispersed slurries that often outweigh the advantages. For example, slurries containing two or more components often are inhomogeneous after either pressure filtration[2] or centrifugation[4] because of mass segregation and phase separation. In addition, the absence of attractive interactions in bodies consolidated from dispersed slurries allows them to flow and lose their shape after being removed from the die cavity.

However, it has been recently discovered[5] that attractive alumina particle networks produced by the addition of salt can achieve high packing densities without particle segregation[4] and have plastic-like rheological properties.[6] These slurries, termed coagulated, are prepared by adding a high concentration of electrolyte to a slurry that initially had a highly repulsive potential at a pH weli below the isoelectric point.

Rheological measurements of the yield stress and viscosity of these Al_2O_3 slurries[7] show that a network exists whenever the electrolyte concentration is above the critical coagulation concentration (c.c.c.) and that the network strength increases with the amount of electrolyte. However, there is a limiting concentration of electrolyte beyond which the network strength does not increase any further.

Significantly, this limiting value of yield stress is an order of magnitude less than that of a flocculated slurry prepared at the same volume fraction. Because the particle network in coagulated slurries is much weaker relative to flocculated slurries, particle rearrangement is expected to be easier and lead to higher parking densities. In addition, it should be possible to eliminate mass segregation effects in a coagulated slurry since the viscosity of the slurry is high. A possible explanation for these rheological properties is that a short-range repulsive potential, perhaps produced by hydration layers, is present in the coagulated systems that allows particles to be attractive, but non-touching.[8]

Colloidal slurries can be consolidated into dense compacts by pressure filtration, by capillary pressure (slip-casting), and by sedimentation as in a centrifuge.[9-17] The latter technique has been studied theoretically and experimentally for the case of hard sphere dispersions and flocculated networks. Buscall and White[15] and Auzerias, Jackson, and Russel[20] have presented models for relating the volume fraction to the pressure gradients in the centrifuge tube. Schilling and Aksay[21] demonstrated how gamma-ray attenuation measurements could be used to study packing evolution of alumina sediments.

In this study we show how a systematic variation in network strength effects the particle packing density in alumina slurries undergoing centrifugation. Results are presented for dispersed slurries, coagulated slurries containing different amounts of electrolyte, and flocced slurries at the isoelectric point. Particle packing gradients are obtained with a simple x-ray and image analysis technique and pressure gradients are calculated with the usual equations for flocculated slurries.[15,20] We find that our results on these materials are consistent with previous[7] rheological measurements of the shear yield stress and viscosity and that they confirm the advantages of using slurries coagulated with an electrolyte.

2. Experimental Procedure

As described elsewhere[7], aqueous slurries containing 0.20 volume fraction α-Al_2O_3[a] were prepared at pH 4 and 9. Slurries at pH 4 were prepared without added salt and with NH_4Cl at concentrations of 0.25, 0.50, 1.0, 1.5, and 2.0 M. Slurries at pH 4 without added salt are dispersed whereas those that contain salt are beyond the critical coagulation concentration. These latter slurries are called coagulated whereas those at pH 9 are called flocced.

The slurries were centrifuged in tubes (27 mm in diameter and 115 mm in length) with conical bottoms. In some cases the conical bottom was filled with an epoxy resin. Two centrifuges [b,c] were used in order to cover a range of centrifugal pressures. The centrifuge that produced low pressures [b] (< 1 MPa) was equipped with a swinging bucket rotor, while the one that produced higher pressures [c] was equipped with a fixed angle rotor.

Prior to other experiments, the time required for the particle networks to pack to a relative density that was in static equilibrium with the applied centrifugal speed was determined by monitoring the height of the consolidated body within the tube as a function of time. Figure 1 illustrates representative results of these experiments. Our typical procedure was to prepare a slurry, add it to a previously weighed centrifuge tube, and then weigh the tube again before centrifuging. In all but two cases, the supernatants were poured off after spinning, and the tubes were reweighed. After being placed in a drying oven at 60°C for several days, the tubes and compacts were weighed again. Assuming only water evaporated during drying, the average, relative packing fraction of the saturated compacts was calculated using known densities for Al_2O_3 and water. Any NH_4Cl not poured off in the supernatant

---

[a] Sumitomo, Japan, AKP-15
[b] IEC Size 2 Model V
[c] Dupont Sorvall RC-5B with rotor SS-34

of the coagulated slurries was accounted for in the determination of relative packing fractions.

The gradient in relative packing fraction was determined for saturated compacts formed at the two lowest centrifuge speeds. These specimens were allowed to spin for more than 12 h. Their final packing fraction gradient was measured using x-ray absorption analysis[d] and an image analyzer[e] without removing the supernatant. Since x-rays are absorbed in proportion to the density of objects on the same thickness, the transmitted x-ray signal (gray scale reading) is proportional to the relative density of the consolidated powder. The x-ray instrument allowed the specimens to be analyzed in their vertical position, such that the loosely packed portions of each compact was not disturbed. The gradient in packing fraction was related to x-ray gray scales obtained from identical tubes containing 0.10, 0.20, 0.30, and 0.40 volume fraction of dispersed Al_2O_3 slurries. The x-ray gray scale of each calibration slurry was scanned in the vertical direction along the centerline of the tube, and the gray scale reading at ten different points (excluding ends as discussed below) was measured to obtain an average value. The gray scale values of the centrifuged specimens were determined in an identical manner, with readings taken every 0.3 to 0.6 mm from the top to the bottom of the compact. Using the calibration curve, the gray scale measurements were converted to relative packing density. In all of the specimens studied with x-ray absorption, the conical bottoms of the tubes were filled with epoxy in order to eliminate the confusion of gray scale readings associated with changes in sample thickness.

Packing density data as a function of distance, h, from the top of the compact was used to calculate the pressure along the length of the tube using the following equation

---

[d] IRT Model 257 Fluoroscan X-Ray Inspection System & IRT HOMX-161 microfocus X-Ray system with a spot size of nominally 10μm, San Diego, CA

[e] ADR System 700 Automated Digital Radiography Software, IRT San Diego, CA

$$P(h) = \Delta\rho(2\pi v)^2 \int_0^h dh' \, \phi(h')[R - (L - h')] + P_0. \quad (1)$$

Here $\Delta\rho$ is the difference in density between Al_2O_3 (ρ = 3.98 g/cc) and water, v is the rotational frequency, $\phi(h)$ is the packing density as a function of the distance (h) from the top, R is the distance from the center of the rotor to the bottom of the compact, and L is the equilibrium height of the compact. P_0 is the pressure due to mass of particles at the top of the compact where density measurements were inaccurate due to the edge effect described below. The estimation of P_0 is described below. Friction effects at the container wall were neglected.

Gray scale gradients at the edge of specimens (termed the edge effect) are a result of x-rays of a point (or line) source that projects through specimens of finite thickness.[22] To ensure that these edge effects were not a major source of error in the density determinations, a solid aluminum rod was examined with approximately the same dimensions and positioning within the x-ray instrument as the centrifuged compacts. This calibration showed that the density was uniform (±1.5 %) for all portions of the specimen except for the top 4 mm and the bottom 1.2 mm. Thus, only gray scale values in the center portion of each specimen, which excluded these top and bottom portions, were used to determine the relative packing density.

In order to determine P_0 in eq. (1), the mass of the particles in the top 4 mm of the compact, m_t, was estimated by subtracting the mass in the rest of the specimen from the total mass, m_0. The mass of particles in the bottom 1.2 mm of the compact, m_b, where packing fraction measurements were also not reliable, was estimated by assuming that particles packed in this portion had a uniform packing fraction identical to that measured just above it. The mass of the central portion of the

specimen, m_c, was determined by integrating $\phi(h')$ obtained from the x-ray technique described above. Thus,

$$m_t = m_o - (m_c + m_b) \tag{2}$$

and

$$P_0 = \frac{1}{A} 2\pi v^2 m_t (R - L + h_0) \tag{3}$$

where h_o = 4 mm and A is the area of the centrifuge tube.

3. Experimental Results

Figure 1 is representative of the approach to an equilibrium height during centrifugation of the coagulated and flocculated systems. Studies done at other centrifugal speeds showed a similar trend, i.e. 2.5 hours or less to reach the plateau. As mentioned above, samples at the two lowest speeds were spun and monitored for more than 12 hours to ensure equilibrium had been reached. Monitoring of the height of a dispersed slurry was not possible due to its cloudy supernatant (see discussion below).

Consistent with pressure filtration studies previously reported by Lange and Miller[1], Fig. 2 shows that the relative packing density of bodies centrifuged from flocculated slurries was less than those from dispersed slurries. In addition, for network pressures ≥ 0.5 MPa, the packing fraction achieved for the dispersed slurry was relatively independent of pressure, whereas the packing fraction of the flocculated slurry increased with pressure over the complete range of pressures examined. Values obtained at network pressure < 0.5 MPa were determined by the x-ray absorption method, whereas values at higher pressures were obtained by

weight changes before and after drying (described above) and thus represent an average value for the compact. Figure 2 also contains the results for the packing density of two slurries compacted by pressure filtration at 14 MPa. It shows that pressure filtration appears to produce a higher particle packing than centrifugation of dispersed slurries. *This difference might be attributed to the observation that the supernatant of the dispersed slurry was cloudy after centrifuging, clearly showing that mass segregation occurred during centrifugation. Velamakanni and Lange[2] have shown that mass segregation can lead to lower particle packing fraction.*

Figure 3a (pressure range ≤ 0.01 MPa) and Figure 3b (pressure range ≥ 0.01 MPa) show that the pressure dependence of the relative packing density of all of the coagulated slurries lies between those of the dispersed and flocculated slurries. At low pressures, all of the coagulated slurries had a lower packing fraction than a dispersed slurry at the same pressure. For clarity, only data for the highest (2.0 M) and lowest (0.25 M) salt additions are shown. The difference in packing fraction between dispersed and coagulated slurries was less at intermediate pressures, and, at the highest pressures, they appeared to reach a plateau, similar to the one found for pressure filtered slurries (see Figure 3b). Of particular note is that at higher pressures (> 0.5 MPa), coagulated slurries pack to a higher packing fraction than dispersed slurries. Unlike dispersed slurries, the supernatant of the coagulated slurries was always clear, regardless of the network pressure.

The packing fraction of the coagulated slurries appears to decrease with increasing electrolyte concentration (not shown in Figure 3). This was most apparent for a coagulated slurry with 0.25 M NH_4Cl which had a noticeably higher packing fraction than all other coagulated slurries studied. Although this slurry had the highest packing fraction of all of the coagulated slurries examined, it did not have the same integrity at the top of the compact as other coagulated slurries. Similar to dispersed slurries, the top of the sediment was only loosely packed and

could be easily poured off. On the other hand, the coagulated slurries with concentrations of NH_4Cl > 0.25 M formed compacts which appeared stiff when touched, despite their lower packing densities.

4. Discussion

Research in the fields of powder metallurgy, soil mechanics and ceramics engineering show that the compaction of non-saturated, granular materials by rearrangement can often be described by a linear relationship between the relative density of the granular compact and the logarithm of the applied pressure.[23] As shown by Kuhn et al.[24], the forces transmitted through a particle network by an applied pressure can be in static equilibrium, viz., allowing a stable packing arrangement for a given applied pressure. They showed that particle rearrangement occurs when the applied pressure generates a critical contact force for bridging particles that produces a local network instability. *Particles subjected to this critical force are similar to the keystone that is elastically forced through an arch due to an excessive overburden to propagate a structural catastrophe.* In particle networks, instabilities of this nature produce a denser, more stable network that prevails until an increase in pressure produces a new instability, followed by an increase in packing density.

Thus as the applied pressure increases, a stable particle network prevails until the pressure causes rearrangement and an incremental, non-recoverable increase in packing density. With this rearrangement phenomenon, the packing density will increase to a maximum value where no available space remains to relocate another particle. For randomly packed networks, the maximum packing density for identical spheres is ~ 0.64.[25] For real powders, it is well known that the maximum packing density depends on particle shape and size distribution.[26]

For the Al_2O_3 powders used in this study, the maximum packing density appears to be 0.62 ± 0.02 and is achieved for both dispersed and coagulated slurries at

pressure > 0.5 MPa. At lower pressures, the packing density of the dispersed and coagulated slurries are pressure dependent. All of the coagulated slurries have a similar dependence of packing density on pressure ($d\phi/d\ln P$) which is larger than the dispersed slurries. The packing density of flocculated slurries had the greatest pressure dependence and never achieved the maximum packing density for the pressures used in this study. Over the range of pressures where the packing density of each slurry was pressure dependent, the relation between the relative density and the logarithm of the applied pressure is nearly linear, consistent with literature data for non-saturated systems.[23]

The different pressure dependencies shown by the different slurries must be related to a basic phenomenon of network instability, viz., the critical force required to push a load bearing particle into a vacant site. [24] The coefficient of friction of the particles is expected to be critically related to this instability, viz., particles that slide easier will become unstable at a smaller force. Homola et al.[27] were the first to establish, through the use of the surface force apparatus, an experimental relation between surface forces and the coefficient of friction. Their experiments showed that when a short-range, repulsive, hydration potential existed between mica surfaces, the coefficient of friction was low (~0.1) and the surfaces would easily slide. On the other hand, when only an attractive van der Waals potential existed, the same surfaces fractured prior to sliding. These results suggest that a short-range repulsive force acts as a lubricant in a similar manner as the apparent 'lubrication' produced between like poles of two magnets.

The relationship between interparticle potential and particle separation for different attractive networks are schematically shown in Figure 4. These functions can be used to qualitatively describe how a short-range repulsive potential can produce a 'lubrication' effect. When such a potential exists, the repulsive potential part is proceeded by an asymmetric potential well as shown in Figure 4. For

conditions where the kinetic energy of the particle is much less than the well depth, the equilibrium particle separation distance is H_o. The slope of this curve, -dV/dH, is a force, and when $H < H_o$, an increasing compressive force is need to bring the particles closer together. This compressive force can be imagined to sheath each particle with a compliant material described by the force - separation function for $H_o > H \geq 0$. This material elastically deforms much more than the particles themselves, and thus allows particles in contact to slide pass one another in a way that requires lower forces to produce the rearrangement needed for consolidation.[24] On the other hand, if no short-range potential exists as is the case for the lower curve by in Figure 4, the equilibrium separation distance is at $H_o = 0$, i.e., the particles touch. For this case, the compliant layer no longer exists, and the elastic properties of the particles themselves must be used to determine the critical force need to produce the instability for increased particle packing. Thus as the potential well becomes deeper, the short-range repulsive potential becomes less effective in 'lubricating' the rearrangement processes needed to pack particles.[8]

Both the long-range and short-range interparticle potentials in dispersed and coagulated slurries, respectively, are expected to produce 'lubricating' effects when compared to monotonically attractive van der Waals potential. That is, both dispersed and coagulated slurries are expected to achieve their maximum packing density at lower network pressures relative to flocculated slurries.

The pressure required to increase the packing density has been referred to as the compressive yield stress.[15] From a mechanics point of view this stress may not be related to the shear yield stress because the latter occurs at constant volume. Furthermore, the fraction of bonds which are in tension during shear is higher than the fraction that are in tension during compression. Previous comparisons of the compressive yield stress measured in sedimentation experiments with the shear yield stress indicate that the latter is much smaller, but that they both have a similar

dependence on volume fraction.[15] Experiments reported here indicate that the two may have similar dependencies on added salt in coagulated slurries. The shear yield stress measurements for coagulated slurries indicate that they increase with added salt to a maximum value and that the shear yield stress for flocced slurries is an order of magnitude greater.[7] The compaction behavior also indicates that the pressures required for densification are also much higher for flocced slurries. The magnitude of the compressive yield stress and the shear yield stress should be related to the minimum of the interparticle potential and to the maximum force required to separate the particles, and thus, both are measures of the strength of the particle network.

5. Conclusion

Al_2O_3 slurries initially dispersed at low pH and coagulated with high concentrations of salt have advantages over both dispersed and flocculated slurries. They can be consolidated to high packing densities with relative small pressures just like dispersed slurries. The compact body, however, has mechanical integrity like flocculated material. Although unexpected on the basis of DLVO theory, the behavior is believed to be due to a short range repulsive potential which reduces the influence of the van der Waals interactions. This combination is expected to give rise to an energy well which causes particles to aggregate, but which is not as deep as slurries at the isoelectric point (flocculated slurries). The compaction stress that produces a given particle packing density has been found to depend on electrolyte concentration in a manner similar to the shear yield stress.

Acknowledgments

The authors would like to thank Dr. Bhaskar Velamakanni for his assistance, and the Office of Naval Research for the their support of this work under contract # N 0 0 0 1 4 - 9 0 - J - 1 4 4 1

References

[1] Lange, F. F., and Miller, K. T., "Pressure Filtration: Consolidation Kinetics and Mechanics," *Am Ceramic Soc. Bulletin*, **66(10)**:1498-1504, 1987.

[2] Velamakanni, B. V., and Lange, F. F., "Effect of Interparticle Potentials and Sedimentation on Particle Packing Density of Bimodal Particle Distributions During Pressure Filtration," *J. Am. Ceram. Soc.*, **74(1)**: 166-172, 1991.

[3] Lange, F. F., Velamakanni, B. V., and Evans, A. G., "Methods for Processing Metal-Reinforced Ceramic Composites," *J. Am. Ceram. Soc.*, **73(2)**: 388-393, 1990.

[4] Chang, J. C., Velamakanni, B. V., Lange, F. F., and Pearson, D. S., "Centrifugal Consolidation of Al_2O_3/ZrO_2 Composite Slurries vs. Interparticle Potentials: Particle Packing and Mass Segregation," *J. Am. Ceram. S.*, **74(9)**: 2201-2204, 1991.

[5] Velamakanni, B. V., Chang, J. C., Lange, F. F., and Pearson, D. S., "New Method for Efficient Colloidal Particle Packing via Modulation of Repulsive Lubricating Hydration Forces," *Langmuir*, **6**:1323-1325, 1990.

[6] Velamakanni, B. V., Lange, F. F., Zok, F. C., and Pearson, D. S., "Influence of Interparticle Forces on Rheology of Pressure Consolidated Ceramic Particulate Bodies," unpublished work.

[7] Chang, J. C., Lange, F. F., and Pearson, D. S., "The Viscosity and Yield Stress of Al_2O_3 Slurries Containing Large Concentrations of Electrolyte," to be submitted.

[8] Chang, J. C., Lange, F. F., and Pearson, D. S., to be submitted.

[9] Aksay, I. A., "Microstructure Control Through Colloidal Consolidation," in *Advances in Ceramics, vol. 9: The Forming of Ceramics*, John A. Mangels, ed., The American Ceramic Society, Inc., Westerville, Ohio, 1984, p.94-104.

[10] Davis, K. E., and Russel, W. B., "A Model of Crystal Growth in the Sedimentation and Ultrafiltration of Colloidal Hard Spheres," in *Advances in Ceramics, vol. 21: Ceramic Powder Science*, G. L. Messing, K. S. Mazdiyasni, J. W. Mc Cauley, and R. A. Haber, eds., The American Ceramic Society, Inc., Westerville, Ohio, 1987, p.573-585.

[11] Aksay, I. A., and Schilling, C. H., "Mechanics of Colloidal Filtration," in *Advances in Ceramics, vol. 9: The Forming of Ceramics*, John A. Mangels, ed., The American Ceramic Society, Inc., Westerville, Ohio, 1984, p.85-94.

[12] Schilling, C. H., Shih, W.-H., and Aksay, I. A., "Advances in Drained Shaping of Ceramics," in *Ceramic Transactions, vol. 22: Ceramic Powder Science IV*, Shin-

ichi Hirano, Gary L. Messing, and Hans Hausner, eds., The American Ceramic Society, Inc., Westerville, Ohio, 1991, p.307-317.

[13] Nienburg, H., and Harbach, Friedrich, "Pressure Filtration of Fine Ceramic Suspensions," in *Ceramic Transactions, vol. 22: Ceramic Powder Science IV*, Shin-ichi Hirano, Gary L. Messing, and Hans Hausner, eds., The American Ceramic Society, Inc., Westerville, Ohio, 1991, p.321-327.

[14] Buscall, R., "The Elastic Properties of Structured Dispersions: A Simple Centrifuge Method of Examination," *Colloids and Surfaces*, 5:269-283, 1982.

[15] Buscall, R. , and White, L. R., "The Consolidation of Concentrated Suspensions, Part I: The Theory of Sedimentation," *J. Chem. Soc., Faraday Trans. I*, 83:873-891, 1987.

[16] Buscall, R., "The Sedimentation of Concentrated Colloidal Suspensions," *Colloids and Surfaces*, 43:33-53, 1990.

[17] Landman, K. A., White, L. R., Buscall, R., "The Continuous-Flow Gravity Thickener: Steady State Behavior," *AIChE Journal*, 34(2):239-252, 1988.

[18] Buscall, R., Mills, P. D. A., Goodwin, J. W., and Lawson, D. W., "Scaling Behavior of the Rheology of Aggregate Networks formed from Colloidal Particles," *J. Chem. Soc., Faraday Trans. I.*, 84(12): 4249-4260, 1988.

[19] Buscall, R., Mc Gowan, I. J., Mills, P. D. A., Stewart, R. F., Sutton, D., White, L. R., and Yates, G. E., "The Rheology of Strongly-Flocculated Suspensions," *J. Non-Newtonian Fluid Mechanics*, 24:183-202, 1987.

[20] Auzerais, F. M., Jackson, R., and Russel, W. B., "The Resolution of Shocks and the Effects of Compressible Sediments in Transient Settling," *J. Fluid Mechanics*, 195: 437-462, 1988.

[21] Schilling, C. H., and Aksay, I. A., "Gamma-Ray Attenuation Analysis of Packing Structure Evolution During Powder Consolidation," in *Ceramic Transactions Volume 1: Ceramic Powder Science II*, Gary L. Messing, Edwin R. Fuller, Jr., and Hans Hausner, eds., The American Ceramic Society, Inc., Westerville, 1987, 800-808.

[22] Goldstein, J. I., Newbury, D. E., Echlin, P., Joy, D. C., Fiori, C., and Lifshin, E., *Scanning Electron Microscopy and X-ray Microanalysis*, Plenum Press, New York, 1984.

[23] J. J. Benbow, "Mechanics of Compaction," *Enlargement and Compaction of Particulate Solids*, N. G. Stanley-Wood, ed., Butterworth, Boston, MA, 1983, p167.

[24] Kuhn, L. T., Mc Meeking, R. M., Lange, F. F., "A Model for Powder Consolidation," *J. Am. Ceram. Soc.*, 74(3): 682-685, 1991.

[25] McGeary, R. K., "Mechanical Packing of Spherical Particles," *J. Am. Ceram. Soc.*, **44(10)**: 513-522, 1961.

[26] Messing, G. L., and Onada, Jr., G. Y., "Inhomogeneity-Packing Density Relations in Binary Powders," *J. Am. Ceram. Soc.*, **61(1-2)**: 1-5, 1978.

[27] Homola, A. M., Israelachvili, J. N., Gee, M. L. and McGuiggan, P. M. "Measurements of and Relation Between the Adhesion and Friction of Two Surfaces Separated by Molecularly Thin Liquid Films," *J. Tribology*, **111**: 675, 1989.

Figure Captions

Figure 1. Approach to equilibrium of centrifuged Al_2O_3 slurries at pH 4 with 0.5 and 1.5 M NH_4Cl and at pH 9. Samples were spun at 600rpm.

Figure 2. Centrifuged and pressure filtrated Al_2O_3 slurries at pH 4 and 9. Pressure filtrated samples are indicated. Packing fraction gradient was obtained by x-ray analysis for samples consolidated at pressures less than 0.1 MPa.

Figure 3a. Centrifuged Al_2O_3 slurries at pH 4 and at pH 4 with 0.25 and 2.0 M NH_4Cl. Packing fraction gradient was determined by x-ray analysis.

Figure 3b. Centrifuged and pressure filtrated Al_2O_3 slurries at pH 4 and 9, and at pH 4 with 0.25 and 2.0 M NH4Cl. Pressure filtrated samples are indicated. Packing fraction gradient was obtained by x-ray analysis for samples consolidated at pressures less than 0.1 MPa.

Figure 4. Interaction potential of 0.20 μm in diameter Al_2O_3 at pH 4 with 1.0 M NH_4Cl and at pH 9 ($V_T = V_A$), assuming DLVO theory and an additional hydration potential term. Constant potential is assumed with ψ = 40 mV and A = 4.91E-20 J.

Figure 1

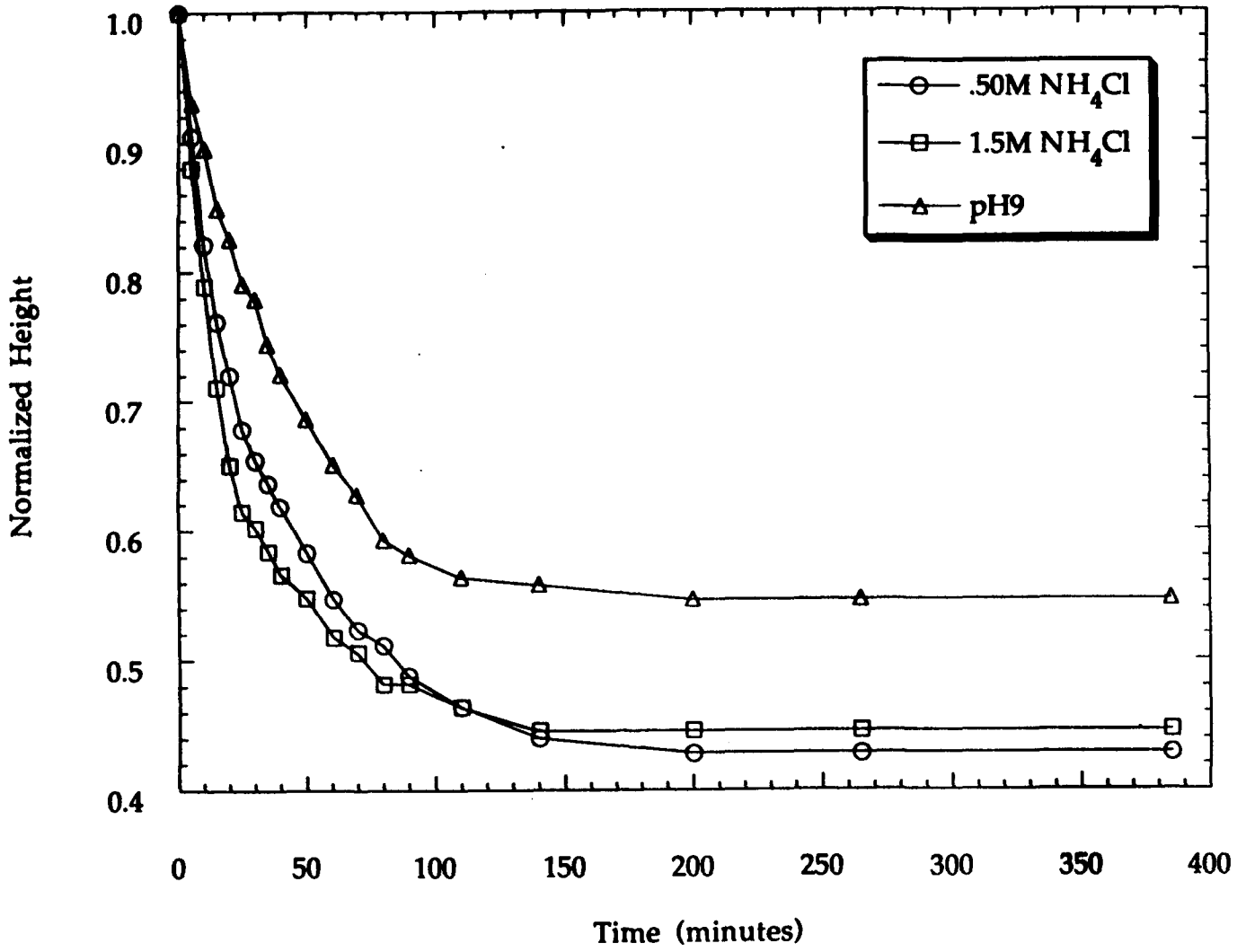
1.0
0.9
0.8
0.7
0.6
0.5
0.4
Normalized Height
0
50
100
150
200
250
300
350
400
Time (minutes)
.50M NH4Cl
1.5M NH4Cl
pH9

Figure 2

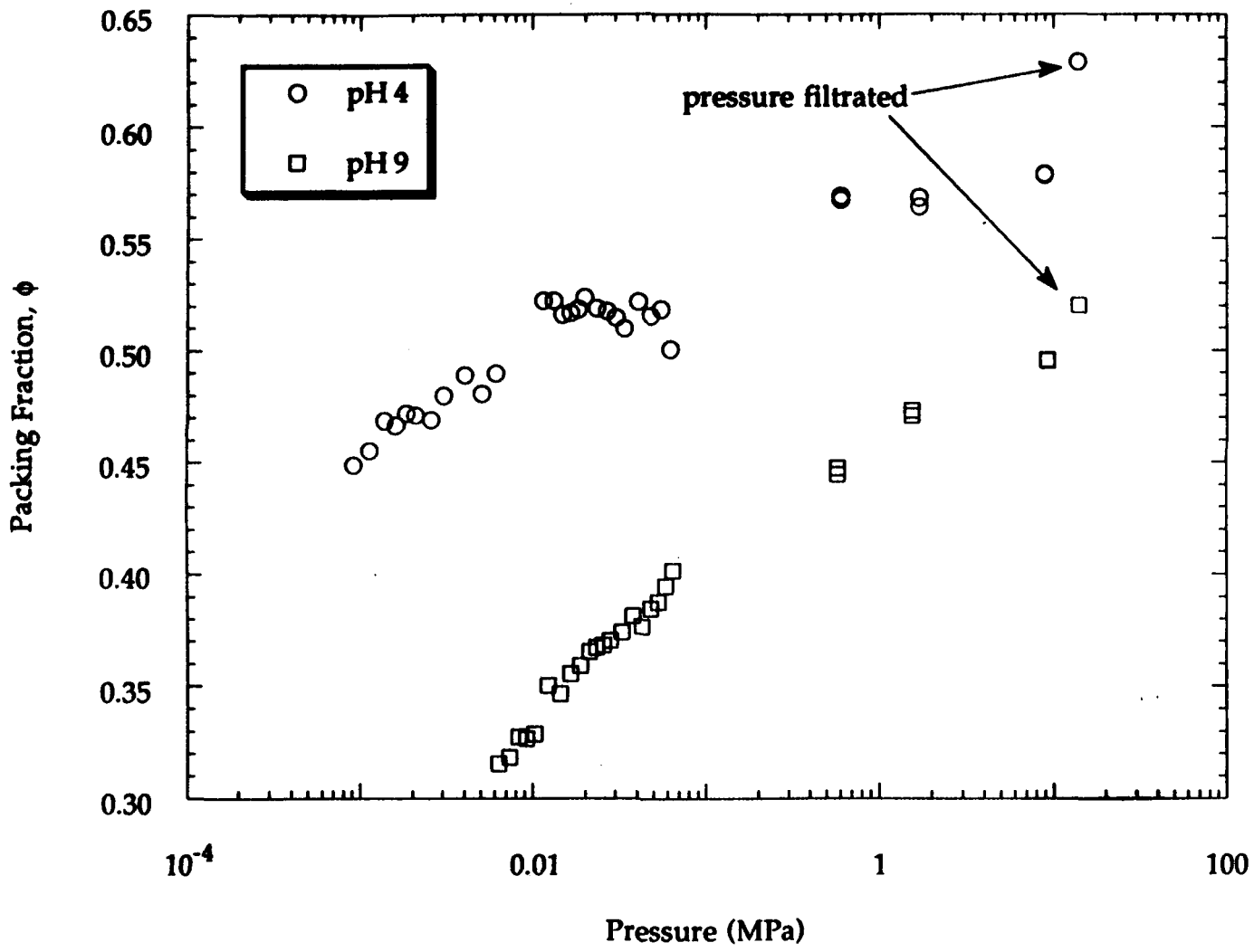
0.65
0.60
0.55
0.50
0.45
0.40
0.35
0.30
Packing Fraction, ϕ
pH 4
pH 9
pressure filtrated
10-4
0.01
1
100
Pressure (MPa)

Figure 3a

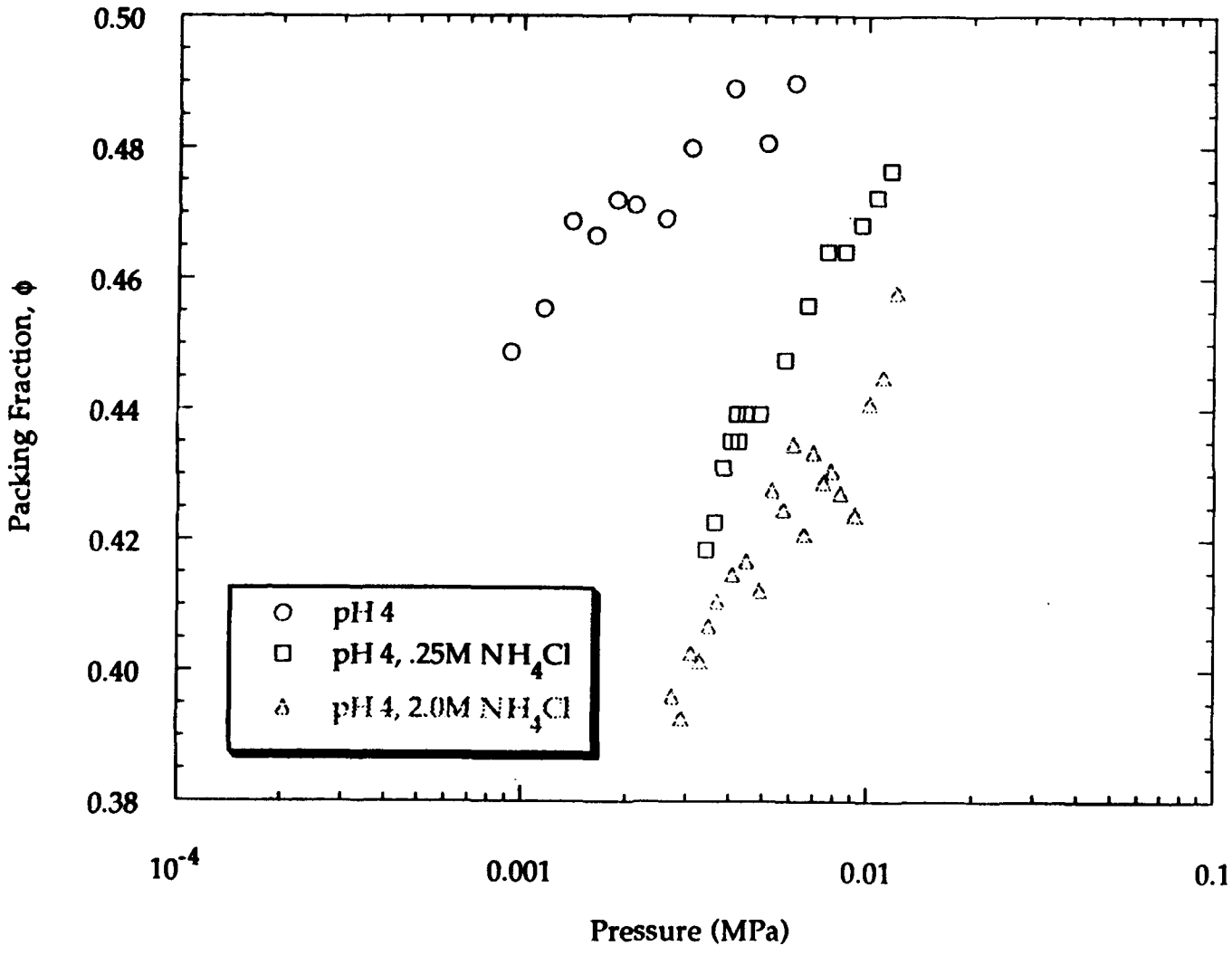
0.50
0.48
0.46
0.44
0.42
0.40
0.38
Packing Fraction, ϕ
pH 4
pH 4, .25M NH4Cl
pH 4, 2.0M NH4Cl
10-4
0.001
0.01
0.1
Pressure (MPa)

Figure 3b

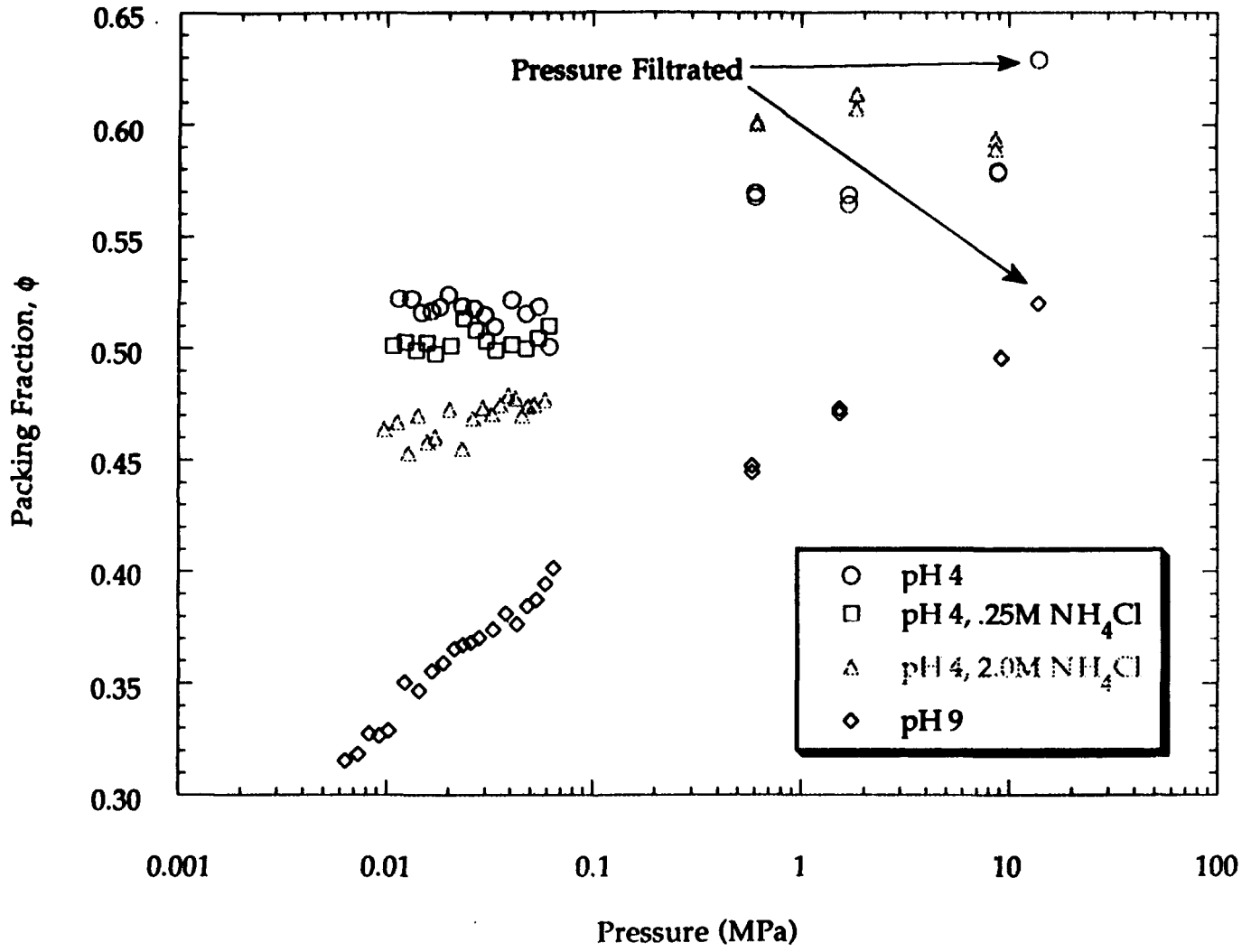
0.65
0.60
0.55
0.50
0.45
0.40
0.35
0.30
Packing Fraction, ϕ
Pressure Filtrated
pH 4
pH 4, .25M NH4Cl
pH 4, 2.0M NH4Cl
pH 9
0.001
0.01
0.1
1
10
100
Pressure (MPa)

Figure 4

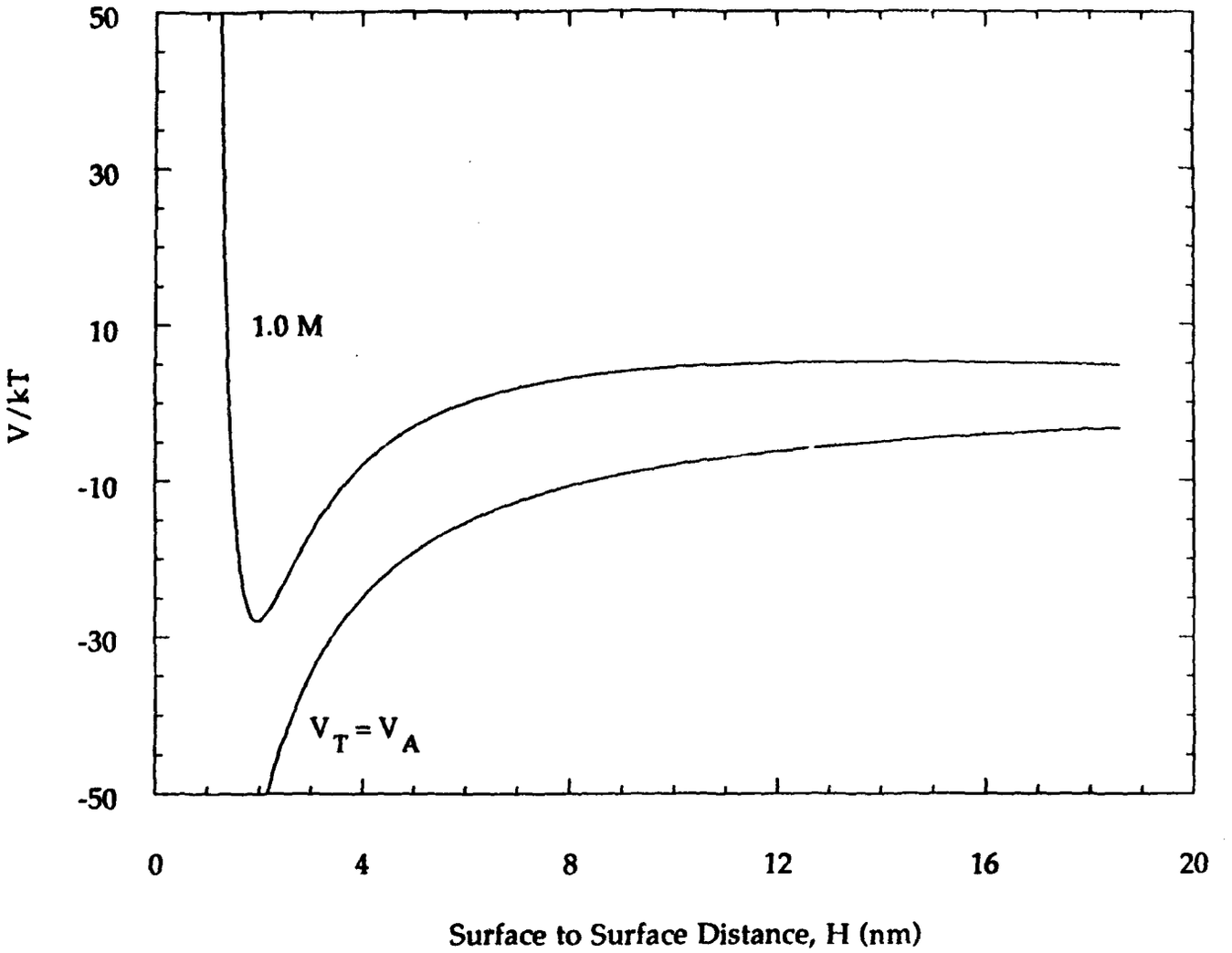
50
30
10
-10
-30
-50
V/kT
1.0 M
$V_T = V_A$
0
4
8
12
16
20
Surface to Surface Distance, H (nm)

MATERIALS

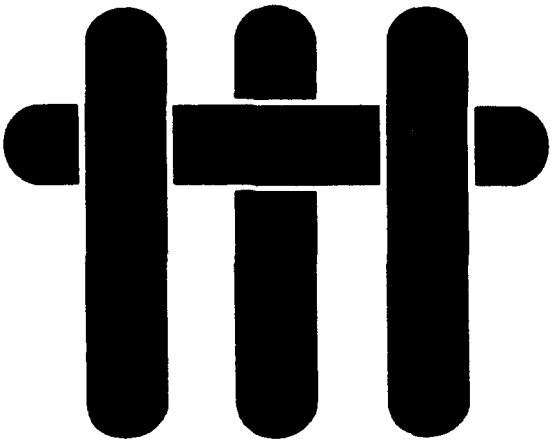

Technical Report Number 10

The Rheology and Packing Behavior of Alumina Slurries Containing Ammonium Citrate CounterIons

Erik P. Luther, Joseph A. Yanez, George V. Franks,
Fred F. Lange and Dale S. Pearson

Office of Naval Research

Grant No. N00014-90-J-1441

Fred F. Lange

Principal Investigator

Materials Department
University of California
Santa Barbara, CA 93106

198

MATERIALS

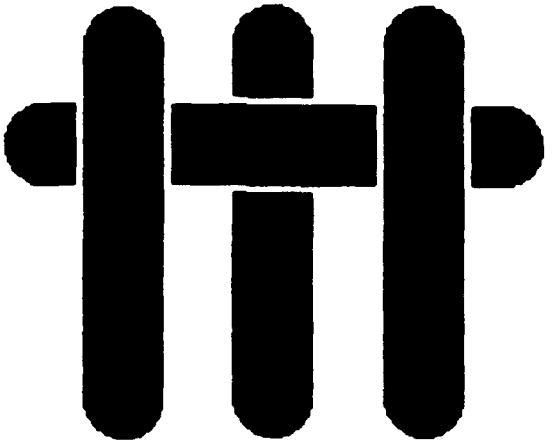

The Rheology and Packing Behavior of Alumina Slurries with Ammonium Citrate

Erik P. Luther, Joseph A. Yanez, George V. Franks,
Fred F. Lange and Dale S. Pearson

Materials Department
College of Engineering
University of California, Santa Barbara
Santa Barbara, CA 93106

The Rheology and Packing Behavior of Alumina Slurries with Ammonium Citrate

Erik P. Luther, Joseph A. Yanez, George V. Franks,
Fred F. Lange and Dale S. Pearson

Materials Department
College of Engineering
University of California
Santa Barbara, CA 93106

The behavior of alumina slurries with added ammonium citrate tri-basic, a potential determining ion, is compared to the behavior of slurries with ammonium chloride, an indifferent electrolyte. Adding salt to dispersed slurries has been shown to remove the long-range electrostatic repulsion and produce a short-range repulsion. Due to van der Waals attraction, the net potential is attractive. Ammonium citrate lowers the isoelectric point of alumina from pH 9 to pH 3 by neutralizing positive surface sites. At pH 8 with added ammonium citrate, alumina slurries are coagulated. These slurries pack to high densities and have lower viscosities than flocced slurries because of the short-range repulsion which effectively lubricates particles allowing for rearrangement. Packing density and viscosity measurements show little difference between slurries coagulated with ammonium citrate and ammonium chloride. When ammonium chloride is added to slurries flocced at pH 9 no difference is seen in the viscosity or yield stress. Slurries with added ammonium citrate are flocced at pH 3 and exhibit yield stresses similar to slurries flocced at pH 9. However, when excess ammonium citrate is added, the yield stress decreases, behavior which is not observed when ammonium chloride is added.

I. Introduction

It has been shown that dispersed slurries can be coagulated by the addition of indifferent electrolyte.[1,2] The addition of electrolyte eliminates the electrostatic repulsion between particles, leaving van der Waals attraction and a third potential not predicted by DLVO theory. The potential introduced by adding salt is a short-range repulsion that prevents particle-particle contact but does not overwhelm the van der Waals attraction at long range.

High relative packing densities can be obtained with coagulated slurries without the problem of particle segregation because of the presence of a weak attraction between particles.[3] Consolidated bodies are plastically deformable when saturated which allows for reshaping into complex forms.[4] Viscosity and yield stress measurements show that increasing amounts of indifferent electrolyte increases the strength of the network formed until a maximum is reached; however, this maximum is still less than that of a flocced slurry.[2] Further additions of salt do not greatly effect the system.

Currently we believe that the source of the short-range repulsion is the presence of a hydration layer similar to that found between mica surfaces[5,6] and for clays.[7] Recently Ducker et al.[8] have confirmed the existence of a short-range repulsion due to added salt between sapphire plates in the surface force apparatus.

Leong et al.[9] have demonstrated that the yield stress of flocced zirconia slurries is reduced by the addition of citric acid, a potential determining ion. The addition of potassium nitrate, an indifferent ion, did not affect the yield stress.[10] We have added ammonium citrate to alumina slurries to examine the effect of potential determining ions on the viscosity, packing behavior, yield stress, and shear modulus of the slurry.

II. Experimental

Aluminum oxide powder[a] with an average particle size of 0.2 μm was dispersed in deionized water (14 MΩ) with ultrasound.[b] A solids loading of 20 vol% was used throughout. Slurries were prepared 24 hours before testing. Additions of ammonium chloride and ammonium citrate tri-basic were made at least 1 hour before testing. The pH of slurries was adjusted before testing with HNO_3 and KOH or NH_4OH. Slurries at pH 4 with no added electrolyte are dispersed. Slurries at pH 9 with no added electrolyte are flocced.

Zeta potential measurements[c] were made on dilute suspensions with 0.01M NH_4Cl and on suspensions of a fixed concentration of alumina with increasing amounts of ammonium citrate tri-basic. Settling experiments were performed in graduated cylinders with increasing amounts of ammonium citrate tri-basic.

Viscosity measurements were made with a Rheometrics rheometer[d] using a couette type measuring cell (25 mm radius 77 mm long). Slurries were subjected to a decreasing rate sweep starting at 1000 s^{-1} and ending at 0.1 s^{-1} or until the torque was below the sensitivity of the instrument (1 g-cm). Yield stress and shear modulus measurements[d] were made using a vane tool (12.7mm radius 36mm long) in steady and dynamic modes. (Yield stress and shear modulus measurements will be discussed in more detail in a subsequent paper.[11] A description of the vane tool can be found in references 12 and 13). Steady shear experiments consisted of shearing the sample at a constant strain rate. In steady shear, the yield stress was determined to occur at the point where the log stress versus log strain deviated from a slope of

---

a AKP-50. Sumitomo Chemical Co. Ltd., Osaka, Japan
b Model W-380. Heat Systems Ultrasonics Inc., Farmingdale, NY
c Zetameter System 3.0. Zeta-meter Inc., Long Island City, NY
d Model RMS-800. Rheometrics Inc., Piscataway, NJ

one. Dynamic experiments consisted of an amplitude sweep at fixed frequency (1rad/sec) and a frequency sweep at fixed amplitude. In an amplitude sweep, the stress at which the storage modulus deviated from a constant value was the yield stress. A dynamic frequency sweep was run to determine if the yield stress was frequency dependent. At frequencies greater than about 0.3 rad/sec the yield stress was independent of frequency but at lower frequencies the yield stress was frequency dependent. The stress and strain on the vane tool was calculated assuming a couette geometry.

Slurries were consolidated by pressure filtration. Pressure filtration was carried out in a cylindrical device reported elsewhere.[3] Particle packing densities of the saturated bodies were determined by weighing the body before and after drying. The weight change was assumed to be due only to evaporated water. The theoretical density of alumina was taken to be r = 3.94 g/cc.

III. Results

(1) Zeta Potential

The zeta potential of alumina as a function of citrate concentration is shown in figure 1. The isoelectric point occurred at pH 9 when an indifferent electrolyte was added (ammonium chloride). The addition of large amounts of ammonium citrate, a potential determining ion, lowered the isoelectric point to pH 3. Small amounts of ammonium citrate slowly lowered the isoelectric point from pH 9 to pH 3. The amount of citrate needed to shift the the isoelectric point to pH 3 is a function of the solids loading of the slurry. The relationship between salt concentration and solids loading is not understood; however, it is clear that the citrate concentration needed to fully shift the isoelectric point does not correspond well to the settling and viscosity measurements.

(2) Settling

Alumina slurries with increasing amounts of ammonium citrate were allowed to settle undisturbed for over 1 week. The supernate of the slurry with 0.035 M ammonium citrate was cloudy and the sediment diffuse. The supernate of the slurry at 0.040 M was less cloudy and the sediment was distinct. The critical coagulation concentration(CCC) lies between these two salt concentrations. At concentrations greater than the CCC, increasing concentrations of salt increased the sediment height (lower densities) but to much lower heights than for a slurry flocced at pH 9.

(3) Viscosity

The viscosity versus shear rate of alumina slurries is shown in figure 2. Dispersed alumina slurries (pH 4, 0 M) were almost Newtonian. The addition of ammonium citrate spontaneously increased the pH of dispersed slurries from 4 to ~8. At low salt concentrations (pH8, 0.01M) the slurry was strongly shear thinning due to incomplete coverage of the alumina particles with citrate. It can be seen that at ammonium citrate concentrations approximately equal to the CCC (pH 8, 0.03 M) the slurry was indistinguishable from a dispersed slurry. This is because the alumina surface has been fully covered by citrate. Since the citrate ions are charged, a large zeta potential os present yielding a dispersed slurry. The viscosity of the alumina slurries increased with increasing amounts of salt to a maximum at about 0.5 M as the electrostatic repulsion is screened. Further salt additions had no effect. The maximum viscosity reached by adding salt was about an order of magnitude less than for a flocced slurry (pH 9, 0 M). This is very similar to the behavior of alumina slurries coagulated with ammonium chloride. (A short-range repulsion is apparently developed as discussed in reference 1). As seen in figure 3, the viscosity of alumina slurries coagulated

at pH 8 with 0.5 M ammonium citrate or at pH 4 with 2 M ammonium chloride was identical to a slurry at pH 8 with 0.03 M ammonium citrate and 1 M ammonium chloride.

The viscosity of alumina slurries at pH 3, the isoelectric point when ammonium citrate was added, is shown in figure 4. At ammonium citrate concentrations below 0.015 M the viscosity of the slurry was similar to that of a dispersed slurry. This is because not enough citrate is present to fully neutralize the charge on the alumina particles. The viscosity was strongly shear thinning and close but not equal to the viscosity of a flocced slurry at salt concentrations over 0.015 M. At these salt concentrations, the isoelectric point of the alumina is pH 3, thus the slurry is flocced.

(4) Yield Stress

Figure 5 shows the yield stress as a function of citrate added for slurries at pH 3 obtained from steady shear experiments (strain rate=0.001rad/sec). Figure 6 shows the stress versus strain curves for the same slurries. Although there is some ambiguity as to where the yield stress occurs, the deviation from linearity is clear. It can be seen that flocced slurries (pH 9, 0 M), have the highest yield stress, i.e., the strongest network. Yield stresses were determined as a function of citrate added at the new isoelectric point (pH 3.0). The yield stress of a slurry with the critical coagulation concentration of added citrate (pH 3, 0.035M) was close to that of a flocced slurry (pH 9, 0 M). When more salt was added, the yield stress continued to drop with increasing salt added until a minimum yield stress was achieved, after which further increases in salt concentration had no effect. In contrast, when ammonium chloride was added to slurries at pH 9, there was no effect on the yield stress. These slurries were indistinguishable from flocced systems. Slurries at pH 8 with ammonium citrate had yield stresses too low to measure.

(5) Shear Modulus

The shear modulus was determined in both steady and dynamic modes. Like the yield stress measurements the shear modulus was determined to be a function of salt added, see figure 7. The shear modulus in steady shear experiments was determined by calculating the slope of the stress versus strain curve prior to yield. The shear modulus (i.e., storage modulus) is a parameter calculated directly in dynamic experiments. The shear modulus values calculated by each technique agree well.

(6) Particle Packing

Dispersed, flocced and coagulated alumina slurries were consolidated by pressure filtration and the relative densities are listed in table 1. The packing density of coagulated slurries (pH 8 with 0.5 M ammonium citrate) was almost as high as those of dispersed slurries, i.e., 58% and 60% respectively. Slurries coagulated with ammonium chloride also result in high packing densities. Slurries coagulated with either salt are stabilized by a short-range repulsion which aids particle rearrangement. Flocced slurries packed to much lower densities. Slurries at pH 9 with no added salt packed to 50% and slurries at pH 3 with 0.1 M ammonium citrate also packed to 50%.

IV. Discussion

(1) Surface Coverage

Previous research has shown that indifferent electrolytes such as NH_4Cl, KI and NH_4NO_3 coagulate alumina slurries.[2] We have shown that ammonium citrate, a potential determining ion, can also coagulate alumina slurries. The added electrolyte removes the electrostatic repulsion between charged particles leaving the ubiquitous van der Waals attractive potential. A third force arises from the presence of salt. This is a repulsive, short-range potential not predicted by DLVO theory. This repulsion prevents particle-

particle contact; however, a weakly attractive network is formed due to the van der Waals potential which acts over a longer range.

Ammonium citrate tri-basic is a trivalent ion which is fully dissociated at pH 8 where we coagulate our system. The pK_a values occur at pH 3.1, pH 4.8 and pH 6.4.[14] At pH 3, where we flocc the slurry, half of the ions have one charged site.

Currently we believe the source of the short-range repulsive potential to be due to the attraction of the hydrated salt ion to the particle surface creating a layer that must be removed in order for particles to come into contact similar to the hydration layers found on mica surfaces.[5,6] Ammonium citrate, a potential determining ion, is more strongly bound to the particle surface than ions previously studied as evidenced by the lowering of the isoelectric point. The citrate ion is attracted to the positive surface sites of the alumina and neutralizes them leaving the negatively charged sites which yields a lower isoelectric point. The point where just enough ammonium citrate tri-basic is present to neutralize the surface and be in equilibrium in solution at pH 3 was found to occur at a citrate concentration of 0.001 M by zeta potential measurements. Although the citrate concentration seems low, the concentration of ammonium citrate to alumina surface area is very high (10 g/m^2) because a large fraction of ammonium citrate is bound to the surface but each ion only neutralizes a single charged site. This value is much higher than the critical coagulation concentration found for slurries with solids loadings of 20 vol%. As stated before, the relationship between solids loading and particle surface coverage has not been established. The CCC should be approximately equal to the concentration of salt where the surface is neutralized.

(2) Rheology

Viscosity measurements indicate that despite the large size and strong bonding of the citrate ion there are many similarities between the behavior of slurries coagulated with ammonium citrate and an indifferent electrolyte. When salt is added to a dispersed slurry, the viscosity increases and becomes shear thinning. At some maximum salt concentration further additions of salt no longer influence the viscosity. The difference between the maximum viscosity reached by adding salt and the viscosity of a flocced slurry is about an order of magnitude regardless of which salt is added. There are some differences when ammonium citrate is added, however. At low citrate concentrations, there is incomplete surface coverage of the alumina powder and thus the slurry has a high viscosity. The particles are strongly attractive because, although the iep has been lowered, it has not yet dropped to pH 3. This is shown for a slurry with only 0.01 M citrate at pH 8 in figure 2. When enough citrate is added to just cover the alumina surface (0.03 M), the viscosity is Newtonian, i.e., dispersed. In other words, the surface is covered and there is little in solution to eliminate the electrostatic repulsion. Once a 'new' charged surface has been created by covering the alumina particles with citrate (lowering the iep to pH 3), the slurry can be coagulated by adding an indifferent electrolyte such as ammonium chloride as shown in figure 4.

In agreement with the viscosity data, the critical coagulation concentration determined by the settling experiment occurs at a salt concentration of between 0.035 M and 0.04 M for slurries at pH 8. Complete surface coverage should thus occur sometime before a concentration of 0.035 M similar to the value of 0.03 M necessary to disperse a slurry at pH 8. (This is a citrate to alumina ratio of 0.09 g/m2, much less than that needed to cover the surface as determined by the zeta potential measurements).

The isoelectric point with added citrate occurs at pH 3 and so a slurry with enough citrate to fully cover the surface should be flocced at pH 3. The amount of citrate needed to reach the maximum viscosity for slurries at pH 3 was only 0.015 M (0.045 g/m^2). This is about half of the concentration needed at pH 8 to cover the surface. The charge on each ion is only one at pH 3 while it is three at pH 8 which would seem to indicate that more citrate would be needed. The amount of citrate adsorbed to the particle surface therefore must be greater at lower pH.

There is an important difference between the properties of slurries with ammonium citrate and those coagulated with ammonium chloride that is apparent when these slurries are flocculated. Alumina slurries at pH 9 with and without ammonium chloride yield nearly identical viscosities. Alumina slurries with the critical coagulation concentration of citrate at pH 3 with ammonium citrate have viscosities which are slightly lower than for slurries at pH 9. Since the citrate ion is much larger (~0.6 nm) than the ions previously studied (~0.2 nm), a steric stabilization mechanism might be considered. This has been cited as the cause for the reduction of the yield stress in zirconia suspensions reported by Leong et al.[9] We have also observed a decrease in the yield stress in alumina slurries due to the presence of excess ammonium citrate that does not occur when ammonium chloride is present. However, we find that slurries with the CCC of citrate have nearly identical yield stresses to flocced slurries. Research by Bergstrom et al.[15] indicates that the thickness of a steric layer necessary to obtain good packing densities must be larger than about 1 nm. Steric layers of less than about 1 nm were strongly attractive possessing very large compressive yield stresses. Further, these measurements were performed in organic solvents where the van der Waals attraction is less than in water; therefore, an even larger

molecule would be necessary to provide steric stabilization in aqueous slurries. This implies that a single layer of citrate ions on the particle surface would not be sufficient to cause steric stabilization. A significant reduction in the yield stress only occurs when large amounts of citrate (compared to the CCC) are present. It is possible that several layers of citrate ions are required to provide steric stabilization. Although we do not know the exact concentration of citrate that produces a monolayer of citrate on the alumina particles, if there were insufficient citrate ions to lower the isoelectric point of the slurry to pH 3, than the slurry would be even less attractive; i.e., possess a lower yield stress. An alternate explanation is the presence of the development of the short-range repulsion which was previously only observed for coagulated slurries. The role of the salt in the formation of the short-range repulsion is not fully understood so it is unclear if the presence of salt in the flocced slurries would produce a short-range repulsion.

The manner in which the yield stress is identified in our work is different from that presented in zirconia suspensions. In that research, the yield point was determined to be where the stress reached its maximum value whereas we interpret that to be the point where destruction of the attractive particle network and its reforming are balanced. Since this point occurs at quite large strains, it is clear that the original particle-particle contacts have long since been sheared. We identify the yield stress as the point where the stress versus strain curve goes non-linear in steady state experiments and the point where G' drops from a constant value in dynamic experiments.

V. Conclusions

We have found that potential determining ions can coagulate alumina slurries much as indifferent electrolytes do. The relative packing density of

consolidated bodies made from coagulated slurries are nearly the same as for bodies made from dispersed slurries regardless of the electrolyte used. The viscosity of coagulated slurries achieves the same maximum value regardless of whether ammonium citrate or ammonium chloride is added. The size of the ion at the particle surface does not seem to affect the strength of the short-range repulsion in coagulated slurries. The same viscosity can also be reached by adding enough ammonium citrate to completely cover the alumina surface, in effect creating a 'new' charged surface and coagulating the new system with ammonium chloride. Besides the obvious change in working pH and salt concentration, there are some important differences between potential determining ions and indifferent electrolytes. The yield stress of flocced slurries at pH 3 with the CCC of citrate is identical to slurries flocced at pH 9. Adding larger amounts of citrate lowers the yield stress until a minimum is reached where further additions of electrolyte have no effect. The viscosity of flocced slurries at pH 3 with added citrate never reaches the same value as a slurry flocced at pH 9. Adding ammonium chloride to flocced slurries has no effect on the viscosity or the yield stress. Steric stabilization does not satisfactorily explain the behavior since the size of a single citrate ion is too small to prevent the van der Waals attraction from flocing the slurry.

Acknowledgement
The authors would like to thank Bhaskar Velamakanni for helpful discussions on the behavior of potential determining ions.

References

1 B.V. Velamakanni, J.C. Chang, F.F. Lange and D.S. Pearson, "New Method for Efficient Colloidal Particle Packing via Modulation of Repulsive Lubricating Hydration Forces", Langmuir, 6, 1323-5 (1990).

2 J.C. Chang, F.F. Lange and D.S. Pearson, "Viscosity and Yield Stress of Al_2O_3 Slurries Containing Large Concentrations of Electrolyte", J. Am. Ceram. Soc. (in press).

3 J.C. Chang, F.F. Lange and D.S. Pearson, "Centrifugal Consolidation of Al2O3 and Al2O3/ZrO2 Composite Slurries vs. Interparticle Potentials: Particle Packing and Mass Segregation", J. Am. Ceram. Soc., 74, 2201-4 (1991).

4 B.V. Velamakanni, F.F. Lange and D.S. Pearson, "Influence of Interparticle Forces on Rheology of Consolidated Ceramic Particulate Bodies", J. Am. Ceram. Soc. (in press).

5 R.M. Pashley, "DLVO and Hydration Forces between Mica Surfaces in Li^+, Na^+, K^+ and Cs^+ Electrolyte Solutions: A Correlation of Double-Layer and Hydration Forces with Surface Cation Exchange Properties", J. Coll. Inter. Sci., 83, 531-46 (1981).

6 J.N. Israelachvilli and R.M. Pashley, "DLVO and Hydration Forces Between Mica Surfaces in Mg^{2+}, Ca^{2+}, Sr^{2+} and Ba^{2+} Chloride Solutions", J. Coll. Inter. Sci., 97, 446-55 (1984).

7 H. van Olpen, *An Introduction to Clay Colloid Chemistry,* John Wiley and Sons, New York, 1977, p 99.

8 W.A. Ducker, Z. Xu, J.N. Israelachvilli and D.R. Clarke, "The Forces Between Alumina Surfaces in Salt Solutions: Non-DLVO Forces and Their Effect on Colloid Processing", to be published.

9 Y.K. Leong, T.W. Healy, D.V. Boger, "Surface Chemistry and Rheology of ZrO2 Suspensions Containing Polyacrylate: Effects of Molecular Weight and ZrO2 Surface Area", Proceedings of the 94th Annual Meeting of The American Ceramic Society, Minneapolis MN, 12-16 April 1992, in press, Ceramic Transactions.

10 Y.K. Leong, N. Katiforis, D.B. O'C Harding, T.W. Healy and D.V. Boger, "Role of Rheology in Colloidal Processing of ZrO_2", J. Materials Proc. and Manuf. Sci. (in press).

11 J. Yanez, T. Shikata, D.S. Pearson, and F.F. Lange,"Shear Modulus of Attractive, Particle Networks vs. Depth of Potential Well", to be submitted.

12 Q.D. Nguyen, and D. Boger, "Yield Stress Measurement for Concentrated Suspensions", J. Rheology, 27,321-49 (1983).

13 Q.D. Nguyen, and D. Boger, "Direct Yield Stress Measurement with the Vane Method", J. Rheology, 29,335-47 (1985a).

14 R.G. Bates and G.D. Pinching, "Resolution of the Dissociation Constants of Citric Acid at 0 to 50°, and Determination of Certain Related Thermodynamic Functions", 71, 1274-83 (1949).

15 L. Bergstrom, C.H. Schilling and I. A. Aksay, "Consolidation Behavior of Flocculated Alumina Suspensions", J. Am. Ceram. Soc., 75, 3305-14 (1992).

Table I. Relative Packing Densities (%)

Slurry State	pH	Salt Conc.	Density
Dispersed	pH 4	0M	59.9%
Coagulated	pH 8	0.5 M citrate	58.6%
Coagulated	pH 4	1.5 M chloride	58.0%
Flocced	pH 9	0 M	50.1%
Flocced	pH 3	0.1 M citrate	50.5%

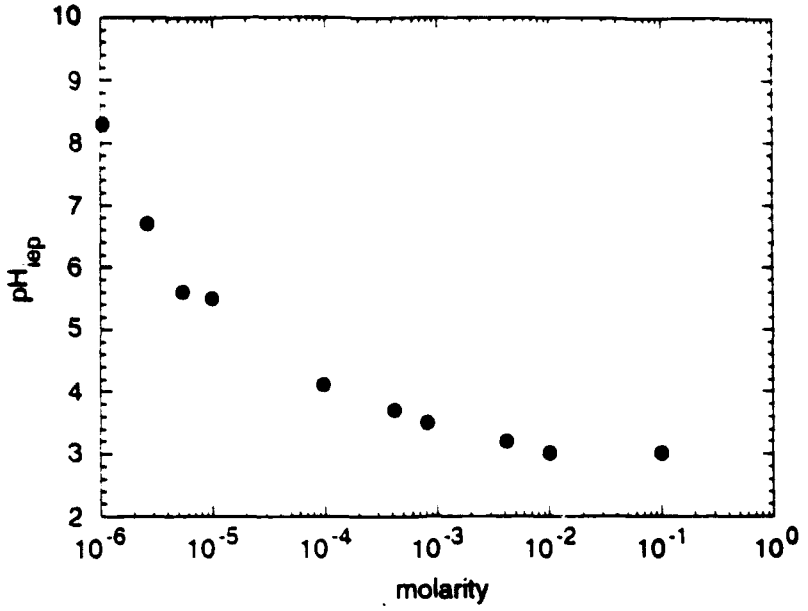

Figure 1 The reduction in isoelectric point with increasing amounts of citrate tribasic. The solids loading of the suspension is 0.005vol%.

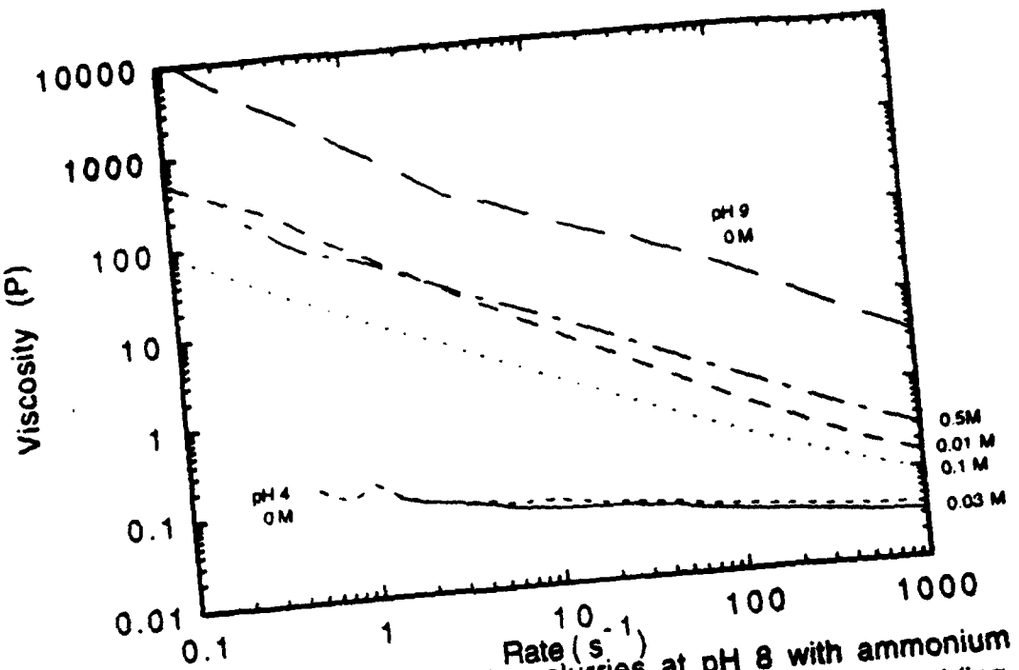

Figure 2 Viscosity of alumina slurries at pH 8 with ammonium citrate unless noted. The maximum viscosity reached by adding salt is an order of magnitude less than the viscosity of a flocced slurry.

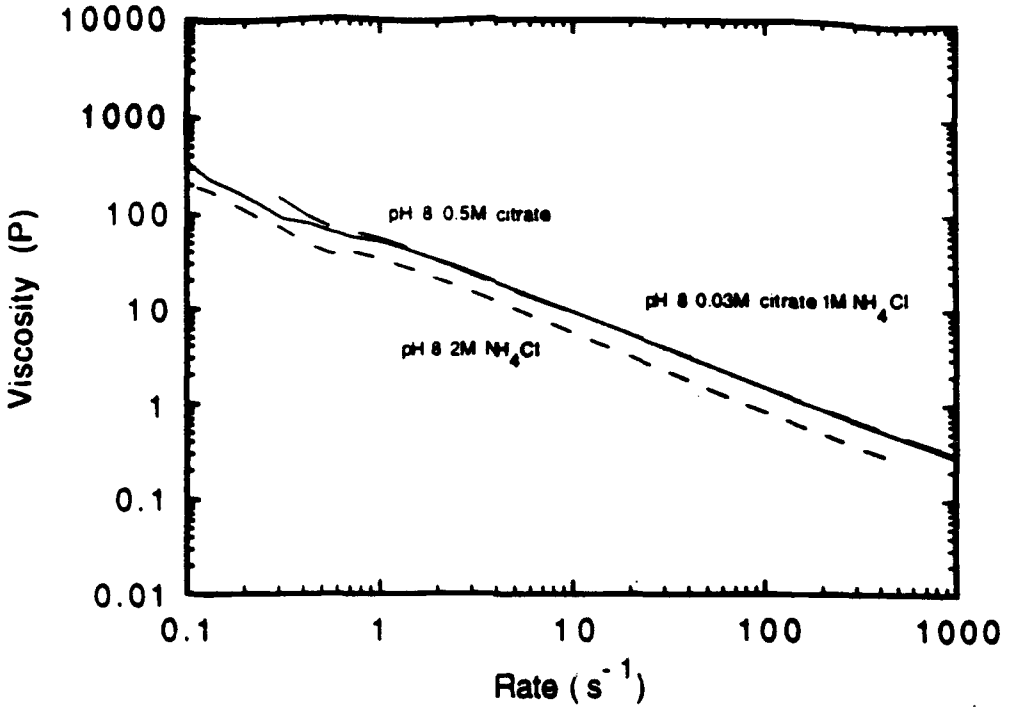

Figure 3 Viscosity of alumina slurries with 2M ammonium chloride, 0.5M ammonium citrate and 0.03M citrate and 1M chloride. All slurries display the same viscosity.

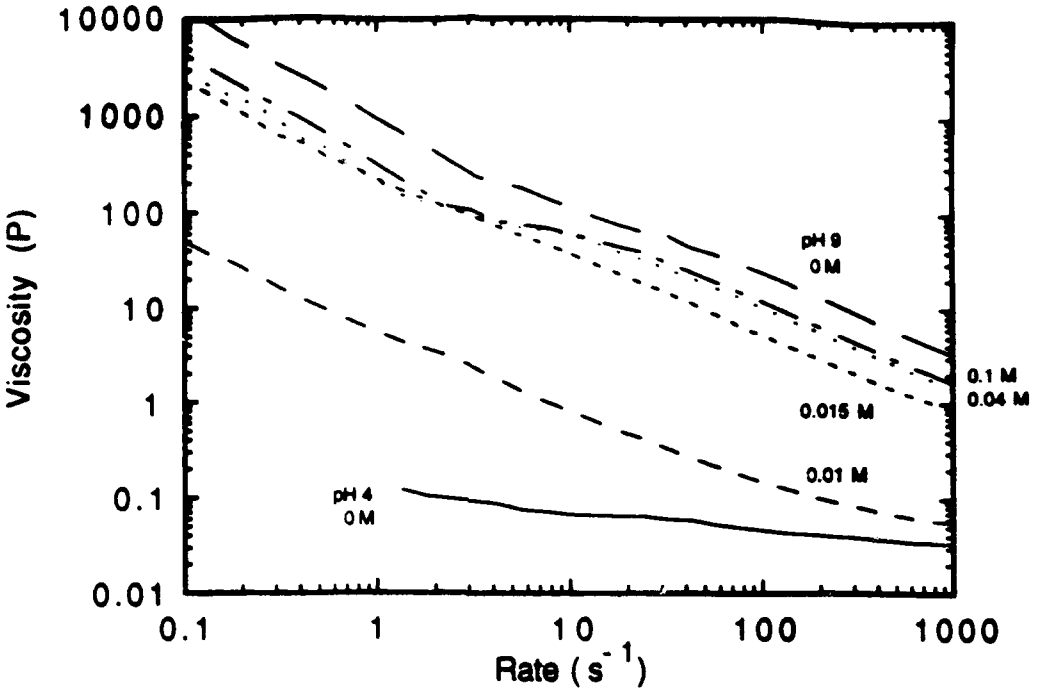

Figure 4 Viscosity of alumina slurries at pH 3 with ammonium citrate unless noted. The viscosity of a slurry at pH 3 with added ammonium citrate is less than the viscosity of a flocced slurry.

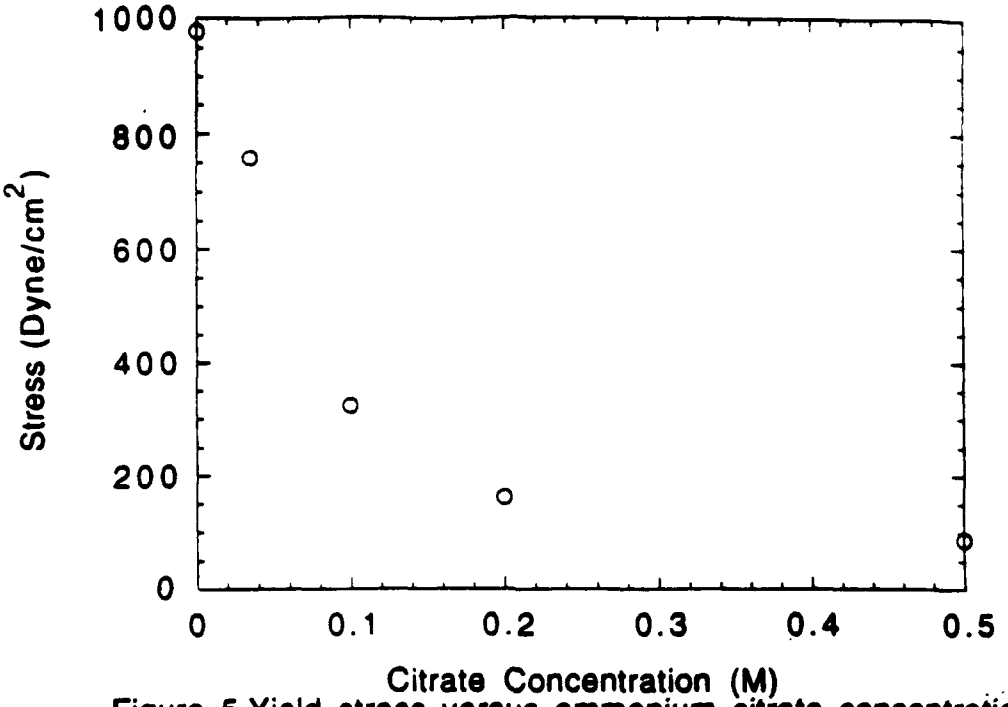

Figure 5 Yield stress versus ammonium citrate concentration showing a decrease in yield stress with increasing salt. All slurries are at pH 3 except 0M at pH 9.

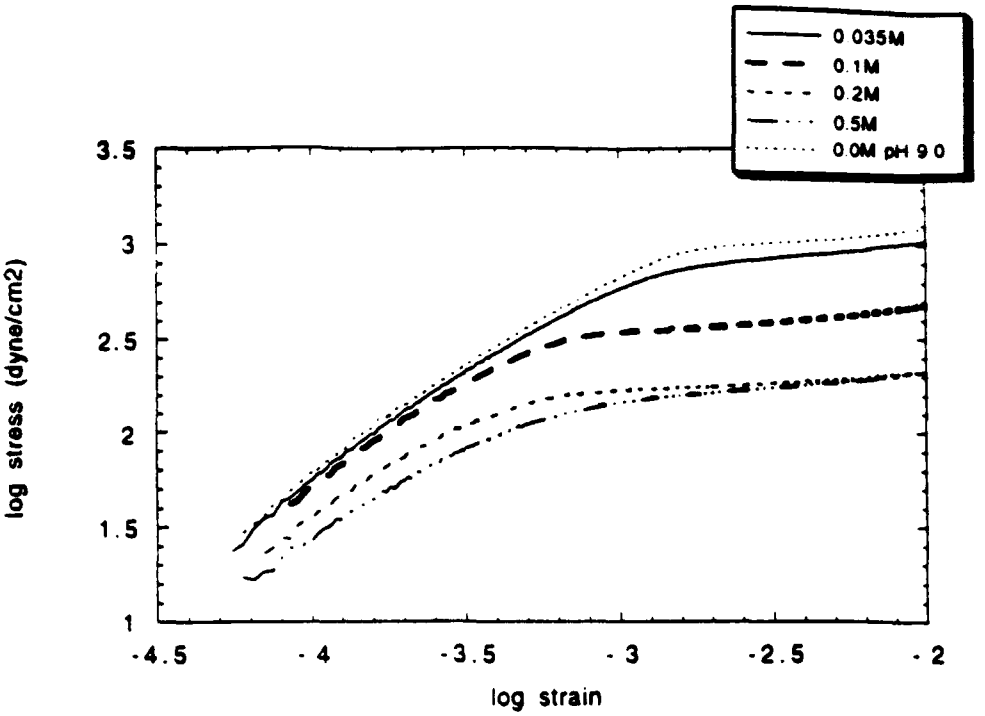

Figure 6 Stress versus strain of 20 vol% alumina slurries. Yield stress occurs where the curve deviates from linearity.

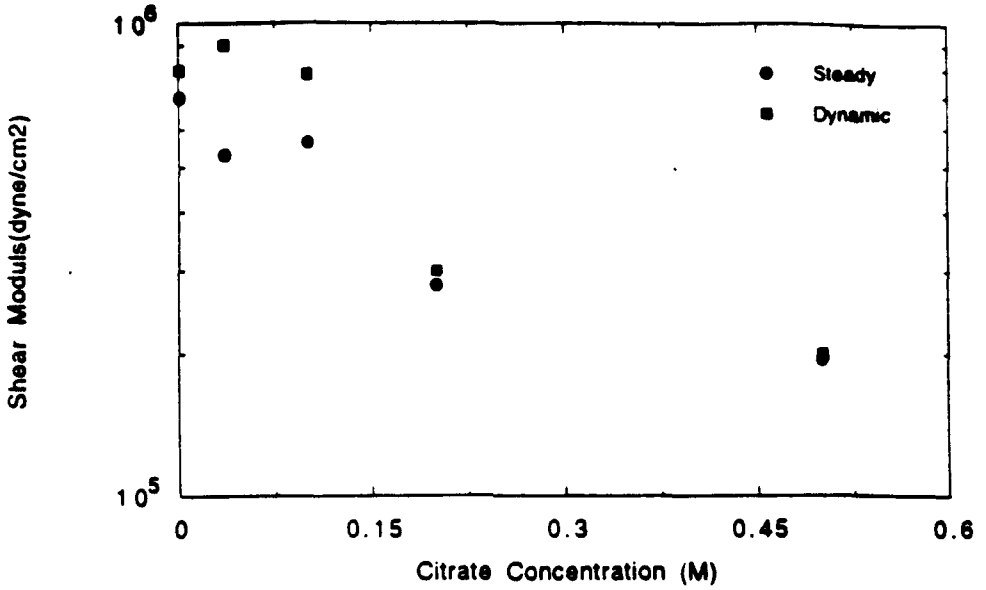

Figure 7 Shear Modulus of 20 vol% alumina slurries tested in steady and dynamic modes.

MATERIALS

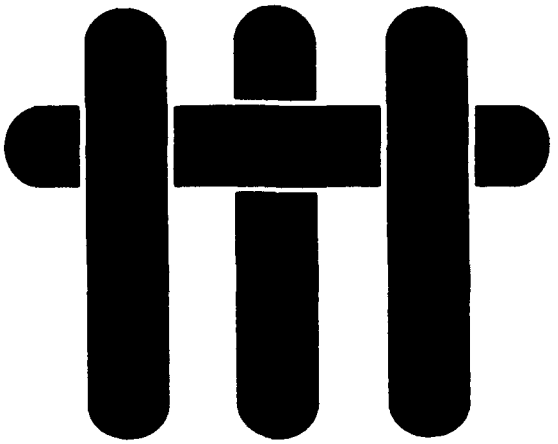

Technical Report Number 11

US Patent 5,188, 780
Method for Preparation of Dense Ceramic Products

Fred F. Lange and Bhaskar V. Velamakanni

Office of Naval Research

Grant No. N00014-90-J-1441

Fred F. Lange

Principal Investigator

Materials Department
University of California
Santa Barbara, CA 93106

US005188780A

United States Patent [19]

Lange et al.

[11] Patent Number: 5,188,780

[45] Date of Patent: Feb. 23, 1993

[54] **METHOD FOR PREPARATION OF DENSE CERAMIC PRODUCTS**

[75] Inventors: Frederick F. Lange, Santa Barbara, Calif.; Bhaskar V. Velamakanni, Woodbury, Minn.

[73] Assignee: Regents of the University of California, Oakland, Calif.

[21] Appl. No.: 687,251

[22] Filed: Apr. 18, 1991

[51] Int. Cl.[5] C04B 35/64

[52] U.S. Cl. 264/63; 264/56; 264/311; 501/1

[58] Field of Search 264/63, 311, 56; 501/1

[56] References Cited

U.S. PATENT DOCUMENTS

3,888,662	6/1975	Boeckeler	264/63
4,569,920	2/1986	Smith-Johannsen	501/1
4,624,808	11/1986	Lange	264/56
4,800,051	1/1989	Yan	264/56

OTHER PUBLICATIONS

Pashley, DLVO and Hydration Forces between Mica Surfaces in Li^+, Na^+, K^+, Cs^+ Electrolyte Solutions: A Correlation of Double-Layer and Hydration Forces with Surface Cation Exchange Properties J. of Colloid Interfaxe Science, vol. 83, No. 2, 531-546, Oct. 1981.

James, Characterization of Colloids in Aqueous Systems, Advances in Ceramics, vol. 21, 349-409, Ceramic Powder Science, 1987.

Lange, Powder Processing Science and Technology for Increased Reliability, J. Amer. Ceram. Soc., 72, [1], 3-15, (1989).

Horn, Surface Forces and Their Action in Ceramic Materials, J. Am. Ceram. Soc., 73 [5], 1117-1135 (1990).

Primary Examiner—James Derrington

Attorney, Agent, or Firm—Robbins, Dalgarn, Berliner & Carson

[57] **ABSTRACT**

A method of preparing dense ceramic product is described, wherein a coagulated network of ceramic powder particles in water is formed and then treated to increase the volume fraction of particles, thereby forming a water-saturated powder compact. The compact is formed into a desired shape and fired to provide the dense ceramic product. A coagulated network may advantageously be formed by mixing a ceramic powder with water at a pH that produces a net surface charge, to form a dispersed slurry and adding a sufficient amount of salt to the dispersed slurry to cause particles within the slurry to form the coagulated network. In view of the unique rheological properties of the powder compacts prepared from coagulated networks of ceramic powder particles, the compact may be processed into complex, near-net-shaped forms by introducing the compact into a mold and subjecting the mold to vibration, whereby the compact adopts the shape of the mold; once removed from the mold, the compact retains its shape without distortion.

17 Claims, 2 Drawing Sheets

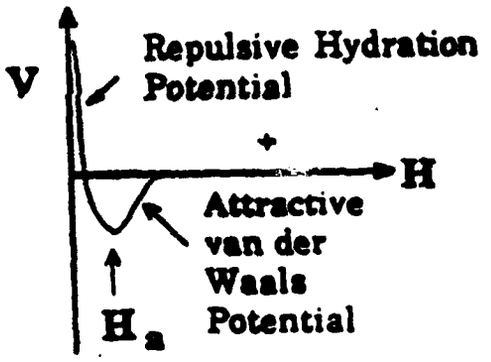

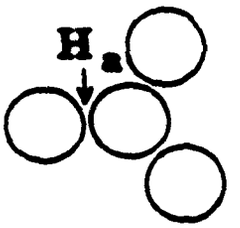

Coagulated

Weakly attractive, non-touching network

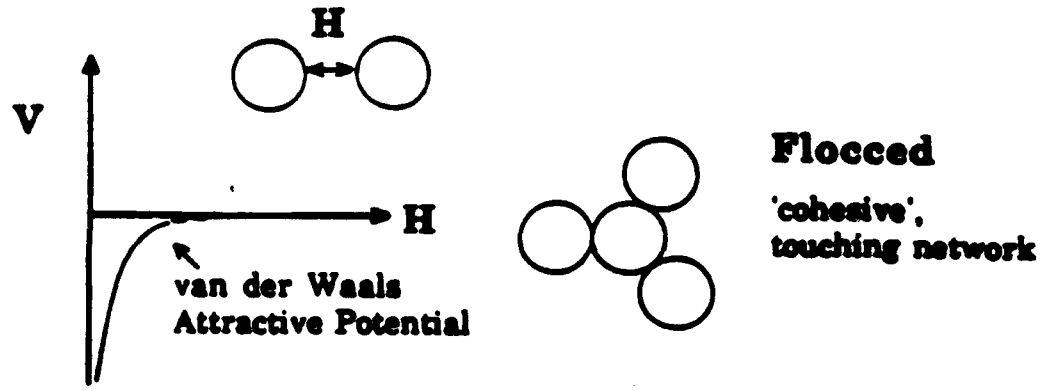

FIG. 1a

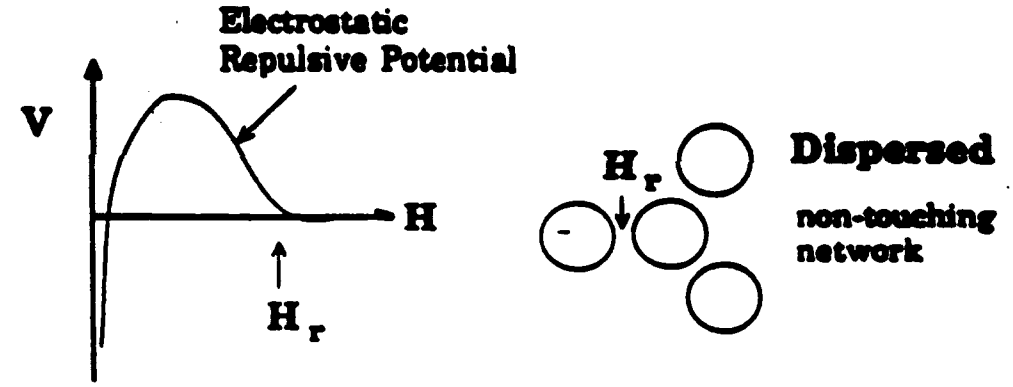

FIG. 1b

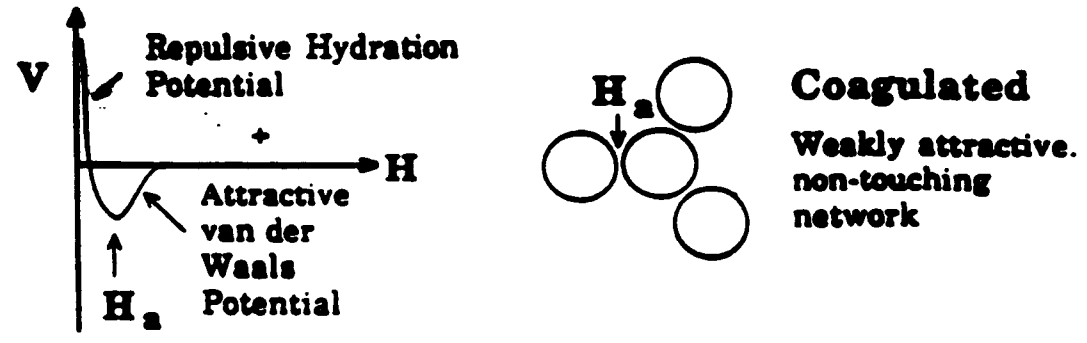

FIG. 1c

FIG. 2

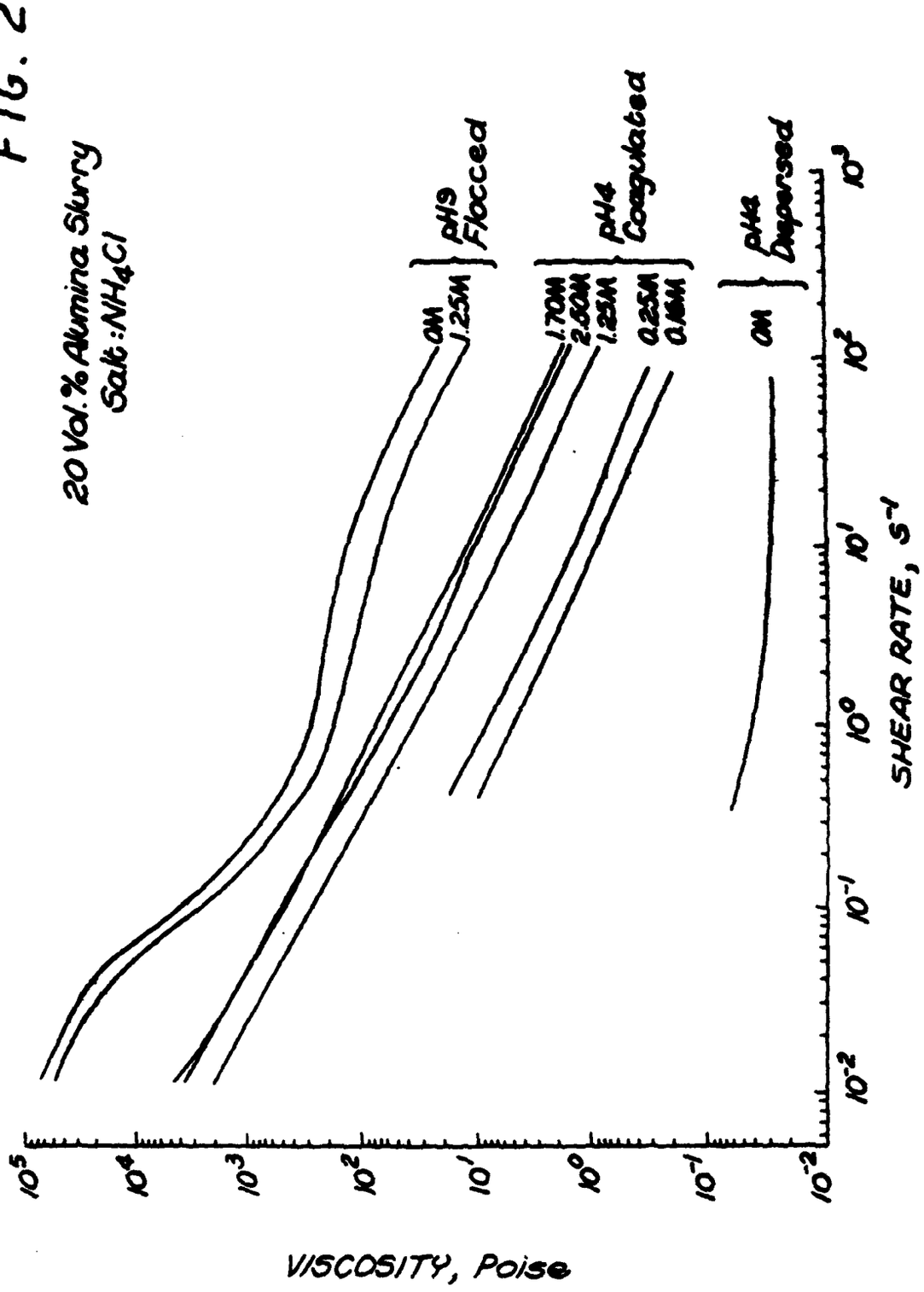
20 Vol.% Alumina Slurry
Salt: NH_4Cl
pH9 Flocced
0M
1.25M
pH4 Coagulated
1.70M
2.50M
1.25M
0.25M
0.16M
pH4 Dispersed
0M
SHEAR RATE, s^{-1}
10^{3}
10^{2}
10^{1}
10^{0}
10^{-1}
10^{-2}
10^{5}
10^{4}
10^{3}
10^{2}
10^{1}
10^{0}
10^{-1}
10^{-2}
VISCOSITY, Poise

METHOD FOR PREPARATION OF DENSE CERAMIC PRODUCTS

This invention was made with Government support under Grant (or Contract) No. N00014-90-J-1441, awarded by the Office of Naval Research. The Government has certain rights in this invention.

BACKGROUND OF THE INVENTION

The present invention relates to methods for preparation of ceramic products. In particular, the present invention relates to methods wherein compositions comprising ceramic powders are formed into a desired shape and fired to prepare the final densified product.

Current processing methods generally employ ceramics particulates dispersed in a suitable medium with volume fractions of solids close to or below the powder's maximum packing fraction. Techniques such as injection molding have found application for heat engine components (turbine rotors, stators, vanes, transition ducts, back-shrouds, etc). Other common techniques, such as tape casting and plastic extrusion, are also being used to prepare products such as electronic packaging.

Despite their widespread applications, these known techniques have significant limitations. In particular, with the exception of injection molding, the known techniques are generally not adequate to permit the preparation of ceramic products having complex shapes.

Most advanced ceramics are formed as powder compacts that are made dense by a heat treatment. Injection molding suffers from the large (between 35 and 50 volume-%) polymer content that must be slowly removed prior to high-temperature processing. Typical industrial practices for making complex-shaped ceramics have used organic liquids for dispersing fine ceramic particulates with polymeric binders and plasticizers (which may comprise as much as 50 vol. %) for easy forming and handling. Environmental restrictions and economic concerns strongly encourage the development of alternative processing methods which do not employ organic solvents or polymeric additives. In addition to their potential for toxicity, the polymeric binders and plasticizers used in injection molding pose several processing problems with respect to incomplete binder burn out (resulting in residual impurities and defects) and excessive burn out time (about 40 to 50 hrs/cc). During the removal of additives, the ceramics may undergo substantial shrinkage and distort from their desired shape. In addition, impurities left behind after binder burnout (which is often incomplete) may severely limit the mechanical properties of the ceramic. Accordingly, there is a need in the art for methods to prepare densely-packed compositions consisting essentially only of ceramic powders so as to obviate the serious problems associated with binders and plasticizers.

Powder processing involves four basic steps: (1) powder manufacture; (2) powder preparation for consolidation; (3) consolidation to an engineering shape; and (4) densification and microstructural development to eliminate void space and produce the microstructure that optimizes properties. Each step has the potential for introducing detrimental heterogeneities that either persist during further processing or develop into new heterogeneities during densification and microstructural development. Many microstructure heterogeneities stem from the powder itself; agglomerates are a major heterogeneity in powders, as are inorganic and organic inclusions. Heterogeneities are responsible for both dielectric and mechanical breakdown; with respect to the latter, each heterogeneity is a stress concentrator, and thus a potential flaw which can initiate failure prematurely. Current processing methods inherently lack a clear approach for controlling microstructure heterogeneities and uncontrolled phase distributions. Therefore, there is also a need in the art for methods which optimize processing reliability by minimizing heterogeneities and uncontrolled phase distributions.

In the search for approaches to improve known methods for preparation of ceramic products, significant consideration has been given to the nature of the interaction between ceramic powder particles suspended in a liquid medium. This interaction has generally been considered to consist primarily of electrostatic interparticle repulsive forces and van der Waals attractive forces [see generally, R. O. James, "Characterization of Colloids in Aqueous Systems," *Advances in Ceramics*, Vol. 21, pp. 349–410 (1987)]. Van der Waals interparticle potentials are always attractive between like particles. In the absence of any repulsive potential, the van der Waals potential produces very strong, attractive interparticle forces at small (<5nm) interparticle separations. In this situation, particles which are initially separated and free to move are attracted to one another and quickly attach to first form small, low density clusters. This cohesive, touching network (a flocced network as schematically illustrated in FIG. 1*a*) requires great effort to break apart. Moreover, particles colliding with nascent agglomerates as are formed in such a flocced network are unlikely to become associated with the agglomerates at precisely the position required for formation of a close-packed configuration. Therefore, the attractive forces which created flocculation tend to prevent the achievement of the densest possible packing of powder particles.

To avoid flocculation, repulsive interparticle potentials sufficient to overcome the attractive van der Waals potential must be introduced. Long range, repulsive, electrostatic interparticle potentials are developed when a surface becomes charged. Charged oxide surfaces can be produced in water when the surface reacts with either H_3O^+ or OH^- ions. By controlling the pH, a net surface charge is developed which is positive (acidic conditions), neutral, or negative (basic conditions). The pH producing the maximum surface charge (either positive or negative) depends on the surface chemistry and its equilibrium with H_3O^+ or OH^-. The surface is neutral at an intermediate pH, where the surface contains equal proportions of positive and negative sites, as well as neutral sites. Some of the ions in the solution with an opposite charge relative to the surface (known as counterions) are attracted by the surface to form a diffuse layer. Counterions do not chemically bond to the surface, but hover in solution near the surface in an attempt to shield the surface charge. For a given surface chemistry, the magnitude of the repulsive electrostatic potential depends on the magnitude of the surface charge obtained at a certain pH and on the concentration of counterions.

The DLVO theory, well known to the colloid chemist, adds the van der Waals attractive potential and the repulsive electrostatic potential to produce a combined interparticle potential that can either be repulsive or

attractive, depending on the magnitude of the repulsive potential [see generally, Horn, Roger G., "Surface Forces and Their Action in Ceramic Materials," J. Am. Ceram. Soc. 73(5):1117 (1990)]. One form of a combined interactive potential (high surface charge and low salt content) is shown in FIG. 1*b*. For this condition, as particles approach one another, they encounter a repulsive energy barrier. The particles repel one another if the energy barrier is greater than their kinetic energy. When the volume fraction of particles is increased sufficiently such that they crowd together, the particles attempt to 'sit' at positions that minimize their interaction potential, viz., at a separation distance (usually >20 nm) to form a non-touching, but interactive network schematically shown in FIG. 1*b*. As the particles are not touching one another, this is called a 'dispersed' network.

If the repulsive component of this combined potential is reduced (*e.g.*, by decreasing the surface charge through a change in pH), a condition can be achieved where the repulsive barrier is no longer sufficient to prevent particles from slipping into the deep potential well caused by the van der Waals attractive potential so as to produce the strongly cohesive, touching network described above. According to the DLVO theory, particles should always fall into a deep potential well to form a cohesive flocced network when conditions are much less than optimum, even though the combined repulsive interaction (magnitude of the repulsive barrier and equilibrium separation distance) may be controlled and optimized by, e.g., controlling pH. DLVO theory thus offers no help in understanding whether or how one might control the depth of the attractive well.

It is an object of the present invention to provide techniques for preparing ceramic products from particles which have been as densely packed as possible, using a minimum amount of non-ceramic additives (such as binders and plasticizers).

It is a further object of the present invention to provide manufacturing technology capable of producing high-volume, near-net-shape powder compacts that can be subsequently densified by heat treatment.

It is an additional object of the present invention to provide methods which permit the formation of complex shapes during initial stages of processing that are within a tolerance envelop of the desired shapes after the final stages of processing, such that any shrinkage associated with densification might change the dimensions but not the shape of the final product.

It is yet another object of the present invention to provide fabrication methods for preparation of dense, complex-shaped ceramic products, which methods are simple and inexpensive to use, yet able to handle complex shapes.

SUMMARY OF THE INVENTION

Pursuant to the present invention, complex and near-net-shaped ceramic powder compacts are formed using a technique which involves forming a liquid saturated powder compact, consolidating the compact (for example, by pressure filtration or centrifugation), and shaping the compact to the desired dimensions. To prepare the shaped body, the compact may advantageously be introduced into a suitably-shaped mold cavity and vibrated gently. During vibration, the liquid saturated powder compact becomes sufficiently fluid to fill the cavity. After the vibration is stopped, however, the powder compact (now having the shape of the cavity) becomes sufficiently stiff to retain its shape without distortion. The unique rheology of the powder compact is produced in accordance with the invention by manipulating interparticle forces of the ceramic powder to develop a weakly attractive particle network, with properties distinct from either the flocced networks or the dispersed networks predicted by DLVO theory.

BRIEF DESCRIPTION OF THE DRAWINGS

The invention may be better understood with reference to the accompanying drawings, in which:

FIGS. 1*a*-1*c* are schematic representations of flocced, dispersed and coagulated networks, respectively; and

FIG. 2 is a graph showing the viscosity vs shear rate for a series of aqueous slurries containing 20 volume % of an aluminum oxide powder.

DETAILED DESCRIPTION OF THE INVENTION

In accordance with the present invention, short-range surface repulsive forces which may be introduced on highly charged ceramic particles in aqueous media are used to provide a lubricating effect between particles. Due to such lubrication effects, the ceramic particles in the slurry may be packed to a density which could not heretofore be achieved due to the formation of cohesive, flocced networks. Therefore, by exploitation of the lubrication effects, a maximum particle packing density is obtained when the slurry is formed into a consolidated body, for example by pressure filtration or centrifugation.

The saturated consolidated body exhibits plastic flow behavior similar to that heretofore observed only for some types of clay bodies. The consolidated bodies prepared in accordance with the present invention, exhibiting plasticity and a very high particle packing density, can be made to flow and fill even a complex-shaped die cavity simply by placing the saturated powder compact in the cavity and subjecting the material to vibration (for example, by shaking). Little effort is generally required to form complex-shaped molded products; moreover, the thus-formed products tend to maintain their complex shapes even after removal from the mold. After drying, the products may be densified by a conventional high temperature heat treatment. Unlike the heretofore known materials, the near-net-shaped compacts retain their molded shape upon densification, with substantially uniform shrinkage.

The weakly attractive interparticle forces are produced by a combination of the longer range, electrostatic repulsive forces and attractive van der Waals forces contemplated according to DLVO theory with a third type of very short range ($\leq$5 nm), repulsive hydration forces. These short range, repulsive hydration forces prevent the attractive particles from touching one another. Accordingly, under appropriate conditions these forces allow particles to slide pass one another easily and pack to a higher density during consolidation than would otherwise be the case either with dry solid particles or with touching particle networks. This third, repulsive potential only acts when the separation distance between the surfaces is very small (i.e., less than about 5 nm), where the attractive van der Waals potential becomes strong.

The formation and properties of hydration layers in solutions of plate-like clay particles is known, and the influence of hydration layers on interactions between

molecularly smooth mica surfaces has been reported [Pashley, R. M., "DLVO and Hydration Forces between Mica Surfaces in Li^+, Na^+, K^+, and Cs^+ Electrolyte Solutions: A Correlation of Double-Layer and Hydration Forces with Surface Cation Exchange Properties," *J. Colloid and Interface Science* 83(2):531-546 (1981)]. It has now unexpectedly been found that this hydration layer repulsion phenomenon is not limited to situations where plate-like surfaces (as are found with clay particles) exhibit surface-charging behavior.

In experiments with Al_2O_3 powders, salt was added to an aqueous Al_2O_3slurry prepared at a pH known to produce a positive surface charge and a highly dispersed particle network. Hydrated anions were attracted to the positively charged Al_2O_3 surface. When sufficient salt was added to the slurry it was noted that the dispersed network was altered to what superficially appeared as a flocced network predicted by the DLVO theory. After further experiments, it was concluded that the salt did change the dispersed network to an attractive network, but that this new attractive network was not cohesive. That is, unlike a flocced network, the particles in this network could easily be rearranged.

Additions of more counterions continuously reduced the electrostatic repulsive potential. This dispersed particle network became an attractive network above an optimal concentration of counterions due to the persistent van der Waals potential. As the hydrated counterions reduced the electrostatic repulsive potential, they also appeared to form a hydrated surface layer; thus, they built a strong, short range repulsive hydration potential. Instead of falling into the deep potential well to produce a cohesive, touching network predicted by DLVO theory, the particles slipped into a well with a more modest depth to produce an attractive, but non-touching, particle network called a "coagulated" network (as schematically illustrated in FIG. 1*c*).

In accordance with preferred embodiments of the present invention, coagulated ceramic particle networks are formed by adjustment of the pH of a dispersed slurry of the particles and of the amount of salt added to the slurry. This in turn controls the residual long range electrostatic repulsive potential, and possibly the strength of the short range repulsive hydration potential as well. No additional effects are observed when the salt concentration is greater than an optimal value (i.e., an amount of salt which reduces the long-range electrostatic repulsive potential to zero). This suggests that hydrated counterions are no longer attracted to the surface, all of the electrostatic repulsive potential is dissipated, and the system resides in the deepest potential well that can be established when the repulsive hydration potential is summed with only the attractive van der Waals potential. This state appears to produce the strongest, non-touching coagulated particle network, but a much weaker network relative to the flocced network.

The particular salt or salts employed is not critical to the present invention; a wide variety of organic and inorganic salts would in principle be useful in developing a coagulated particle network due to the short range repulsive potential of the charged ceramic particles. Depending upon the composition of the specific ceramic particles, however, in certain instances particular types of salts might be inappropriate by virtue of the possibility that the salts would react with the ceramic particles, and such salts would therefore be avoided in those instances. Otherwise, the choice of salt would readily be made by one familiar with the nature and properties of the ceramic powder. Inorganic salts, such as NaCl, NH_4Cl, NaI, etc., are suitable for use with most ceramic powders and are considered in detail in the accompanying examples.

In accordance with a preferred embodiment of the present invention, a water saturated powder compact containing a weakly attractive particle network for use in accordance with the inventive method may be produced by the following sequence of operations: (1) forming a dispersed slurry (i.e., a mixture of powder and liquid) by mixing a ceramic powder (generally comprising less than 30 volume % powder) with water at a pH that produces a net surface charge and a highly repulsive interparticle force; (2) adding a sufficient amount of a salt to the dispersed slurry to cause particles within the slurry to attract one another; and (3) increasing the volume fraction of particles (by, e.g., pressure filtration or centrifugation) to form a water saturated powder compact with a uniform and very high particle packing density. The coagulated slurry has a higher viscosity at a given volume fraction of powder relative to a dispersed slurry. Thus, if the volume fraction of powder were too high in the coagulated slurry (i.e., substantially greater than about 30 volume %), its rheology would be that of a paste, rather than a flowable slurry suitable for pouring and further processing (e.g., pressure filtration or centrifugation). After consolidation, the attractive forces between particles within the powder compact saturated with water are sufficiently strong to prevent body flow, but sufficiently weak to produce flow when the body is subjected to a modest vibration. The compact is then formed into a desired shape and fired to provide the final ceramic product.

The implications of the particle networks have direct bearing on the particle packing density as well as on the rheology of pressure-consolidated particulate bodies and on processing ceramics and their composites. Fig. 2 shows the viscosity vs shear rate for a series of aqueous slurries containing 20 volume % of an aluminum oxide powder. The viscosity of the dispersed slurry (prepared at pH =4, without added salt) is low and relatively independent of shear rate; it represents the behavior of a highly repulsive particle network (FIG. 1*b*). The viscosity of the flocced slurry (pH=9, with and without salt additions) is highest relative to other slurries and exhibits extensive shear thinning indicative of a strongly cohesive, touching particle network (FIG. 1*a*). The influence of salt (NH_4Cl) additions on the viscosity of dispersed 20 volume % alumina slurries (at pH=4) is shown by a series of curves between the curves for the dispersed and flocced slurries. As shown, the added salt increases the viscosity of the slurry and produces shear thinning behavior indicative of a weekly attractive, non-touching, coagulated network (FIG. 1*c*).

The behavior of the coagulated slurries was dependent on NH_4Cl concentration, i.e., their viscosity at any shear rate increased over four orders of magnitude. No further changes in viscosity were observed when the salt concentration exceeded a saturation maximum of 1.7 M NH_4Cl, which is the maximum practical value of added salt for this system. While the degree (slope of the viscosity vs shear rate curve) of shear thinning is similar to that of flocced slurries, the magnitude of the viscosity at any shear rate depended on the amount of added salt. At a salt content greater than or equal to the saturation maximum (which, in this case, is also the maximum practical salt concentration), the viscosity of

the coagulated slurries is about one order of magnitude lower than that for the flocced slurries. This behavior suggests that a similar attractive network exists within both the coagulated and flocced slurries, but that the magnitude of interparticle attraction is altered by the salt concentration.

As shown in FIG. 1c, the particles in coagulated slurries are weakly held together in a shallow "hydration minimum". The depth of the hydration minimum controls the strength of the attractive but non-touching particle network in the coagulated slurries. The data shown in FIG. 2 strongly suggests that the attractive particle network becomes stronger with added salt, but never as strong as the flocced network.

In accordance with preferred embodiments of the present invention, the addition of appropriate amounts and types of salts is employed to decrease the magnitude of the long range electrostatic repulsive force. Powders that react with acidic or basic water are positively charged on the acidic side (i.e., at low pH) and negatively charged on the basic side (at high pH). Depending on the surface chemistry of a given powder, at a particular pH the particles are neutral (i.e., the number of positive surface sites equals the number of negative sites). This pH is defined as the point of zero charge (PZC). One may determine the PZC, and thus the pH that separates positively from negatively charged surfaces, by a variety of known techniques. Using electrophoretic techniques, for example, the slurry is placed between a potential gradient and the particle velocity is determined. For alumina, the PZC is about pH 9; for silica, about pH 4. For silicon nitride, the PZC is between about pH 4 (if the surface is highly oxidized to resemble silica) and about pH 7 (for a less oxidized surface).

The pH range to which the powder is appropriately brought before adding the salt is variable, and is determined relative to the PZC for that powder. Preferably, the pH is as close as possible to the value(s) where the surface charge may be brought to the maximum (i.e., a pH at an optimum variance from the PZC). For example, for alumina powder an optimum pH is between about 2 and 4; this range produces the largest positively-charged surface, and thus the largest interfacial potential difference (zeta potential). For other powders, the optimum pH range for formation of a coagulated network may be determined in a manner known per se using, e.g., electrophoretic measurements which define the zeta potential vs. pH.

Up to a particular salt concentration for each ceramic particle system, increasing additions of salt increase the magnitude of the attractive interparticle forces. Determination of an effective salt concentration range for use with any given ceramic powder material may be carried out empirically in a manner known per se by those skilled in the art of colloid chemistry. The desired coagulated network can be formed within a range of added salt concentrations; for example, with alumina powder, it may range between about 0.1 and about 1.7M NH_4Cl. Any concentration within this range would be a sufficient amount of added salt to form a coagulated network. As shown in FIG. 2, the amount of salt added within this range only changes the strength of the coagulated network; the method of the invention may be carried out with any network strength, as long as the desired coagulated network is formed.

Determination of the minimum amount of salt necessary to just produce an attractive particle network may be determined for any given powder by first producing a dispersed slurry at the appropriate pH and then adding small, known increments of salt until the particles within the slurry attract one another. In dilute slurries (for example, those containing less than about 1 to 3 volume-% of powder), the formation of an attractive network may be monitored visually; groups of particles come together to form noticeable agglomerates, changing the texture of the slurry.

Alternatively, the minimum amount of salt necessary to form an attractive particle network may be determined using sedimentation columns. Slurries containing different salt contents are allowed to sediment in columns for several hours. The slurry with the minimum salt content that develops a clear supernatant defines the minimum salt content necessary for attractive network formation. This concentration is known as the critical coagulation concentration.

The maximum practical value of salt content (i.e., the salt concentration above which further additions of salt have no effect on network strength) is determined through viscosity versus shear rate measurements, as are shown in FIG. 2. Above the maximum practical salt concentration, there is no observed change in viscosity. At or near the maximum practical concentration, there is achieved an interparticle network of maximum strength. For purposes of the present invention, however, it is not essential that the strongest interparticle network be formed.

Slurries used to form the saturated powder compacts used in this method exhibit extensive shear thinning behavior, i.e., they decrease their viscosity by more than three orders of magnitude with increasing shear rate. The saturated powder compacts used in the inventive method of forming complex-shaped articles themselves exhibit extensive shear rate thinning. This allows the compact to behave in a sufficiently liquid-like manner when vibrated to fill a complex mold cavity, but allows the newly-shaped article to retain its shape once the vibration is stopped. It is development of the coagulated network (the particles are weakly attractive but non-touching due to short range repulsive forces) which imparts to both the slurry and the saturated powder compact derived therefrom the characteristic rheological properties exploited in accordance with the present invention. Both the slurry and the particle compact behave in a manner heretofore observed only with materials like clay; while clay materials appear to develop their short range repulsive potential naturally, it has heretofore not been observed and would not have been expected that ceramic powders could be manipulated in a manner such that materials with such properties could be prepared therefrom.

Colloidal powder treatments (sedimentation and/or filtration) can be used to eliminate many heterogeneities common to powders and ensure more uniform phase distribution. This permits the preparation of ceramics of enhanced uniformity and with greater reliability. In addition, this method is not only extremely simple, inexpensive and safe but also avoids the use of organic solvents, polymeric binders and plasticizers.

To consolidate particles into saturated powder compacts, the volume fraction of particles within a slurry is increased by particle partitioning methods, such as pressure filtration and/or centrifugation. Increasing the volume fraction of particles also changes the slurry rheology. The highest volume fraction of particle that can be packed together for a given consolidation pres-

sure will depend on the interparticle potential. The viscosity of the densely packed particle slurry is extremely high and it behaves much like a solid at slow shear rates. These densely packed slurries can thus be considered as saturated powder compacts. The rheology of the saturated powder compacts depends on the interparticle potential.

Pressure filtration is one suitable method for consolidating powders. A slurry (for example, alumina powder in water) confined within a cylinder is acted upon at one end by a plunger which forces the fluid within the slurry through a filter at the other end. Particles within the slurry are trapped at the filter to build up a consolidated layer as fluid is forced through the layer and then through the filter. Pressure filtration concentrates the particles within the slurry to form a layer consisting of densely packed particles. After a single layer of particles is trapped by the filter, the trapped particles themselves become part of the filter through which fluid must flow t trap more particles. The consolidated layer thickens in proportion to the amount of slurry filtered; consolidation stops when the top of the layer encounters the plunger. At this point, all of the particles which were initially in the slurry are densely packed within the consolidated body and any space left within the densely packed particles is filled with fluid. The consolidated body is then removed from the cylinder. Additional fluid can be removed by evaporative drying.

For powders comprising dense, spherical particles, pressure filtration studies have shown that interparticle forces have the greatest effect on particle packing density. Dispersed slurries (highly repulsive interparticle forces) produce much higher packing densities than flocced slurries (highly attractive interparticle forces); particularly high particle packing densities can be achieved pursuant to the present invention using coagulated slurries (short range hydration layer repulsion).

Centrifugation is another technique for fractionating colloidal slurries. Particles in a slurry are centrifuged into a mold, followed by decantation of the supernatant liquid and removal of the packed particulate body from the mold. The stress is applied to each element of the component rather than to its exterior. An obvious consideration is the effect of polydispersity in particle size, as sedimentation rates during centrifugal acceleration vary with particle size and density. The use of flocced or coagulated rather than dispersed particulate systems can overcome this difficulty, as a flocced or a coagulated system consolidates as a network rather than by motion of individual particles. Uniform packing densities in centrifuged particulate bodies can be also achieved by processing with concentrated dispersed slurries; however, as indicated above, processing with concentrated dispersed slurries is extremely complex. Centrifugation can be conveniently used to uniformly pack polydispersed particles from coagulated slurries without being concerned about mass segregation.

The influence of interparticle forces on the rheology of consolidated bodies has been characterized with the help of stress relaxation experiments. A fixed compressive strain was applied to saturated consolidated bodies made by pressure filtration and the accompanied stress relaxation as a function of time was recorded. The stress relaxation behavior is an indirect indication of the rheology of the consolidated bodies. As consolidated particulate bodies consisting of attractive forces tend to be solid-like or elastic, these bodies only relax to about 70% of the peak stress. However, consolidated bodies made from dispersed as well as coagulated slurries exhibit plastic behavior. The consolidated bodies made from coagulated slurries consistently appear to have better shape retention characteristics when compared to a body made from a dispersed slurry, because they exhibit a yield stress for plastic flow. An important characteristic of the bodies made from coagulated slurries is that the plastic flow behavior is retained when stored without moisture loss for as much as a week to ten days.

The inventive method is applicable to the preparation of complex shaped bodies from a wide variety of different ceramic powders. For purposes of the present invention, ceramic powders are contemplated as including all non-metallic, inorganic materials which may be formed into a desired shape and then treated (typically, by heating) to form a final ceramic product. As is well known in the art, this class of ceramic powders includes a wide variety of different classes of compounds, including in particular oxides, nitrides, borides, carbides and tellurides. For example, the following materials have all been used to prepare ceramic products: alumina, zirconia, titania, silica, lead oxide, silicon carbide, silicon nitride and yttria, as well as mixtures thereof. Further, powders containing more than one metal ion (e.g., binary and ternary compounds) are also clearly suitable for use in accordance with the present invention. In addition, while the materials are generally employed in a particulate form, for particular end uses it may be desirable to use these materials in alternative formulations as are well known in the art (such as disks, whiskers, etc.).

The following examples serve to illustrate various aspects of the present invention.

EXAMPLES

Example 1

Slurry Preparation

Aqueous slurries containing 20 vol. % α-alumina powder (0.4 μm median size) were used in this study. All the slurries were prepared by first dispersing the as-received powder in deionized water at pH4 without ionic strength adjustments. At pH4 (O M NH_4Cl) the zeta potential of alumina is sufficiently large to keep particles dispersed through strong electrostatic repulsion. A high shear-field, obtained by immersing an ultrasonic horn in the slurry, aided in breaking apart soft agglomerates. Finally, ionic strength and/or pH adjustments of slurries were made as required. Analytical grade HNO_3 and NH_4OH were used for pH adjustments; analytical grade NH_4Cl was used for ionic strength adjustments.

The following terminology is adopted to distinguish between the three types of alumina slurries that were used in this study: (1) slurries at pH 9 with and without NH_4Cl are "flocced"; (2) slurries at pH4 without NH_4Cl are "dispersed"; and (3) slurries at pH4 with NH_4Cl are "coagulated". In the present study, the ionic strength in coagulated slurries is adjusted to 1.5 M.

Consolidation

Pressure filtration was used to make consolidated ceramic bodies using the coagulated alumina slurry. A predetermined volume of slurry was poured into a cylindrical filtration die 2.54 cm in diameter to make consolidated bodies having a thickness of 1 to 1.5 cm once filtration was complete. A final consolidation pressure

of 14.6 MPa was used in all the experiments. The alumina powder used in the present study could be packed to a maximum density of 0.62. After pressure filtering the coagulated slurry, the consolidation body was ejected from the die and was immediately transferred into a zip-lock plastic bag containing a moist paper towel and sealed to prevent the sample from drying. The presence of the moist towel was to ensure 100% humidity in the sealed bag so as to prevent the body from drying during storage.

Epoxy Mold Preparation

A tapered rotor shaped plastic male die (3 cm in diameter and 2.5 cm in height) was prepared using an epoxy mold containing the rotor-shaped cavity. The epoxy mold was prepared by the following procedure. The plastic die was initially coated with a silicone die release agent. Then the die was placed upright resting on its wide base in a paper cup. A sufficient amount of quick set epoxy resin was prepared and carefully pored over the plastic die in the cup. After allowing the assembly to set for 15 minutes, the die was separated from the epoxy resin. This procedure allowed making casting molds with excellent dimensional stability and surface smoothness. These molds were used subsequently for casting the plastic ceramic.

Ceramic Shape Forming

Prior to ceramic molding, the epoxy mold was given a thin coat of high vacuum silicone grease to allow the molded ceramic to be easily removed. The saturated powder compact (stored in a plastic bag) was then placed in the cavity of the mold. The mold containing the saturated powder compact was then caused to flow into every part and corner of the mold by gently tapping the mold on the table. This tapping produced sufficient vibrations to impart viscous flow to the plastic body, which facilitated filling every part of the mold. In addition to the plastic flow, during the course of tapping expulsion of air bubbles initially trapped between the plastic body and the mold walls was observed to have taken place. Once all the material is evenly distributed in the mold, the tapping was stopped and the saturated particulate body (along with the mold) was weighed. After 24 hours of air drying and 12 hours of oven drying at 60° C., the shaped body shrank (about 1%); this facilitated removal of the cast body without damage. Assuming that the body contained only alumina powder and water, the saturated packing density was again determined by weighing the body before and after drying. The shaped ceramic had a relative packing density of 62%, i.e., identical to the saturated powder compact body formed by pressure filtration.

Heat Treatment of the Ceramic

The dried ceramic particulate articles were first heat treated at 300° C. to sublime NH_4Cl from the ceramic. Thereafter, the ceramic was densified at 1550° C. for 3 minutes. The densified alumina body had a relative density of 98% (i.e., 98% of the theoretical density of aluminum oxide).

Example 2

Attempts were also made to form a complex ceramic shape (e.g., a gear) using the procedure described in Example 1. Although the attempts were extremely successful with respect to making the epoxy mold, filling the mold with the saturated consolidated body (pH4, 1.5 M NH_4Cl), and drying the ceramic without cracking, the dried ceramic could not be removed from the mold without damage. Therefore, a second casting procedure was adopted, in which silicone rubber was substituted as the mold material. Once cured, silicone rubber exhibits some flexibility, yet it is rigid enough to be an ideal material for forming complex shapes.

Silicone Rubber Mold

Except for the different mold making material, for making a mold containing a gear-shaped cavity the procedure is similar to that of the epoxy mold preparation procedure described in Example 1. Dow Corning silicone rubber (3112 RTV) wa mixed thoroughly with 10 vol. Dow Corning catalyst (RTV 1) and then the mixture was degassed to expel any entrapped air. The mixture was then carefully poured over a greased metal gear. After 12 hours of curing at room temperature, the metal gear was removed from the hardened rubber cast by simply pushing the gear out of the mold.

Casting of the Ceramic Gear

Making of the saturated consolidated body, shaping it in silicone rubber mold, and drying the ceramic in the mold was done as per the procedure described in Example 1. Finally, the dried ceramic was ejected out of the mold with gentle squeezing. About 95% of the gear teeth remained unbroken. An optical micrograph comparison of the ceramic gear adjacent to the metal gear confirmed that the quality of gear reproduction as well as the surface reproduction was excellent, particularly in view of the small dimensions of the gear teeth (minimum width of 0.72 mm). This demonstrates that the present technique can be used for making complex shaped ceramic parts. Thorough coating of the rubber mold with silicone grease (stripping agent) prior to ceramic casting is observed to be a most important factor in producing a ceramic gear with all of its teeth remaining. The dried and sintered ceramic prepared in this manner showed remarkable reproduction of the original gear.

Example 3

Lubricating surface layers as formed on alumina particles in Examples 1 and 2 can also be introduced into other ceramic systems such as zirconia, titania, silica, silicon carbide, silicon nitride, etc. In the present example, surface hydration layers were introduced on zirconia containing 3 mole % yttria (Tosoh-Zirconia TZ-3Y, Minato-ku, Japan). A 10 vol. % zirconia was dispersed in water at pH 2.8 and equilibrated while the slurry was being ultrasonicated. Later, the surface lubricating layers were formed on zirconia by adding 1.5 NH_4Cl and the pH readjusted to 2.8. The slurry was then pressure filtered, as per the procedure described in Example 1. The consolidated body was thereafter placed in the epoxy mold (consisting of a rotor-shaped cavity, as described in Example 1) and the entire assembly was tapped for the plastic consolidated body to flow into the mold. The shaped ceramic was allowed to dry in the mold; after drying, the relative particle packing density of the ceramic was 50%. The dried ceramic was ejected from the mold as per the procedure described in Example 1.

Example 4

All commercial submicron sized ceramic powders consist of heterogeneities such as coarse particles, hard

agglomerates, organic and inorganic inclusions. Such heterogeneities, if not separated from powder prior to consolidation, can act as stress concentrators in the densified ceramic and can adversely affect the mechanical properties of the ceramic. It has been demonstrated that colloidal methods, i.e., methods of controlling and manipulating the forces between particles within a liquid, can be used to fractionate from powders heterogeneities (e.g., agglomerates and inclusions) that would otherwise lead to strength degrading flaw populations. That is, colloidal methods to treat powders have the potential to produce more reliable ceramic materials. Because drying can reintroduce heterogeneities, colloidally treated powders must be packed into a shape from their slurry state. High particle packing densifies the powder compact. In addition, mass and/or phase segregation during consolidation must be avoided.

Preparation of Coagulated Ceramic Slurries Free of Heterogeneities

In both the traditional approach of powder fractionation and the improved method suggested in the present disclosure, the first few steps of the process are essentially the same, i.e., (1) disperse ceramic powder in pure water at a pH where the interparticle interactions are predominately repulsive; (2) ultrasonicate the particulate slurry to break apart the soft agglomerates in the powder; (3) sediment the slurry for a given length of time to separate coarse particle, hard agglomerates and other impurities (for a given particle size the duration of sedimentation can be approximately estimated by Stokes' equation); and (4) carefully siphon the supernatant containing desired colloidal particles into a separate container.

In the traditional approach, the particles in the supernatant are flocced by adjusting the pH to the point of zero charge and allowing the flocced particles to sediment. Flocculation of the desired fraction of the powder in the supernatant serves two functions. First, it concentrates the slurry for downstream processing needs. Second, flocculation prevents segregation of coarse and fine particles during storage and handling. This step is followed by using the slurry for consolidation prior to which one may or may not disperse the slurry. Because of their strongly attractive particulate network, flocced slurries always pack to a lower density than the dispersed state. One may pack the particles to their highest density in the dispersed state in the absence of mass segregation.

Coagulation instead of flocculation offers an ideal and efficient alternative for colloidal fractionation and processing of ceramics powders. In an improved method of colloidal powder fractionation, a salt of known concentration is added to the supernatant containing the dispersed colloidal particles. The addition of the salt to the dispersed slurry destabilizes the particles, leading to coagulation. The coagulated particles sediment and the supernatant can be removed. The slurry containing the coagulated particles can be directly used in consolidation, since particles in the coagulated slurries pack to the maximum density.

The concentrated coagulated slurry can be used to make useful ceramic shapes following the procedure described in Example 1 or 2.

Example 5

Another potential advantage of colloidal methods, in addition to removal of heterogeneities, is its ability to mix two or more powders to produce more uniform multiphase ceramic bodies. This allows one to manufacture composite ceramics. The second phase material can be an alloying agent and/or a reinforcement (particle, whisker, fiber, disc etc.). Typical examples of the first kind of composite are Al_2O_3-ZrO_2, Al_2O_3-MgO, etc. Examples of the other kind of composite include Al_2O_3-SiC (whisker), Si_3N_4-SiC etc.

For making these composites, one either treats individual ceramic powders to fractionate heterogeneities (as per Example 4) followed by either mixing them together and then coagulating them or by mixing the coagulated slurries at a high shear rate sufficient to break apart the coagulated networks and form a new coagulated network containing both phases. When mixed in a slurry state, this type of multicomponent dispersions can be mixed thoroughly and uniformly. The composite coagulated slurry is transformed into useful ceramic components as per the procedure described in Example 1 and 2.

While the invention has been described with reference to exemplary embodiments thereof, it should be noted by those skilled in the art that the disclosures are exemplary only and that various other alternatives, adaptations and modifications may be made within the scope of the present invention. Accordingly, the present invention is not limited to the specific embodiments as illustrated herein, but only by the following claims.

What is claimed is:

1. A method of preparing a dense ceramic product, comprising:
   (1) forming a coagulated network of ceramic powder particles in water by adjustment of the pH of a dispersed slurry of said ceramic powder particles in water to a pH that produces a net surface charge and addition of a sufficient amount of a salt to the dispersed slurry to form said coagulated network;
   (2) treating said coagulated network of ceramic powder particles in water to increase the volume fraction of said powder particles, thereby forming a water saturated powder compact; and
   (3) firing the compact to provide said dense ceramic product.

2. A method according to claim 1, wherein the compact is formed into a desired shape prior to firing.

3. A method according to claim 2, wherein said desired shape is formed by introducing the compact into a mold and subjecting the mold to vibration sufficient to induce flow of the compact, whereby the compact adopts the shape of the mold.

4. A method according to claim 1, wherein said coagulated network is formed by:
   mixing a ceramic powder with water at a pH that produces a net surface charge, to form a dispersed slurry; and
   adding a sufficient amount of salt to the dispersed to cause particles within the slurry to form a coagulated network.

5. A method according to claim 1, wherein the dispersed slurry comprises less than about 30 volume % ceramic powder.

6. A method according to claim 1, wherein said salt is selected from the group consisting of organic salts, inorganic salts and mixtures thereof.

7. A method according to claim 6, wherein said salt is an inorganic salt.

8. A method according to claim 7, wherein said inorganic salt is selected from the group consisting of alkali

halides, alkali earth halides, ammonium halides and mixtures thereof.

9. A method according to claim 1, wherein the ceramic powder is selected from the group consisting of oxides, nitrides, carbides, borides and tellurides.

10. A method according to claim 9, wherein the ceramic powder is selected from the group consisting of alumina, zirconia, titania, silica, silicon carbide, silicon nitride, yttria, lead oxide and mixtures thereof.

11. A method according to claim 1, wherein the volume fraction of particles is increased by pressure filtration.

12. A method according to claim 1, wherein the volume fraction of particles is increased by centrifugation.

13. A method according to claim 1, wherein said firing comprises a first heating step at a first temperature sufficient to evaporate water and pyrolyze salt from the shaped compact, followed by a second heating step at a second temperature sufficient to densify the shaped compact.

14. A method according to claim 1, wherein said coagulated network is formed by:

dispersing the ceramic particles in water at a pH that produces a net surface charge, to form a dispersed slurry;

ultrasonicating the slurry to break apart agglomerates;

sedimenting the slurry to separate remaining strong agglomerates and inclusions;

siphoning off supernatant containing desired colloidal particles; and

adding a sufficient amount of salt to the supernatant to form a coagulated network.

15. A method according to claim 1, wherein said coagulated network of ceramic powder particles in water comprises at least two different types of ceramic powder particles.

16. A method according to claim 15, wherein said coagulated network is formed by:

mixing each ceramic powder separately with water at a pH that produces a net surface charge with that powder, to form a plurality of dispersed slurries;

combining said plurality of dispersed slurries to form a mixed slurry; and

adding a sufficient amount of salt to the mixed slurry to cause particles within the slurry to form a coagulated network.

17. A method according to claim 15, wherein said coagulated network is formed by:

mixing each ceramic powder separately with water at a pH that produces a net surface charge with that powder, to form a plurality of dispersed slurries;

adding a sufficient amount of salt to each of said plurality of dispersed slurries to cause particles within each slurry to form a coagulated network, thereby forming a plurality of coagulated slurries; and

combining said plurality of coagulated slurries at a high shear rate sufficient to break apart said coagulated networks and form a new coagulated network.

* * * * *

MATERIALS

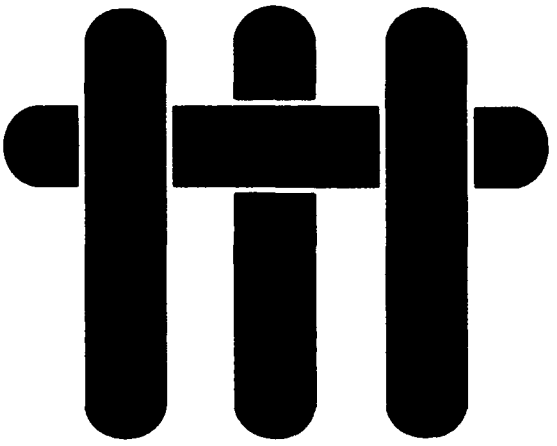

Technical Report Number 12

US Patent 5, 284, 698
Partially Stabilized ZrO_2-Based Laminar Ceramic Composites

David B. Marshall*, Fred F. Lange and Joseph J. Ratto*

* Rockwell International Science Center, Thousand Oaks, CA

Office of Naval Research

Grant No. N00014-90-J-1441

Fred F. Lange

Principal Investigator

Materials Department
University of California
Santa Barbara, CA 93106

US005284698A

United States Patent [19]

Marshall et al.

[11] Patent Number: 5,284,698

[45] Date of Patent: Feb. 8, 1994

[54] **PARTIALLY STABILIZED ZrO_2-BASED LAMINAR CERAMIC COMPOSITES**

[75] Inventors: **David B. Marshall**, Thousand Oaks; **Frederick F. Lange**, Santa Barbara; **Joseph J. Ratto**, Newbury Park, all of Calif.

[73] Assignees: **Rockwell Int'l Corp.**, Seal Beach; **Regents of the University of California**, Oakland, both of Calif.

[21] Appl. No.: **761,581**

[22] Filed: **Sep. 18, 1991**

[51] Int. Cl.[5] **B32B 18/00**

[52] U.S. Cl. **428/216**; 123/41.84; 428/212; 428/697; 428/701; 428/702

[58] Field of Search 428/336, 212, 701, 702, 428/697, 216; 415/174; 123/41.84

[56] **References Cited**

U.S. PATENT DOCUMENTS

4,503,130	5/1985	Bosshart et al.	428/632
4,588,607	5/1986	Matarese et al.	415/174
4,600,038	7/1986	Matsui et al.	123/41.84
4,676,994	6/1987	Demaray	427/255.3
4,966,820	10/1990	Kojima et al.	428/701

OTHER PUBLICATIONS

Jones et al "Hot Corrosion Studies of Zirconia Ceramics" Surface and Coatings Tech, 32(1987) p. 349-358.

Primary Examiner—A. A. Turner

Attorney, Agent, or Firm—John C. McFarren

[57] **ABSTRACT**

In a Ce-ZrO_2-based laminar composite having enhanced fracture toughness, alternating barrier layers comprise a ceramic material that undergoes stress-induced phase transformation, if any, less readily than Ce-ZrO_2. Separation of the barrier layers is normally in the range of about 10-200 μm, with optimum individual barrier layer thicknesses at the lower end of the range. Powders of ceramic materials comprising the individual layers of the composite are dispersed in separate slurries. The pH of the slurries is adjusted to form coagulations in which the particles settle without mass segregation and can be consolidated to high density by centrifuging. After centrifuging, the supernatant liquid can be removed and a desired volume of another slurry can be added on top of the first layer of consolidated material. This process can be repeated indefinitely to form a consolidated structure having individual layers as thin as approximately 10 μm. The consolidated structure may be pressed, shaped, dried, and sintered to form the laminar composite. In the composite, interactions between a barrier layer and the martensitic transformation zone surrounding a crack or indentation spread the transformation zone along the region adjacent to the barrier layer. As a result, barrier layers provide large increases in toughness for cracks growing parallel or normal to the layers.

9 Claims, 2 Drawing Sheets

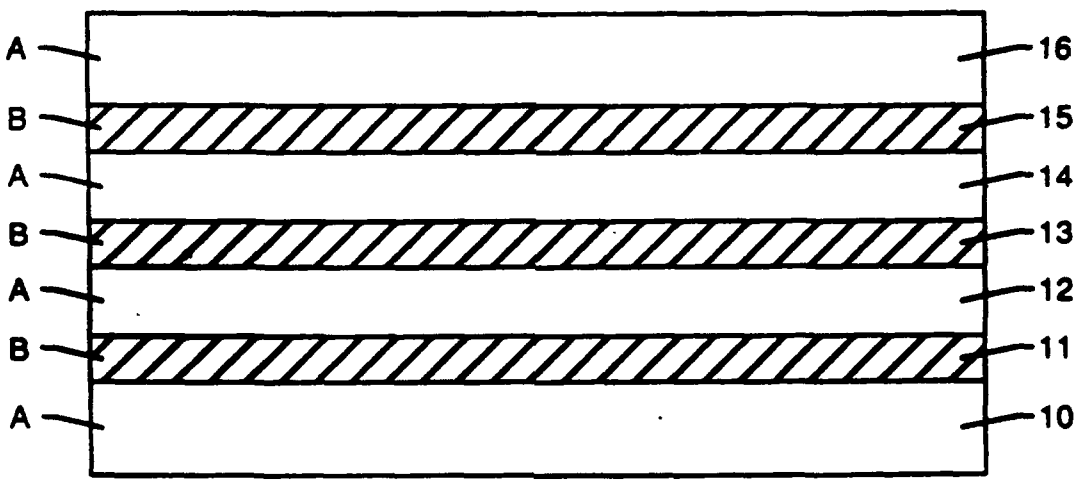

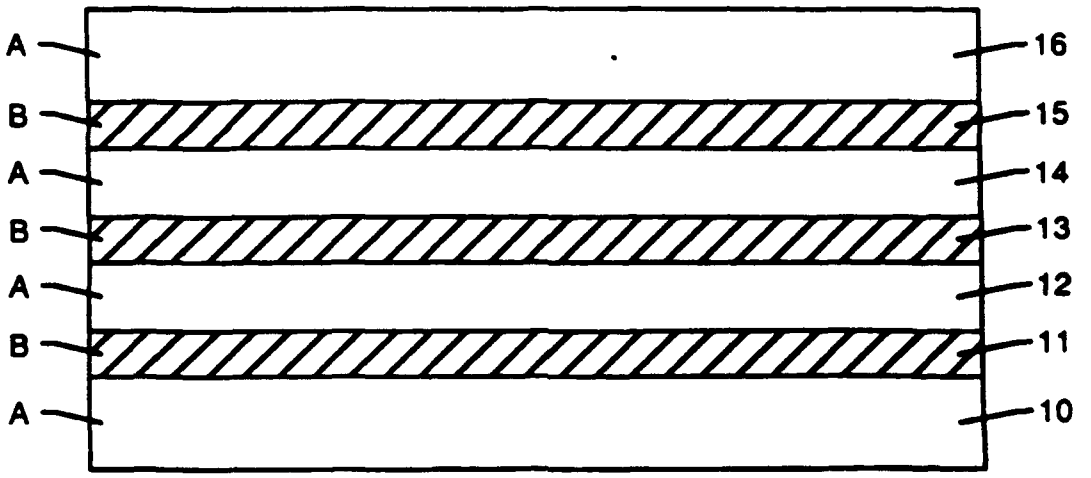

Figure 1

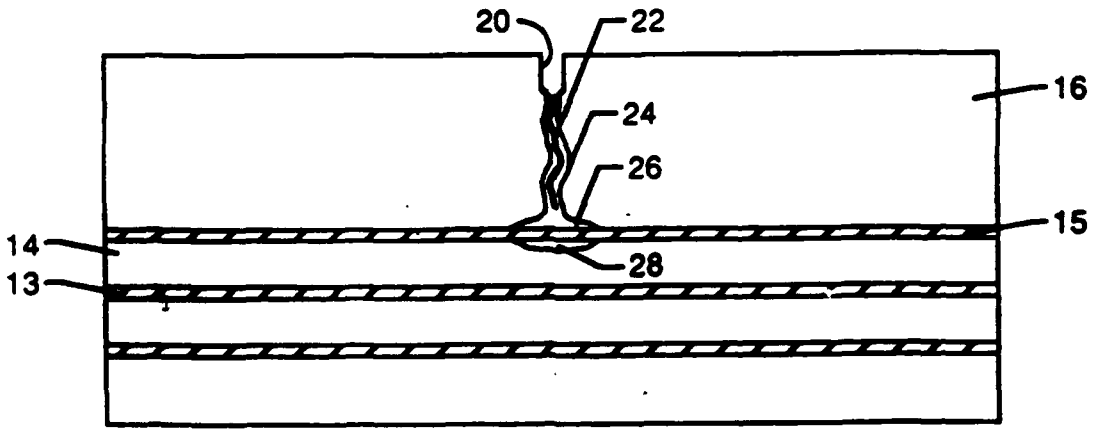

Figure 2

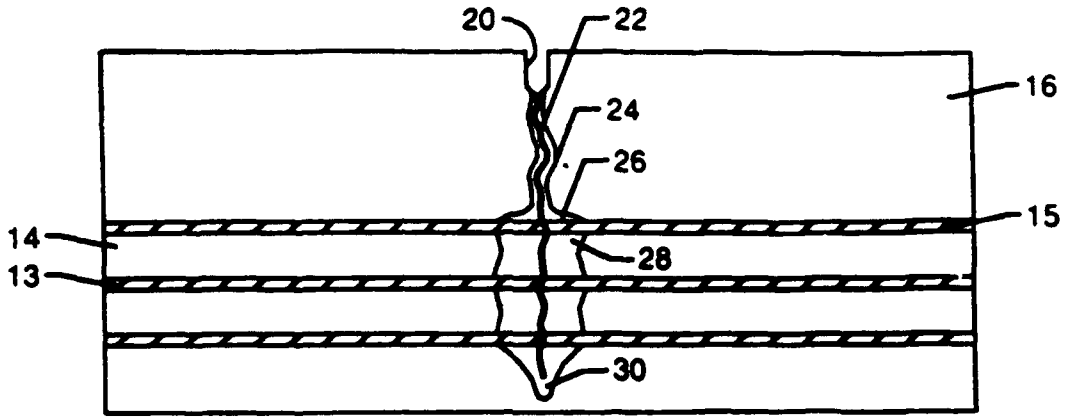

Figure 3

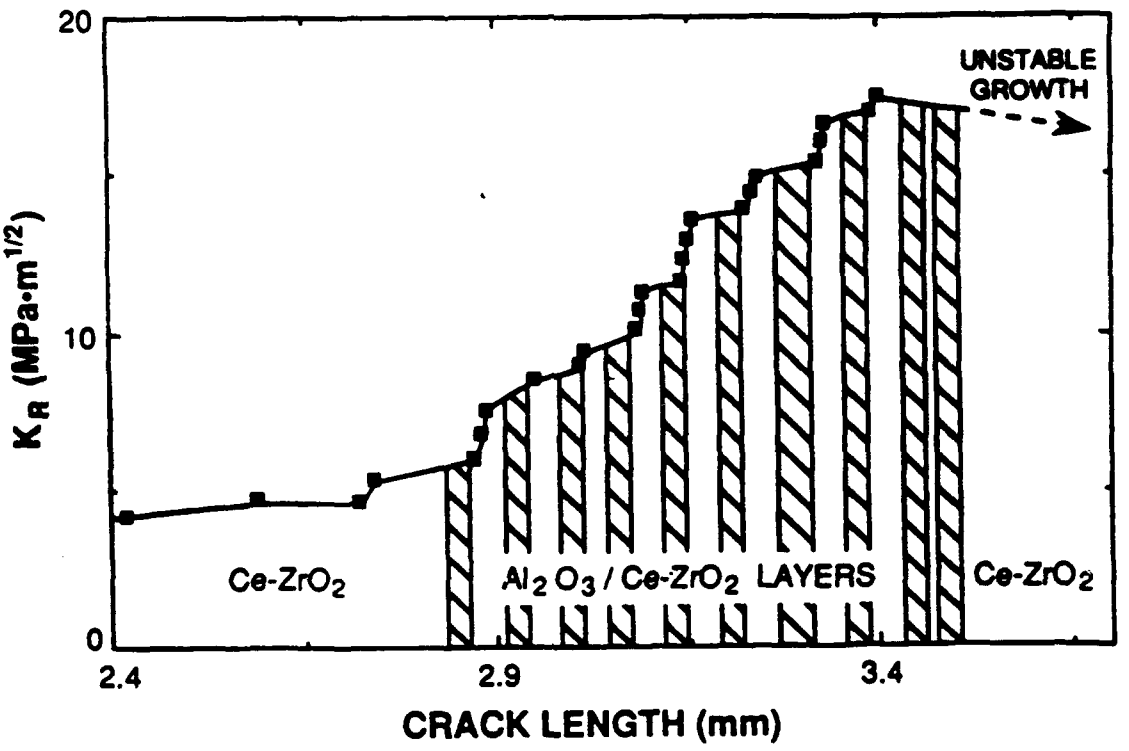

Figure 4

PARTIALLY STABILIZED ZRO$_2$-BASED LAMINAR CERAMIC COMPOSITES

GOVERNMENT RIGHTS

The United States Government has right in this invention under contract number F49620-89-C-0031 awarded by the Department of the Air Force and contract number N00014-90-J-1441 awarded by the Department of the Navy.

TECHNICAL FIELD

The present invention relates to laminar composite materials and, in particular, to laminar ceramic composites having enhanced fracture toughness.

BACKGROUND OF THE INVENTION

In ceria-partially-stabilized zirconia (Ce-ZrO_2, or Ce-TZP), high fracture toughness in the range of 10–14 MPa•m$^{\frac{1}{2}}$ has previously been achieved. Ce-TZP is known to undergo martensitic transformation from the tetragonal to the monoclinic phase as a result of stress. However, the elongated shapes of the stress-induced transformation zones surrounding cracks in Ce-TZP are not optimal for producing beneficial transformation toughening. In other zirconia ceramics of comparable toughness (such as magnesia-partially-stabilized zirconia (Mg-ZrO_2, or Mg-PSZ), for example), the transformation zone extends approximately equal distances ahead of and to the side of a crack. In contrast, the transformation zone in Ce-TZP is very elongated, extending ahead of the crack a distance of 10 to 20 times the width of the zone. The extra transformed material ahead of a crack in Ce-TZP degrades the toughness. Calculation of the crack tip shielding from transformation zones indicates that the increase in fracture toughness due to transformation shielding for the semicircular frontal zone shape characteristic of Mg-PSZ is about twice that for the elongated frontal zone characteristic of Ce-TZP.

The elongated transformation zone in Ce-TZP is thought to result from autocatalytic transformation, i.e., the sequential triggering of transformation in a grain by transformation strains in adjacent grains. Autocatalytic transformation also occurs in Mg-PSZ, as evidenced by the formation of well-defined shear bands within grains. The microstructure of Mg-PSZ may be thought of as dual scale: the individual precipitates that transform from tetragonal to monoclinic phase are lenticular in shape are lenticular in shape (approximately 300 nm in diameter), and they are contained within grains that are larger by about 2 orders of magnitude (approximately 50 μm diameter). Although each transformation band contains many autocatalytically transformed precipitates, the grain boundaries are effective barriers for arresting the propagating band. In Ce-TZP, however, the transforming units are the individual grains; there are no larger scale microstructural units. Thus, there are no large scale barriers to arrest a developing transformation band in Ce-TZP. Based on the foregoing, it is believed that substantial toughness enhancement will result if the microstructure of Ce-TZP is modified to change the shape of the stress-induced transformation zone.

SUMMARY OF THE INVENTION

The present invention relates to laminar ceramic composites and includes a method of introducing large-scale microstructural units into Ce-ZrO_2 (Ce-TZP) for enhancing fracture toughness of the ceramic material. These large-scale microstructural units take the form of barrier layers of materials such as Al_2O_3 or a mixture of Al_2O_3 and Ce-ZrO_2. Based on the foregoing background of the invention, the optimum separation of the barrier layers is believed to be approximately 10–200 μm, with optimum individual barrier layer thicknesses at the lower end of this range.

In the method of the present invention, powders of selected ceramic materials comprising the layers of the composite structure are dispersed in separate containers of water to form slurries. The pH of the slurries is adjusted to remove long range repulsive forces between the powder particles but retain short range repulsive forces. In this state of suspension, or coagulation, the particles settle readily under gravity without mass segregation and can be consolidated to higher density by centrifuging. After centrifuging, the supernatant liquid can be removed and a desired volume of another slurry can be added on top of the first layer of consolidated material. This process can be repeated indefinitely to form a laminar composite structure comprising alternating layers of different ceramic materials. Laminar composites having layers as thin as about 10 μm have been fabricated using this colloidal method of the present invention to consolidate the ceramic powders.

Controlled crack growth experiments and indentation experiments have been used to investigate the influence of barrier layers on crack tip transformation zones and fracture toughness in laminar composites of the present invention. Strong interactions between these layers and the martensitic transformation zones surrounding cracks and indentations have been observed. In both cases, the transformation zones spread along the region adjacent to the barrier layer. The presence of barrier layers thus leads to large increases in toughness and extensive R-curve behavior. This enhanced fracture toughness was observed for cracks growing parallel to the layers as well as for those that were oriented normal to the layers.

A principal object of the present invention is the fabrication of improved laminar ceramic composite materials. A feature of the invention is the use of a colloidal technique combined with centrifuging to consolidate layers of ceramic powders into a laminar composite. An advantage of the invention is fabrication of thin barrier layers of material that modify the stress-induced autocatalytic transformation at crack tips to enhance the fracture toughness of ceramic materials.

BRIEF DESCRIPTION OF THE DRAWINGS

For a more complete understanding of the present invention and for further advantages thereof, the following Detailed Description of the Preferred Embodiments makes reference to the accompanying Drawings, in which:

FIG. 1 is a schematic cross section of a laminar composite of the present invention;

FIG. 2 is a schematic cross section of the laminar composite of FIG. 1 illustrating crack propagation and transformation zone spreading at a barrier layer of the composite;

FIG. 3 is a schematic cross section showing further propagation of the crack of FIG. 2 to illustrate narrowing of the transformation zone after passing through the barrier layers; and

FIG. 4 is a graph plotting test results of toughness versus crack length through a laminar composite having a plurality of barrier layers.

DETAILED DESCRIPTION OF THE PREFERRED EMBODIMENTS

Composites of ZrO_2-based ceramic have been fabricated using a colloidal technique of the present invention to produce a laminar structure having one or more barrier layers. The barrier layers comprise materials such as Al_2O_3 or a mixture (typically 50% by volume) of Al_2O_3 and Ce-ZrO_2. The method comprises sequential centrifuging of slurries containing suspended particles of ceramic powders to form the layered structure, followed by forming (optional), pressing, drying, and sintering at temperatures up to about 1600° C. An aqueous electrolyte (i.e., a salt such as NH_4NO_3 or NH_4Cl, for example) can be used to produce short range repulsive hydration forces and to reduce the magnitude of the longer range electrostatic forces between the particles suspended in the slurry. This condition produces a weakly attractive network of particles that prevents mass segregation during centrifugation. Because of the lubricating action of the short range repulsive forces, the particles can be packed to a high consolidation density.

The relative densities of the Al_2O_3 and Ce-ZrO_2 powders consolidated separately using this colloidal technique were approximately 60 and 50 volume %, respectively. The larger shrinkage of the Ce-ZrO_2 during subsequent sintering caused cracking in some layered composites that contained pure Al_2O_3 layers (the exceptions being some thin layers with thickness less than about 30 μm). This contraction mismatch was minimized by using the mixed composition of 50 volume % Al_2O_3 and Ce-ZrO_2 instead of pure Al_2O_3 for most specimens. Optical micrographs of typical layers of Al_2O_3/Ce-ZrO_2 within a matrix of Ce-ZrO_2 show reasonably uniform layers with thicknesses in the range 10 to 100 μm. A multilayered structure of alternating Ce-ZrO_2 and Al_2O_3/Ce-ZrO_2 layers of 35 μm thickness was produced, as illustrated schematically in FIG. 1.

In a preferred embodiment illustrated in FIG. 1, the material of layers A is ZrO_2 doped with CeO_2 (12 molecular %). The material of layers B is a mixture of 50% by volume of Al_2O_3 and ZrO_2 doped with CeO_2 (12 molecular %). The purpose of the mixed composition in the alternative example is to reduce differential shrinkage between layers A and layers B during the densification process, which involves heat treatment. The material of layers A can be any ZrO_2-based material that undergoes stress-induced martensitic transformation from the tetragonal to the monoclinic crystal structure. The material of layers B may be any material that 1) is chemically compatible with the material of layers A at the temperatures needed to densify material A by sintering; 2) densifies at a similar temperature and with similar shrinkage as does the material of layers A; and 3) does not undergo stress-induced phase transformation or does so less readily than the material of layers A. In addition to the Al_2O_3 described above, other examples of suitable barrier layer materials include the following: ZrO_2 with dopants such as CeO_2, Y_2O_3, MgO, and CaO in concentrations sufficient to render ZrO_2 either fully stabilized in the cubic structure or more resistant to stress-induced tetragonal-to-monoclinic transformation than the material of layers A; titanium diboride; silicon carbide (SiC); hafnium oxide; and mixtures of the foregoing. Although there is no upper limit to the thickness of individual layers of the laminar composite, layers with thicknesses as low as about 10 μm can be fabricated using the colloidal method of the present invention.

In the method of the present invention, ceramic powders comprising the materials of layers A and B are dispersed in separate containers of water to form slurries. Ultrasonic waves may be used to cause mixing, and the pH may be adjusted to about 2 by adding HNO_3. At pH 2 there are long range electrostatic repulsive forces between the powder particles that keep them well separated and dispersed. The long range repulsive forces may be removed to form a weakly attractive network that results when the particles develop a solvation layer which produces a short range, but highly repulsive force. Such particle networks can be formed by adding an indifferent salt to a dispersed slurry in which the initial, long range electrostatic repulsive potential is produced at low pH. When the concentration of the salt is ≧0.1M, the particles become weakly attractive to form a coagulation due to the diminished electrostatic potential. A salt such as NH_4Cl or NH_4NO_3 at about 0.5–2.0M concentration, for example, may be added to the slurries of ceramic powders described above to cause coagulation. In this state of coagulation, the suspended particles are not flocced (i.e., not touching or cohesive), but they settle readily under gravity, without mass segregation, and they may be consolidated to higher densities by centrifuging. Mass segregation at this step is undesirable because it causes cracking during subsequent heat treatment and densification.

To construct the laminar composite illustrated in FIG. 1, a volume of slurry needed to yield the desired thickness of material in layer 10 is placed in a container comprising an outer wall (typically cylindrical), a removeable inner Teflon ® sleeve, and a removeable bottom. The container is then placed in the swinging bucket of a centrifuge and spun at approximately 2000 g for 15 minutes. After centrifuging, the supernatant liquid is removed and a volume of slurry needed to yield the desired thickness of material in layer 12 is placed in the container. The container is centrifuged again, and the whole process repeated for each of the layers 13 through 16. As shown in FIG. 1, the composition of the slurry is alternated (or changed to a different material) for each successive layer of the composite. The process is repeated until the composite structure has the desired number of layers, each having the desired thickness and composition.

At this stage, after all the layers of the composite have been centrifuged, the consolidated laminar composite has rheological properties similar to wet clay. Before drying, uniaxial compressive stress may be applied to the structure to further increase the particle packing density. This can be accomplished, for example, by inserting a microporous filter on top of the consolidated composite while it remains in the container, and then loading in a hydraulic press at a pressure of about 4000 psi. Alternatively, the damp composite structure may be shaped in a mold or rolled out to flatten the material, for example. The flattened composite may then be rolled into a composite rod comprising alternating layers of material having a spiral cross-section. It should be apparent that other shapes and structures of the laminar composite may be visualized and formed by one having ordinary skill in the art.

FIG. 4 is a graph plotting test results of toughness versus crack length through a laminar composite having a plurality of barrier layers.

DETAILED DESCRIPTION OF THE PREFERRED EMBODIMENTS

Composites of ZrO_2-based ceramic have been fabricated using a colloidal technique of the present invention to produce a laminar structure having one or more barrier layers. The barrier layers comprise materials such as Al_2O_3 or a mixture (typically 50% by volume) of Al_2O_3 and Ce-ZrO_2. The method comprises sequential centrifuging of slurries containing suspended particles of ceramic powders to form the layered structure, followed by forming (optional), pressing, drying, and sintering at temperatures up to about 1600° C. An aqueous electrolyte (i.e., a salt such as NH_4NO_3 or NH_4Cl, for example) can be used to produce short range repulsive hydration forces and to reduce the magnitude of the longer range electrostatic forces between the particles suspended in the slurry. This condition produces a weakly attractive network of particles that prevents mass segregation during centrifugation. Because of the lubricating action of the short range repulsive forces, the particles can be packed to a high consolidation density.

The relative densities of the Al_2O_3 and Ce-ZrO_2 powders consolidated separately using this colloidal technique were approximately 60 and 50 volume %, respectively. The larger shrinkage of the Ce-ZrO_2 during subsequent sintering caused cracking in some layered composites that contained pure Al_2O_3 layers (the exceptions being some thin layers with thickness less than about 30 μm). This contraction mismatch was minimized by using the mixed composition of 50 volume % Al_2O_3 and Ce-ZrO_2 instead of pure Al_2O_3 for most specimens. Optical micrographs of typical layers of Al_2O_3/Ce-ZrO_2 within a matrix of Ce-ZrO_2 show reasonably uniform layers with thicknesses in the range 10 to 100 μm. A multilayered structure of alternating Ce-ZrO_2 and Al_2O_3/Ce-ZrO_2 layers of 35 μm thickness was produced, as illustrated schematically in FIG. 1.

In a preferred embodiment illustrated in FIG. 1, the material of layers A is ZrO_2 doped with CeO_2 (12 molecular %). The material of layers B is a mixture of 50% by volume of Al_2O_3 and ZrO_2 doped with CeO_2 (12 molecular %). The purpose of the mixed composition in the alternative example is to reduce differential shrinkage between layers A and layers B during the densification process, which involves heat treatment. The material of layers A can be any ZrO_2-based material that undergoes stress-induced martensitic transformation from the tetragonal to the monoclinic crystal structure. The material of layers B may be any material that 1) is chemically compatible with the material of layers A at the temperatures needed to densify material A by sintering; 2) densifies at a similar temperature and with similar shrinkage as does the material of layers A; and 3) does not undergo stress-induced phase transformation or does so less readily than the material of layers A. In addition to the Al_2O_3 described above, other examples of suitable barrier layer materials include the following: ZrO_2 with dopants such as CeO_2, Y_2O_3, MgO, and CaO in concentrations sufficient to render ZrO_2 either fully stabilized in the cubic structure or more resistant to stress-induced tetragonal-to-monoclinic transformation than the material of layers A; titanium diboride; silicon carbide (SiC); hafnium oxide; and mixtures of the foregoing. Although there is no upper limit to the thickness of individual layers of the laminar composite, layers with thicknesses as low as about 10 μm can be fabricated using the colloidal method of the present invention.

In the method of the present invention, ceramic powders comprising the materials of layers A and B are dispersed in separate containers of water to form slurries. Ultrasonic waves may be used to cause mixing, and the pH may be adjusted to about 2 by adding HNO_3. At pH 2 there are long range electrostatic repulsive forces between the powder particles that keep them well separated and dispersed. The long range repulsive forces may be removed to form a weakly attractive network that results when the particles develop a solvation layer which produces a short range, but highly repulsive force. Such particle networks can be formed by adding an indifferent salt to a dispersed slurry in which the initial, long range electrostatic repulsive potential is produced at low pH. When the concentration of the salt is ≧0.1M, the particles become weakly attractive to form a coagulation due to the diminished electrostatic potential. A salt such as NH_4Cl or NH_4NO_3 at about 0.5–2.0M concentration, for example, may be added to the slurries of ceramic powders described above to cause coagulation. In this state of coagulation, the suspended particles are not flocced (i.e., not touching or cohesive), but they settle readily under gravity, without mass segregation, and they may be consolidated to higher densities by centrifuging. Mass segregation at this step is undesirable because it causes cracking during subsequent heat treatment and densification.

To construct the laminar composite illustrated in FIG. 1, a volume of slurry needed to yield the desired thickness of material in layer 10 is placed in a container comprising an outer wall (typically cylindrical), a removeable inner Teflon® sleeve, and a removeable bottom. The container is then placed in the swinging bucket of a centrifuge and spun at approximately 2000 g for 15 minutes. After centrifuging, the supernatant liquid is removed and a volume of slurry needed to yield the desired thickness of material in layer 12 is placed in the container. The container is centrifuged again, and the whole process repeated for each of the layers 13 through 16. As shown in FIG. 1, the composition of the slurry is alternated (or changed to a different material) for each successive layer of the composite. The process is repeated until the composite structure has the desired number of layers, each having the desired thickness and composition.

At this stage, after all the layers of the composite have been centrifuged, the consolidated laminar composite has rheological properties similar to wet clay. Before drying, uniaxial compressive stress may be applied to the structure to further increase the particle packing density. This can be accomplished, for example, by inserting a microporous filter on top of the consolidated composite while it remains in the container, and then loading in a hydraulic press at a pressure of about 4000 psi. Alternatively, the damp composite structure may be shaped in a mold or rolled out to flatten the material, for example. The flattened composite may then be rolled into a composite rod comprising alternating layers of material having a spiral cross-section. It should be apparent that other shapes and structures of the laminar composite may be visualized and formed by one having ordinary skill in the art.

After consolidation, the laminar composite is removed from the container or mold and dried at 50° C for about 24 hours. The composite can then be packed in ZrO_2 powder and sintered in a furnace using a temperature treatment schedule such as the following (which is provided only as an example, and not as a limitation, of a typical treatment schedule):

Typical Temperature Treatment Schedule

Temperature	Rate	Time
20° C. to 450° C.	Constant	2.0 Hours
450° C. to 600° C.	Constant	15.0 Hours
600° C. to 1000° C.	Constant	15.0 Hours
1000° C. to 1500° C.	Constant	10.0 Hours
1500° C.	N/A	2.0 Hours
1500° C. to 1600° C.	Constant	0.5 Hours
1600° C.	N/A	2.0 Hours
1600° C. to 20° C.	Constant	4.0 Hours

EXPERIMENTAL RESULTS

The influence of individual barrier layers of Al_2O_3 or $Al_2O_3/Ce\text{-}ZrO_2$ on crack growth and transformation zones in $Ce\text{-}ZrO_2$ was investigated by fabricating composites containing widely spaced layers, as illustrated schematically in FIG. 2. Measurements were obtained from controlled crack growth in notched beams, fracture of smooth bars, and indentation experiments using a Vickers indenter.

Crack growth experiments with notched beams were conducted in two steps, using two different loading fixtures, which operated on the stage of an optical microscope and allowed high magnification observation of the side of the beam during loading. All experiments were done in a dry nitrogen atmosphere. The dimensions of the beams were approximately $28 \times 6 \times 1$ mm, with an initial notch 20 of about 170 μm width and about 2 mm depth. A stable crack 22 was initiated from the root of notch 20 under monotonic loading. WC/Co flexure beams were placed in series with the test specimen to make the loading system extremely stiff and allow stable crack growth. The beams were equivalent to very stiff springs in parallel with the specimen and thus functioned as a crack arrester. To stiffen the loading system further, initial crack growth was induced without use of a load cell. After growing crack 22 for approximately 500 μm, the loading system was changed to include a load cell with conventional four-point loading through rollers in order to allow measurement of the fracture toughness (or crack growth resistance). The stress intensity factor was evaluated from the measured loads and crack lengths (obtained from optical micrographs), as is well known in the art.

Results were obtained from a specimen comprising three layers of $Al_2O_3/Ce\text{-}ZrO_2$ widely spaced ahead of notch 22, as shown in FIG. 2. After initiating stably in the immediate vicinity of notch 20, crack 22 grew unstably in layer 16 when the loading system was changed to include the load cell, and arrested approximately 20 μm before layer 15 of $Al_2O_3/Ce\text{-}ZrO_2$, which had a thickness of approximately 35 μm. The width of the transformation zone 24 over the wake of crack 22, as determined by Nomarski interference, was approximately 15 μm. However, near the tip of the arrested crack, the transformation zone 26 extended adjacent to $Al_2O_3/Ce\text{-}ZrO_2$ layer 15 for distances of more than 150 μm each side of the crack. Some transformation 28 occurred on the opposite side of $Al_2O_3/Ce\text{-}ZrO_2$ layer 15, also for a distance of 150 μm both sides of the crack plane.

After further loading, crack 22 grew unstably through $Al_2O_3/Ce\text{-}ZrO_2$ layer 15, into the $Ce\text{-}ZrO_2$ of layer 14, and arrested again approximately 40 μm before layer 13, which had a thickness of 70 μm. The shape of the transformation zone along layer 13 near the crack tip was similar to that of zone 26. These results indicate that the Al_2O_3/ZrO_2 barrier layers have a much larger effect than simply arresting the growth of a transformation zone ahead of a crack: they also promote expansion of the transformation zone outward from the side of the crack, which provides additional crack tip shielding and hence toughening. As illustrated in FIG. 3, a plurality of barrier layers produces a broadened transformation zone as crack 22 progresses through the barrier layer region. However, when crack 22 exits the barrier layer region, transformation zone 30 returns to the narrow, elongated shape characteristic of the $Ce\text{-}ZrO_2$ matrix material.

The applied stress intensity factors were calculated at various stages of of crack growth, using the measured loads and crack lengths. The fracture toughness of the $Ce\text{-}ZrO_2$ matrix was 5 $MPa\cdot m^{\frac{1}{2}}$, whereas the stress intensity factor had to be raised to 10 $MPa\cdot m^{\frac{1}{2}}$ to drive the crack across each barrier layer. After the crack tip passed each barrier layer, the unstable crack growth prevented continued measurement of the stress intensity factor until the crack arrested again. However, when the crack had arrested, the applied stress intensity factor decreased to approximately 5 $MPa\cdot m^{\frac{1}{2}}$, implying that the toughening effect of each barrier layer decreased as it became part of the wake of the crack. Similar results were obtained from specimens containing barrier layers of 100% Al_2O_3 in the same $Ce\text{-}ZrO_2$ matrix.

Vickers indentations in the $Ce\text{-}ZrO_2$ matrix were surrounded by large zones of transformed material, which caused uplift of the surface adjacent to the indentations. There was no cracking caused by the indentations at loads up to 300N. The presence of a nearby $Al_2O_3/Ce\text{-}ZrO_2$ barrier layer within the transformation zone caused spreading of the zone in the region adjacent to the barrier layer, in a pattern similar to the crack tip zone 26 shown in FIG. 2. There was also transformed material on the side opposite the indentation. The presence of the $Al_2O_3/Ce\text{-}ZrO_2$ barrier layer caused substantially larger uplift everywhere on the side of the indentation that was closer to the barrier layer. The surface of the $Al_2O_3/Ce\text{-}ZrO_2$ barrier layer was depressed relative to the adjacent transformed $Ce\text{-}ZrO_2$ material. However, the $Al_2O_3/Ce\text{-}ZrO_2$ barrier layer was uplifted more than the $Ce\text{-}ZrO_2$ surface at corresponding positions on the opposite side of the indentation. This observation provides evidence that the $Al_2O_3/Ce\text{-}ZrO_2$ barrier layer caused spreading of the transformation zone adjacent to the layer in the subsurface regions as well as along the surface, and/or larger concentration of transformed material in the region adjacent to the layer.

The influence of multilayered microstructures on transformation zone shapes and toughening was investigated using a specimen containing 19 layers of alternating $Ce\text{-}ZrO_2$ and $Al_2O_3/Ce\text{-}ZrO_2$, each of 35 μm thickness, in the center of a beam of $Ce\text{-}ZrO_2$. An additional isolated 35 μm layer of Al_2O_3 was located approximately 1 mm from the multilayered region. The toughening experienced by cracks oriented normal to the layers was evaluated by growing a crack in a notched

beam using the loading procedure described above. The tip of the initial crack that was introduced with the stiff loading system was about halfway between the end of the notch and the first of the multiple layers (550 μm from the notch and 440 μm from the first layer). Further loading with the more compliant loading system, which allowed continuous load measurement, caused stable growth up to and through the multiple layers. However, as the crack approached the last of the layers, it extended unstably for 1.5 mm and arrested at a position 400 μm past the isolated layer.

As shown in the plot of FIG. 4, the critical stress intensity factor increased from approximately 5 $MPa\cdot m^{\frac{1}{2}}$ in the $Ce\text{-}ZrO_2$ to 17.5 $MPa\cdot m^{\frac{1}{2}}$ as the crack approached the end of the $Al_2O_3/Ce\text{-}ZrO_2$ barrier layer region. A corresponding increase in the size of the transformation zone surrounding the crack tip was evident in micrographs. Surface distortions due to the volume strain associated with the transformation were detected as far as 300 μm from the crack plane, whereas the zone width in the single phase $Ce\text{-}ZrO_2$ is only approximately 15 μm. After exiting the barrier layer region, the crack experienced unstable growth.

The increased width of the transformation zone within the layered region is clearly evident in optical interference micrographs in which fringes represent contours of surface uplift adjacent to the crack. Surface uplift adjacent to the crack is larger (by a factor of about 2) within the layered region than in the single phase $Ce\text{-}ZrO_2$, even though the uplift is constrained by the higher stiffness $Al_2O_3/Ce\text{-}ZrO_2$ barrier layers, and the average volume fraction of the $Ce\text{-}ZrO_2$ is lower in the layered region. Both the zone width and the magnitude of the surface uplift adjacent to the crack decreased where the crack grew unstably out of the multilayered region into the single phase $Ce\text{-}ZrO_2$, and increased again as the crack passed through the isolated $Al_2O_3/Ce\text{-}ZrO_2$ layer.

The response of cracks oriented parallel to the barrier layers was assessed by loading a double cantilever beam using another fixture on the stage of the optical microscope. The cantilever beam was cut from a region of the specimen that contained a conveniently located large processing flaw, which served as an initial sharp crack (a flat nonsintered region approximately 1 mm diameter at the edge of the multilayered area). A sequence of micrographs was obtained during loading. As the load was increased initially, a zone of material within the single phase $Ce\text{-}ZrO_2$ ahead and to one side of the crack tip transformed before the crack began to grow. With further load increase, the crack grew but was forced to cross the first layer of $Al_2O_3/Ce\text{-}ZrO_2$, presumably because of the compressive stresses due to the transformation zone on one side of the crack. The crack then grew along the first layer of $Ce\text{-}ZrO_2$ within the multilayered region, causing transformation in an increasingly wide zone of adjacent layers. The stress intensity factor was not evaluated during this test because the ends of the beam were glued into the loading fixture rather than being loaded through pins. Nevertheless, it is clear that the layers caused an enhancement of the width of the transformation zone, and hence the toughness, in this orientation as well as in the normal orientation.

The results of the foregoing experiments show that the presence of barrier layers of Al_2O_3 or $Al_2O_3/Ce\text{-}ZrO_2$ in Ce-TZP can dramatically modify the sizes and shapes of the transformation zones around cracks in a manner that increases fracture toughness. Two effects have been identified: truncation of the elongated frontal zone, which approximately doubles the toughening due to crack shielding; and the spreading of transformation zones along the regions adjacent to the barrier layers. Transformation zone spreading is believed to be driven by nontransformability of the barrier layers and/or their higher elastic stiffness. The mechanics of transformation zone spreading, however, has not be analyzed. Combination of the two transformation zone effects causes an increase in the fracture toughness of layered material by a factor of about 3.5 (from 5 $MPa\cdot m^{\frac{1}{2}}$ to 17.5 $MPa\cdot m^{\frac{1}{2}}$).

The $Ce\text{-}ZrO_2$ powder used in the foregoing experiments yields a base material with a fracture toughness of approximately 5 $MPa\cdot m^{\frac{1}{2}}$ and a transformation zone size of approximately 15 μm. These are substantially less than the toughness and zone sizes reported in more transformable $Ce\text{-}ZrO_2$ materials ($K_R = 14$ $MPa\cdot m^{\frac{1}{2}}$, and zone sizes of several hundred microns). However, despite this relatively low starting toughness, the multilayered microstructure was characterized by a crack resistance curve that went as high as 17.5 $MPa\cdot m^{\frac{1}{2}}$, and which had not begun to saturate to a steady state value when the crack encountered the end of the layered microstructure. The peak value of K_R is one of the highest toughness recorded in a ceramic material, being surpassed only by weakly bonded fiber reinforced composites, weakly bonded laminar composites, and some Mg-PSZ materials immediately after heat treatment (Mg-PSZ materials age, however, and lose some of their toughening at room temperature). Furthermore, there is potential for substantially higher fracture toughness in layered microstructures fabricated with higher toughness Ce-TZP starting materials.

The mechanisms of toughening enhancement described above are not restricted to the laminar geometry used in the foregoing experiments. Similar effects may be expected for any high-modulus, nontransforming microstructural units, such as continuous or chopped fibers or platelets, that are distributed over a spatial scale similar to that of the barrier layers. An example that has been observed is the interaction of a transformation zone around an indentation with an isolated sapphire fiber in a Ce-TZP matrix. In direct analogy with the effect of the barrier layers, the sapphire fiber caused spreading of the transformation zone and a larger overall surface uplift in the vicinity of the fiber.

The colloidal technique of the present invention may be used for fabricating layered ceramic structures other than the ZrO_2-based structures described above. For example: multilayered capacitors having alternate layers of dielectric materials, such as barium titanate, between metallic electrodes; multilayered actuators or transduces having alternate layers of ferroelectric ceramic material, such as PZT (lead-zirconium titanate), between metallic electrodes; and solid oxide fuel cells having alternate layers of fuel electrodes (e.g., Ni/ZrO_2), oxygen conducting electrolyte (e.g., Y_2O_3/ZrO_2), and air electrodes (e.g., $La(Sr)MnO_3$). These laminar structures may all be fabricated using variations of the method described above instead of prior art tape casing methods. The colloidal method of the present invention has several advantages over tape casting methods, such as the fabrication of smaller layer dimensions, avoiding problems associated with burning out the binder used with tape casting, and achieving better particle packing, which results in reduced sintering temperatures and the

avoidance of interdiffusion between layers (caused by high-temperature sintering).

Although the present invention has been described with respect to specific embodiments thereof, various changes and modifications can be carried out by those skilled in the art without departing from the scope of the invention. Therefore, it is intended that the present invention encompass such changes and modifications as fall within the scope of the appended claims.

We claim:

1. A ZrO_2-based laminar composite, comprising:

at least two layers of ZrO_2-based ceramic material that undergoes stress-induced martensitic transformation from a tetragonal to a monoclinic structure;

a layer of a second ceramic material consolidated between said layers of ZrO_2-based material to form a barrier layer;

said second ceramic material undergoing stress-induced transformation, if any, less readily than said ZrO_2-based material.

2. The laminar composite of claim 1, wherein said ZrO_2-based ceramic material comprises Ce-doped ZrO_2 ceramic material.

3. The laminar composite of claim 1, wherein said second ceramic material comprises a material selected from the group consisting of Al_2O_3; sapphire fibers; titanium diboride; silicon carbide; hafnium oxide; ZrO_2 doped with a material selected from the group consisting of CeO_2, Y_2O_3, MgO, and CaO; and mixtures of the foregoing.

4. The laminar composite of claim 2, further comprising a plurality of barrier layers formed from said second ceramic material, said barrier layers having individual thicknesses ranging from approximately 10 to 100 μm and consolidated alternately between a plurality of said Ce-doped ZrO_2 ceramic layers.

5. A laminar ceramic composite, comprising:

at least two layers of partially stabilized Ce-doped ZrO_2 ceramic material that undergoes stress-induced martensitic transformation from a tetragonal to a monoclinic structure;

a layer of a second ceramic material consolidated between said layers of said partially stabilized Ce-doped ZrO_2 ceramic material to form a barrier layer;

said second ceramic material undergoing stress-induced transformation, if any, less readily than said partially stabilized Ce-doped ZrO_2 ceramic material.

6. The laminar ceramic composite of claim 5, wherein said second ceramic material comprises a material selected from the group consisting of Al_2O_3; sapphire fibers; titanium diboride; silicon carbide; hafnium oxide; ZrO_2 doped with a material selected from the group consisting of CeO_2, Y_2O_3, MgO, and CaO; and mixtures of the foregoing.

7. The laminar ceramic composite of claim 5, further comprising a plurality of barrier layers formed from said second ceramic material, said barrier layers having individual thicknesses ranging from approximately 10 to 100 μm and consolidated alternately between a plurality of layers of said partially stabilized Ce-doped ZrO_2 ceramic material.

8. A partially stabilized ZrO_2-based laminar ceramic composite, comprising:

a plurality of layers of ZrO_2-based ceramic material that undergoes stress-induced martensitic transformation from a tetragonal to a monoclinic structure;

a plurality of layers of a second ceramic material, said layers of said second ceramic material consolidated alternately between said layers of said ZrO_2-based material and having individual thicknesses ranging from approximately 10 to 100 μm;

said second ceramic material comprising a material selected from the group consisting of Al_2O_3; sapphire fibers; titanium diboride; silicon carbide; hafnium oxide; ZrO_2 doped with a material selected from the group consisting of CeO_2, Y_2O_3, MgO, and CaO; and mixtures of the foregoing.

9. The laminar ceramic composite of claim 8, wherein said ZrO_2-based ceramic material comprises Ce-doped ZrO_2 ceramic material.

* * * * *